

Distribution Agreement

In presenting this thesis or dissertation as a partial fulfillment of the requirements for an advanced degree from Emory University, I hereby grant to Emory University and its agents the non-exclusive license to archive, make accessible, and display my thesis or dissertation in whole or in part in all forms of media, now or hereafter known, including display on the world wide web. I understand that I may select some access restrictions as part of the online submission of this thesis or dissertation. I retain all ownership rights to the copyright of the thesis or dissertation. I also retain the right to use in future works (such as articles or books) all or part of this thesis or dissertation.

DocuSigned by:
Signature: *Alexa Iannitelli*
D124357B7B04452...

Alexa Iannitelli
Name

4/5/2023 | 4:49 PM EDT
Date

Title Noradrenergic dysfunction in neurodegenerative disease

Author Alexa Iannitelli

Degree Doctor of Philosophy

Program Biological and Biomedical Sciences
Neuroscience

Approved by the Committee

DocuSigned by:

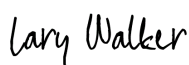
B1EFF48AF52342A...

David Weinschenker
Advisor

DocuSigned by:

B1343C118BE5461...

Ellen Hess
Committee Member

DocuSigned by:

D48D02D6E75C4CE...

Lary Walker
Committee Member

DocuSigned by:

213D62417545412...

Steven Sloan
Committee Member

DocuSigned by:

6E720DF73E2743B...

Mike Caudle
Committee Member

Accepted by the Laney Graduate School

Kimberly Jacob Arriola, PhD, MPH
Dean, James T. Laney School of Graduate Studies

Noradrenergic dysfunction in neurodegenerative disease

By

Alexa F. Iannitelli

B.S., Susquehanna University, 2018

Advisor: David Weinshenker, Ph.D.

An abstract of

A dissertation submitted to the Faculty of the

James T. Laney School of Graduate Studies of Emory University

in partial fulfillment of the requirements for the degree of

Doctor of Philosophy in Neuroscience

2023

Abstract

Noradrenergic dysfunction in neurodegenerative disease

By Alexa F. Iannitelli

Neurodegenerative disease impacts millions of individuals worldwide, with incidence rates climbing alongside the average human lifespan. There are currently no therapeutic treatments for neurodegeneration, and as such, this process poses a public health risk. The two most common neurodegenerative disorders are Alzheimer's and Parkinson's diseases. Both diseases are pathologically characterized by the presence of abnormal protein aggregates, which lead to eventual dysfunction and degeneration of important neural systems. Interestingly, early pathology of both disorders can be found in a brainstem region called the locus coeruleus prior to most other areas of the brain. The locus coeruleus is responsible for central neurotransmission of the neuromodulator norepinephrine, and as such, it is responsible for a wide range of behaviors. As these neurons accumulate pathology, they become dysfunctional, leading to prodromal aspects of both Alzheimer's and Parkinson's diseases. These symptoms most often include sleep disturbances, anxiety, and cognitive decline, and are reported by patients to be among the most troublesome aspects of their disorders. Thus, there is an urgent need for the development of novel treatments for Alzheimer's and Parkinson's diseases. The work presented here assess two rodent models of locus coeruleus dysfunction and degeneration. The first, a selective neurotoxin, ablates axon terminals but spares cell bodies, providing a model of the very early noradrenergic dysfunction that precedes outright degeneration. Mice administered DSP-4 recapitulate phenotypes of neurodegenerative disease, including decreased catecholamine levels, increased inflammation, and novelty-induced anxiety-like behavior. These changes are coupled with a downregulation of important noradrenergic genes, indicating severe cellular harm. To further investigate the impact of noradrenergic dysfunction in a mouse model of neurodegeneration, we adapted an approach for driving pigmentation in the locus coeruleus. We found that pigmentation led to neurodegeneration as early as 1-week post-infusion, coupled with a depletion of catecholamines throughout the brain and increased anxiety-like behavior. On a molecular level, the presence of pigment granules leads to the upregulation of several pathways involved in apoptosis and other stress responses. By 6-weeks, the presence of this pigment in locus coeruleus neurons nearly completely degenerates the region, leaving a robust astrocyte response in its wake. Taken together, these models allow for a comprehensive assessment of noradrenergic dysfunction throughout neurodegeneration, both early on when only fibers are damaged, and also later, when degeneration begins to impact the cell bodies. These insights will inform future research into the precise mechanisms driving locus coeruleus dysfunction and degeneration in Alzheimer's and Parkinson's diseases.

Noradrenergic dysfunction in neurodegenerative disease

By

Alexa F. Iannitelli

B.S., Susquehanna University, 2018

Advisor: David Weinschenker, Ph.D.

A dissertation submitted to the Faculty of the
James T. Laney School of Graduate Studies of Emory University
in partial fulfillment of the requirements for the degree of
Doctor of Philosophy in Neuroscience

2023

Acknowledgements

First and foremost, I would like to thank my advisor, Dr. David Weinshenker, for his unwavering support throughout this journey. I truly could not have asked for a kinder or more caring mentor. Each time I hit a roadblock, David's door was always open to offer practical advice or simply lend a sympathetic ear (somehow always knowing exactly what I needed to hear). Without his guidance and encouragement, I would not be the scientist I am today. I would also like to thank my undergraduate advisor, Dr. James Briggs, for helping me to discover my passion for research. And to my teaching mentors – Dr. Leah Roesch, Dr. Gillian Hue, and Dr. Kristen Frenzel – I am beyond grateful for your wisdom, compassion, and strength. I can only hope to one day be a fraction of the inspiration you are for women in neuroscience.

I am thankful for the scientific input and support I received from my thesis committee. To Drs. Ellen Hess, Lary Walker, and Mike Caudle, for their time and guidance throughout my dissertation research. A very special thank you to Dr. Steven Sloan, who gave me the confidence I needed to take on new and challenging techniques. I am fortunate to have learned so much from all of their expertise and perspectives, and I greatly appreciate the advice and encouragement I received throughout the years.

I would also like to thank the members of the Weinshenker lab who have helped me along the way. To Dr. Dan Manvich, who first introduced me to the locus coeruleus and was endlessly patient when I struggled mounting brain tissue for the first time. To my peers Dr. Rachel Tillage, who was always a source of positivity in the lab, and Anu Korukonda, for her enthusiasm and curiosity about every project, and for always lending a helping hand. And a special thanks to Dr. Kate McCann, for her support and guidance, even in the most difficult times.

I am eternally grateful to have gained the closest of friends through this Ph.D. To Dr. Stephanie Foster, who got me through each week with our regular walks and much-needed talks. To Dr. Danny Lustberg, who always pushed me to be the best scientist I could be. To Dr. Samantha Ortiz-Vanderhoof, whose presence in the lab was brief but made a lasting impression. And finally, to Michael Kelberman, my lab twin. Thank you for letting me be my authentic self, and having my back always. I could not have asked for a better friend to navigate graduate school alongside.

Finally, I would like to thank my family for their support throughout the many years of my education. To my mother, who could not be more proud and never resists the urge to tell me so. To my father, who fostered my curiosity about the natural world from a very young age. To my little sister Olivia, for whom I strive to be the very best version of myself. To Barbara, Laura, and Joe, for their love and support. Most importantly, to my partner Matthew, whose patience throughout this journey should earn him sainthood. Thank you for believing that I can do anything, and giving me the strength to do it. And of course, to Eva, my emotional support critter.

I am eternally grateful for each of these individuals, without whom this dissertation would not have been possible.

This work is dedicated to my uncle, Fred Grotenhuis, who passed away from complications related to Parkinson's disease. Despite his condition, he was the life of every party, and never let his disease keep him from living his best life. I hope that this work will one day help advance treatments for neurodegenerative diseases, so that other patients may continue living their lives to the fullest.

TABLE OF CONTENTS

CHAPTER 1: INTRODUCTION.....	1
1.1 THE LOCUS COERULEUS.....	2
1.1.1 Composition.....	2
1.1.2 Norepinephrine synthesis.....	2
1.1.3 Locus coeruleus function.....	4
1.2 ALZHEIMER'S DISEASE.....	6
1.2.1 Epidemiology and etiology.....	6
1.2.2 Clinical presentation.....	7
1.2.3 Neuropathology.....	9
1.2.4 The role of the locus coeruleus.....	12
1.2.5 Rodent models.....	13
1.3 PARKINSON'S DISEASE.....	15
1.3.1 Epidemiology and etiology.....	15
1.3.2 Clinical presentation.....	18
1.3.3 Pathology.....	21
1.3.4 The role of the locus coeruleus.....	21
1.3.5 Animal models.....	23
1.4 LOCUS COERULEUS SUSCEPTIBILITY.....	26
1.5 NEUROMELANIN.....	28
1.5.1 Characteristics of neuromelanin.....	28
1.5.2 Neuromelanin formation.....	28

1.5.3 Neurotoxicity of neuromelanin.....	30
1.5.4 Previous work in the field.....	32
1.6 DISSERTATION AIMS.....	34
CHAPTER 2: THE NEUROTOXIN DSP-4 DYSREGULATES THE LOCUS COERULEUS-NOREPINEPHRINE SYSTEM AND RECAPITULATES MOLECULAR AND BEHAVIORAL ASPECTS OF PRODROMAL NEURODEGENERATIVE DISEASE.....	36
2.1 ABSTRACT.....	37
2.2 INTRODUCTION.....	38
2.3 MATERIALS AND METHODS.....	40
2.4 RESULTS.....	48
2.5 DISCUSSION.....	53
CHAPTER 3: CONSEQUENCES OF PIGMENTATION ON LOCUS COERULEUS SURVIVAL AND FUNCTIONING.....	69
3.1 ABSTRACT.....	70
3.2 INTRODUCTION.....	71
3.3 MATERIALS AND METHODS.....	74
3.4 RESULTS.....	81
3.5 DISCUSSION.....	87
CHAPTER 4: DISCUSSION.....	101

4.1 SUMMARY.....	102
4.2 CONCLUSIONS AND FUTURE DIRECTIONS.....	102
4.2.1 DSP-4.....	102
4.2.2 Neuromelanin.....	105
4.3 CONCLUDING REMARKS.....	110
REFERENCES.....	112

FIGURES

Figure 1.1 Formation of endogenous neuromelanin granules.....	35
Figure 2.1 DSP-4 decreases tissue NE and metabolite levels and increases turnover.....	59
Figure 2.2 DSP-4 induces degeneration of noradrenergic terminals and oxidative stress but leaves LC cell bodies intact.....	60
Figure 2.3 DSP-4 alters astrocyte and microglia activation across the LC-NE system.....	61
Figure 2.4 DSP-4 triggers changes in the LC transcriptome.....	62
Figure 2.5 DSP-4 treatment does not alter baseline or footshock-induced LC activity.....	64
Figure 2.6 DSP-4 increases novelty-induced anxiety and arc expression.....	65
Figure 3.1 hTyr induces pigmentation in the LC reminiscent of endogenous NM.....	92
Figure 3.2 The presence of pigmentation damages LC cell bodies and fibers at 1-week.....	93
Figure 3.3 hTyr-induced pigmentation decreases tissue NE and metabolite levels and increases turnover at 1 week.....	94
Figure 3.4 hTyr-induced pigmentation increases novelty-induced anxiety but not contextual fear memory at 1 week.....	95

Figure 3.5 hTyr-driven pigmentation triggers changes in the LC transcriptome.....	96
Figure 3.6 Prolonged pigment expression results in granule accumulation and LC degeneration	97
Figure 3.7 Pigment-induced neurodegeneration triggers astrocyte responses in and around the LC	98
Figure 3.8 hTyr-induced pigmentation depletes tissue NE and metabolite levels and dysregulates turnover at 6 weeks.....	99
Figure 3.9 Pigment accumulation and subsequent neurodegeneration does not affect novelty- induced anxiety or contextual fear memory by 6-weeks.....	100

CHAPTER 1: INTRODUCTION

1.1 THE LOCUS COERULEUS

1.1.1 COMPOSITION

The locus coeruleus (LC) is a small brainstem nucleus, comprised of less than 50,000 neurons in the human brain (Mouton et al., 1994) and just 3,000 neurons in the rodent brain (Sara, 2009). Despite its stature, the LC is critically important in much of our daily cognitive functioning. The LC contains catecholaminergic neurons which rely on the neurotransmitter norepinephrine (NE) for neural communication. The LC is the primary source of central NE and sends unmyelinated axonal projections to virtually every other region of the brain (Foote et al., 1983).

1.1.2 NOREPINEPHRINE SYNTHESIS AND NEUROTRANSMISSION

Norepinephrine Synthesis

NE is produced in vesicles at the axon terminal via the catecholamine synthesis pathway. This pathway begins when an enzymatic reaction converts the essential amino acid Phenylalanine into L-Tyrosine, then the rate-limiting enzyme tyrosine hydroxylase (TH) converts the product to form L-DOPA. This dopamine (DA) precursor is synthesized into the neurotransmitter by DOPA decarboxylase. Once DA is formed in the cytoplasm, it is quickly packaged into vesicles by the vesicular monoamine transporter 2 (VMAT2). Inside the vesicle, the enzyme dopamine beta-hydroxylase (DBH) converts DA into NE. Upon neuronal activation and calcium entry into the terminal, the vesicles then fuse with the plasma membrane and neurotransmission ensues. DBH is highly efficient, resulting in a near-total conversion of DA to NE in LC neurons. However, there have been reports of co-transmission of DA and NE from these neurons under specific conditions (Devoto et al., 2005; Devoto and Flore, 2006; Yamasaki and Takeuchi, 2017).

Noradrenergic Neurotransmission

Following vesicular release, NE binds adrenoceptors located on the postsynaptic neuron. In the brain, these postsynaptic receptors are found in two primary subtypes: alpha-1 and beta. Activation of these G-protein coupled receptors (GPCRs) elicits signaling cascades downstream of the receptor. Alpha-1 receptors are Gq-coupled, activating the phospholipase C pathway, which subsequently increases IP₃ and DAG and increases intracellular calcium concentrations, ultimately resulting in cellular activation (Taylor and Cassagnol, 2022). Beta adrenergic receptors are coupled to the Gs subunit. The binding of these receptors activates adenylyl cyclase and signals via a cAMP-dependent pathway (Alhayek and Preuss, 2022). Like Gq-coupled alpha-1 receptors, beta adrenergic receptors have the effect of activating the postsynaptic neuron.

NE can also bind alpha-2 adrenergic receptors in the brain. In comparison to the expression of alpha-1 and beta receptors, which is largely confined to postsynaptic neurons, alpha-2 receptors most often reside on the dendrites and axon terminals of LC neurons themselves. The alpha-2 adrenergic receptor is Gi-coupled, inhibiting adenylyl cyclase activity and preventing subsequent signaling pathways, which has an overall inhibitory effect on cellular activity. For this reason, alpha-2 receptors are often referred to as “inhibitory autoreceptors”. This feedback mechanism is advantageous, as it suppresses LC activity to prevent over-activation of the nucleus (Aghajanian et al., 1977). Interestingly, differences in the axonal expression of alpha-2 receptors vary between LC neurons based on their projection region (Wagner-Altendorf et al., 2019).

LC neurons can also clear excess neurotransmitters that do not bind receptors, mitigating the effects of extended NE exposure, which can include reactivation of the receptors and eventual dysregulation of receptor expression on the postsynaptic neuron. LC neuron terminals express the norepinephrine transporter (NET), the monoamine transporter that is responsible for returning

excess NE into the presynaptic neuron. In the cytoplasm, NE is either repackaged into synaptic vesicles by VMAT2 or decomposed by monoamine oxidase A (MAO-A) and catechol-O-methyltransferase (COMT), eventually forming its main metabolite MHPG. This process is critically important to the health of the neuron, as free catecholamine metabolites are known to be highly reactive and thus toxic (Kang et al., 2020; Goldstein, 2021).

In addition to NE, several important neuropeptides are known to be co-expressed by LC neurons, including galanin (Holets et al., 1988; Le Maitre et al., 2013), neuropeptide Y (NPY) (Holets et al., 1988), brain-derived neurotrophic factor (BDNF) (Conner et al., 1997; Fawcett et al., 1998), and cocaine and amphetamine-regulated transcript (CART) (Koylu et al., 1999). While NE is released from LC neuron terminals in small clear synaptic vesicles, these neuropeptides rely on large dense-core vesicles, which are preferentially released during periods of heightened activity (Bartfai et al., 1988; Lang et al., 2015).

1.1.3 LOCUS COERULEUS FUNCTION

Firing Patterns of the LC

Firing of the LC can be categorized into tonic and phasic activity. These patterns of activation work together to modulate many of the basic cognitive and attentional functions associated with the LC (Howells et al., 2012). At baseline, the LC displays a tonic firing pattern of ~0.5-2 Hz. Low or no LC activity is observed during sleep, with activation increasing as a function of arousal (Aston-Jones and Bloom, 1981). The highest levels of tonic LC firing, ~3-10 Hz, are displayed during periods of stress (Carter et al., 2010). The LC also displays phasic 15-20 Hz “bursts” in response to novel and salient stimuli (Bouret and Sara, 2005). These unique firing patterns are critical in modulating behavior.

Sleep and Sleep Disorders

Due to its role in arousal, the LC-NE system has long been linked to sleep (Mitchell and Weinschenker, 2010). Optogenetic stimulation of the LC promotes wakefulness (Carter et al., 2010). On the other hand, transgenic mice lacking NE display increased sleepiness (Hunsley and Palmiter, 2004; Porter-Stransky et al., 2019). Interestingly, studies in mice have revealed that even acute stress exposure can result in poor sleep, and these sleep disturbances are largely due to inappropriate LC activity during non-REM sleep (Antila et al., 2022). Other studies have demonstrated that noradrenergic manipulation using pharmacological agents also impacts sleep and arousal (España et al., 2016). Taken together, this evidence closely links the LC-NE system with sleep behavior.

Neuropsychiatric Disorders

As these noradrenergic neurons are strongly activated by stress, the LC-NE system and its diffuse projections play a critical role in the stress response system (Valentino and Van Bockstaele, 2008). Optogenetic stimulation induces anxiety-like stress behaviors in mice (McCall et al., 2015; Tillage et al., 2021), as does the administration of drugs that increase NE transmission (Bremner et al., 1996b, a). Accordingly, the noradrenergic network is dysregulated in several neuropsychiatric disorders related to stress, including anxiety, depression, and posttraumatic stress disorder (Roy, 1988; Bissette et al., 2003; Naegeli et al., 2018). Conversely, low LC activity and decreased NE neurotransmission can attenuate stress-induced anxiety and depression. Several studies have demonstrated that chemogenetic and pharmacological suppression of LC activity has anxiolytic and antidepressant effects in mice (Grant and Weiss, 2001; McCall et al., 2015; Lustberg et al.,

2020b). Similarly, adrenergic drugs, such as the beta-blocker propranolol and the alpha-2 agonists clonidine and guanfacine, are used to treat anxiety and stress disorders in humans (Belkin and Schwartz, 2015; Steenen et al., 2016).

Neurodegenerative Disorders

Dysfunction of the LC-NE system has also been implicated in neurodegenerative diseases, most notably Alzheimer's disease (AD) and Parkinson's disease (PD). While AD and PD differ in their etiology and clinical presentation, early pathology in the LC and LC-associated behavioral changes are hallmarks of both disorders (Weinshenker, 2018).

1.2 ALZHEIMER'S DISEASE

1.2.1 EPIDEMIOLOGY AND ETIOLOGY

AD is the most common neurodegenerative disorder and the leading cause of dementia in older adults, affecting over 30 million individuals worldwide (Alzheimer's Association, 2022). Incidence rates are expected to climb as the population grows older, as the primary risk factor for AD is age. Individuals under the age of 65 possess a 3% risk of developing AD, a rate which escalates to 30% for individuals 85 and older (Alzheimer's Association, 2022). While a vast majority of cases are sporadic, several genetic mutations have been causally associated with early-onset AD, most notably in the *APP*, *PSEN1*, and *PSEN2* genes (Glennner and Wong, 1984; Scheuner et al., 1996). These point mutations are quite rare, occurring in just several families of patients. However, more common genetic risk factors have also been identified, such as a variant of the *ApoE* gene (Castellano et al., 2011; Cerf et al., 2011). Additionally, chronic illnesses such as cardiovascular disease and high blood pressure are known to confer AD risk (Stampfer, 2006).

A quickly emerging area of research also implicates inflammation in the development of AD and other related dementias (Tansey and Lee, 2015; Kinney et al., 2018).

1.2.2 CLINICAL PRESENTATION

Cognition

Memory impairment is the primary symptom of AD and is often the first visible change observed by patients and their families. Declarative memory, or the explicit recall of facts and events, is the most disrupted in AD patients (Budson and Price, 2005; Tippett et al., 2007; Gold and Budson, 2008). Declarative memory is further separated into semantic and episodic memories, the dysfunction of which can manifest in AD patients as difficulty remembering where keys were placed or what the state capital is, respectively. These memory impairments likely result from the temporal and frontal lobe atrophy that occurs in AD (Davies et al., 2004; Starr et al., 2005). Remarkably, patients are often able to compensate for this memory loss for some time, masking their symptoms from family and friends. However, as the disease progresses and these symptoms become more severe, clinical intervention is required.

Affect

In addition to memory impairment, a majority of AD patients also experience behavioral and psychological symptoms resulting from dysregulation in the cholinergic, noradrenergic, and serotonergic neuromodulatory systems (Lanari et al., 2006). These symptoms are heterogenous in their presentation, ranging from affective symptoms such as agitation, depression, anxiety, and apathy in the early or prodromal period, to psychosis in late-stage AD. While these behavioral symptoms are often considered secondary to the memory impairments experienced by AD patients,

they pose a great risk to quality of life and increase the likelihood of institutionalization (Cohen et al., 1993).

Noradrenergic dysfunction in AD contributes to several of these affective symptoms. Neurodegeneration of LC neurons, and subsequent loss of NE in its projection regions, is linked to neuropsychiatric symptoms including depression and aggression (Herrmann et al., 2004; Jacobs et al., 2021a). Furthermore, LC integrity is closely associated with the severity of cognitive and memory impairments seen in patients (Jacobs et al., 2021a; Cassidy et al., 2022). Evidence suggests that LC dysregulation may also play an important role in the sleep disturbances associated with AD (Van Egroo et al., 2022). Not only does AD pathology contribute to sleep disorders, but sleep deprivation also worsens pathology, leading to a feedback loop of exacerbating symptoms (Ju et al., 2014).

Clinical Diagnosis

A definitive diagnosis requires postmortem analysis of the brain through histology, a method that does not align with patient care. Thus, several measures have been developed to allow physicians to diagnose “probable AD” in patients (McKhann et al., 1984). The most common assessments are the Mini-Mental State Examination (MMSE), a bedside test that evaluates changes in an individual’s cognitive abilities, and The Diagnostic and Statistical Manual of Mental Disorders (Fourth Edition [DSM-IV]), which outlines criteria for diagnosis based on observed impairments in memory, language, calculation, orientation, and judgment (Alzheimer's Association, 2022). Importantly, an AD diagnosis also requires the exclusion of other neurodegenerative disorders that present with similar cognitive symptoms, such as Parkinson’s disease and frontotemporal dementia (Bekris et al., 2010b).

Non-cognitive assessments can complement these clinical evaluations, providing additional support for an AD diagnosis. Recent advancements in technology have led to the emergence of neuroimaging and biomarker measurements to evaluate AD onset and track disease progression. Computerized tomography (CT) scans and magnetic resonance imaging (MRI) were among the first techniques to be adapted for neuroimaging in dementia patients. Neurodegeneration in the hippocampus is perhaps the most robust structural change that occurs in the brains of AD patients, making this region an appealing target for neuroimaging (Braak and Braak, 1995; Small, 2006). However, atrophy of the hippocampus is also observed in other neurodegenerative disorders, limiting the application of this technique for the definitive diagnosis of AD (Small, 2006). Additionally, advancements in the characterization of AD neuropathology (described below) have led to the development of several promising biomarkers. Evaluating the circulating levels of these pathological targets in patients has allowed for an *in vivo* assessment of AD pathology and progression (Blennow and Zetterberg, 2018). Scientists and clinicians are advancing these diagnostic technologies at a remarkable rate, which bodes well for the early detection and effective treatment of AD in patients.

1.2.3 NEUROPATHOLOGY

The symptoms of AD follow neuron atrophy and death, a process that is instigated by aberrant protein accumulation. AD is unique from other proteinopathies and neurodegenerative diseases, in that the clinical diagnosis requires the presence of two separate protein aggregates: beta-amyloid and tau.

Beta-amyloid

Beta-amyloid is one of two proteins comprising the neuropathology of AD. This protein is produced through the proteolytic cleavage of the transmembrane amyloid precursor protein (APP), a process that is part of normal cell metabolism (Haass et al., 1992). In AD, beta-amyloid aggregates and forms harmful extracellular plaques in the brain. Postmortem histology studies suggest that this pathology begins in cortical regions, worsening and spreading toward deeper brain regions as AD progresses (Thal et al., 2002).

Combined with the identification of rare but causative mutations in genes related to beta-amyloid cleavage, these studies built the foundation for an emerging viewpoint in the field, centered around the instigating role of amyloid deposition in AD etiology. This theory, coined the “amyloid cascade hypothesis”, suggests that dysfunction in the production and clearance of beta-amyloid is not just a symptom of AD pathogenesis, but is the driving force behind other disease outcomes, such as oxidative stress, inflammation, and neurodegeneration (Hardy and Selkoe, 2002; Selkoe and Hardy, 2016).

Despite the appeal of this hypothesis as a promising target for disease intervention, the application of this theory has encountered potentially insurmountable challenges. Perhaps most importantly, the burden of beta-amyloid plaques in the brain is not strongly correlated with cognitive functioning in patients (Villemagne et al., 2011). By the same token, attempting to target beta-amyloid plaques in AD patients with a novel monoclonal antibody treatment has resulted in modest, if any, improvements in cognitive functioning (Karran and De Strooper, 2022; Kim et al., 2022). This lack of clinical support for the amyloid hypothesis necessitates a broadening of research efforts in the field of AD.

Tau

In addition to beta-amyloid deposits, aggregates of the microtubule-associated protein tau are found in the brains of AD patients, and the presence of both constitutes an official diagnosis. Hyperphosphorylation and subsequent misfolding of tau lead to the formation of neurofibrillary tangles (NFT). In contrast to extracellular beta-amyloid deposits, NFTs are intracellular, posing a risk to cellular functioning as they aggregate. While beta-amyloid is first displayed in cortical regions, tau pathology begins in the LC and continues to spread as AD progresses (Braak et al., 2011; Weinshenker, 2018). Importantly, NFT burden is well correlated with cognitive symptoms and disease severity (Tomlinson et al., 1970; Jacobs et al., 2021b).

The precise mechanisms of tau toxicity are not comprehensively understood, but current convention suggests tau pathology may result in any or all of the following: loss of function, gain of function, and/or mis-localization. As the primary function of tau is to stabilize the cytoskeleton in healthy neurons, it is perhaps unsurprising that tau accumulation negatively impacts neuronal architecture (Brunden et al., 2009; Noble et al., 2011). Hyperphosphorylated tau may also facilitate a breakdown of the stabilizing network by sequestering functional tau and other microtubule-associated proteins (Alonso et al., 1996). Additionally, significant tau burden may hinder axonal transport and interfere with cellular trafficking (Mandelkow et al., 2003; Cuchillo-Ibanez et al., 2008; Dixit et al., 2008). Aberrant forms of tau may also possess a harmful gain-of-function phenotype through their inherent toxicity (Berger et al., 2007), which results in increased levels of oxidative stress (Stamer et al., 2002). Finally, evidence for the mis-localization of tau is found in its presence in dendritic spines, which leads to synaptic dysfunction and negatively impacts cognition *in vivo* (Hoover et al., 2010; Miller et al., 2014). In fact, it has been proposed that this

disruption to synapses may be one of the earliest occurrences in the pathogenesis of AD and other tauopathies (Noble et al., 2011).

Although several rodent models have demonstrated that tau mutations can lead to neurological phenotypes (Allen et al., 2002; Yoshiyama et al., 2007), causal genetic variants have not been observed in human patients. Likely, beta-amyloid and tau pathologies synergize to alter neuronal functioning in AD (Spires-Jones and Hyman, 2014; Pickett et al., 2019). Thus, research efforts must consider both pathologies as key components in the development and progression of AD.

1.2.4 THE ROLE OF THE LOCUS COERULEUS

Biomarkers and Biological Implications

While the LC displays tau pathology early in AD, noradrenergic cell bodies are not lost until mid- to late-stage disease (Tomlinson et al., 1981; Braak et al., 2011). It has been proposed that during this time, the LC is characterized by dysfunction rather than degeneration, and noradrenergic hyperactivity predominates (Weinshenker, 2018). There is clinical evidence to support this theory, such as increased levels and turnover of NE in the cerebrospinal fluid of patients (Palmer et al., 1987; Hoogendijk et al., 1999; Henjum et al., 2022). However, as AD progresses, significant LC fiber and cell body deterioration are evident (Mather and Harley, 2016). This loss of LC integrity is correlated with cognitive decline in humans (Kelly et al., 2017; Weinshenker, 2018; Jacobs et al., 2021b). The inverse of this is seen in high LC neuron density conferring protection against regular, age-related cognitive decline (Wilson et al., 2013).

Behavioral Symptoms

As LC activity promotes arousal and stress responses, increased, rather than decreased, NE signaling is consistent with many of the prodromal symptoms of AD (Weinshenker, 2018). These symptoms vary between patients but may include anxiety, depression, agitation, and/or sleep disturbances. Additionally, neuropsychiatric symptoms in AD correlate with high LC signal contrast and respond to the blockade of adrenergic receptors (Peskind et al., 2005; Cassidy et al., 2022).

1.2.5 RODENT MODELS

Most preclinical models of AD have focused on beta-amyloid accumulation, and studies that do consider tau often neglect the critical role that the LC plays in this pathogenesis. However, there have been few reports of endogenous LC dysfunction or degeneration in transgenic animal models of AD (Liu et al., 2008; Guerin et al., 2009; Cohen et al., 2013; Liu et al., 2013), supporting the importance of investigating the noradrenergic system in preclinical models. Several rodent models specifically targeting the LC have been developed, and these research efforts have provided insight into the compensatory mechanisms and behavioral abnormalities that result from noradrenergic dysfunction and degeneration in AD.

TgF344-AD

TgF34 rats express the mutant forms of APP (APP^{sw}) and presenilin 1 (PS1E9), both of which cause AD in humans. These phenotypes displayed by these transgenic rats mimic several important characteristics of AD, including age-dependent amyloid pathology, cognitive impairment, and neurodegeneration in the forebrain (Cohen et al., 2013). These rats also display endogenous

hyperphosphorylated tau without the expression of a human tau transgene, which is somewhat surprising because mice carrying the identical transgene do not develop tau pathology (Games et al., 1995; Duff et al., 1996; Jankowsky et al., 2001). This tau pathology is first detectable in the LC at 6 months, resulting in progressive loss of NE in the hippocampus, as well as LC fiber loss in the medial entorhinal cortex and dentate gyrus (Rorabaugh et al., 2017). This pathology contributes to impaired cognition in the Morris water maze task, but remarkably, this behavior is rescued by chemogenetic activation of the LC (Rorabaugh et al., 2017). Further investigation into the behavioral phenotypes of the TgF344-AD rats has revealed age-dependent anxiety-like behavior in the transgenic animals as compared to controls (Kelberman et al., 2022).

DSP-4

Another method for investigating noradrenergic dysfunction in neurodegenerative disease relies on the LC-specific neurotoxin N-(2-chloroethyl)-N-ethyl-2-bromobenzylamine (DSP-4) which preferentially damages LC axons (Grzanna et al., 1989; Zhang et al., 1995). Administration of DSP-4 in rodents results in terminal loss and depletion of NE, mimicking neurodegenerative phenotypes (Theron et al., 1993; Wolfman et al., 1994; Harro et al., 1999; Szot et al., 2010). Furthermore, DSP-4 can exacerbate pathology, neuroinflammation, and cognitive and behavioral deficits in transgenic mouse models of AD (Heneka et al., 2006; Kalinin et al., 2007; Rey et al., 2012; Chalermphanupap et al., 2018).

While this neurotoxin has served as a useful model of LC dysfunction and neurodegeneration for decades, it is important to acknowledge its limitations: the effects of DSP-4 are often interpreted as noradrenergic ablation without taking potential compensatory mechanisms into account; most have focused on a single aspect of LC function; and many different

dosing regimens and species have been used, limiting our ability to integrate the findings into a comprehensive picture of how the LC-NE system responds to damage. Recently, our group published a comprehensive characterization of this model, assessing the consequences DSP-4 administration has on molecular, cellular, and behavioral responses of the LC-NE system in parallel (Iannitelli et al., 2022). Our results (detailed in Chapter 2) contribute to the understanding of LC dysfunction in neurodegeneration and may provide a foundation for early diagnostic and intervention strategies for these disorders.

1.3 PARKINSON'S DISEASE

1.3.1 EPIDEMIOLOGY AND ETIOLOGY

PD is the second most common neurodegenerative disorder, affecting more than 10 million people worldwide (Balestrino and Schapira, 2020). Similar to AD, the biggest risk factor for developing PD is age. There is a higher prevalence of PD in countries that report longer average lifespans, with a clinical diagnosis occurring in more than 4% of individuals over the age of 85 (de Rijk et al., 2000). In addition to age, several genetic and environmental factors are well appreciated to contribute to the development of this multifactorial disease.

Genetic Contributions

Although PD was once thought to be largely sporadic in nature, several genetic causes have now been identified (Bekris et al., 2010a). The first of these mutations, identified through genetic analysis of a family displaying an autosomal dominant pattern of inheritance, lies in the *SNCA* gene (Polymeropoulos et al., 1996; Polymeropoulos et al., 1997). Importantly, this gene encodes the alpha-synuclein (a-syn) protein, which can aggregate to form the hallmark Lewy body

pathology of PD. Indeed, duplications and mutations in the *SNCA* gene are associated not only with an increased risk of PD but also with higher plasma levels of a-syn in patients (Mata et al., 2010).

Another causative link has been found in the *LRRK2* gene (Funayama et al., 2002; Paisan-Ruiz et al., 2004), which encodes a tyrosine kinase-like protein (Mata et al., 2006). While the precise functions of *LRRK2* are not well understood, several of its domains are thought to be involved in protein-protein interactions (Zimprich et al., 2004) and exerting increased kinase activity (West et al., 2005; Gloeckner et al., 2006; Ito et al., 2007). Patients with *LRRK2* mutations present with later-onset forms of PD, and display many of the classical symptoms and pathologies (Nicholl et al., 2002; Wszolek et al., 2004; Zimprich et al., 2004).

While mutations in the *SNCA* and *LRRK2* genes are well appreciated as familial causes of PD, loss-of-function variants of both genes have also been identified as susceptibility factors (Bekris et al., 2010a). Additional genetic factors with an autosomal recessive inheritance have been identified, and are primarily associated with early-onset forms of PD. Mutations in the *PARK2* gene encoding the parkin protein causes early-onset PD (Matsumine et al., 1997; Lucking et al., 2000), as do missense and deletion mutations in *DJI* (Bonifati et al., 2003). *PINK1* mutations account for 1-3% of early-onset cases in patients of European ancestry (Valente et al., 2001; Bonifati et al., 2005), and up to 9% of cases in Japanese patients (Li et al., 2005). The earliest onset of PD is seen in families with *ATP13A2* mutations, with patients presenting with symptoms as early as 10 years of age (Najim al-Din et al., 1994; Myhre et al., 2008).

Environmental Factors

Epidemiological evidence suggests pesticide exposure and PD are strongly linked (Allen and Levy, 2013; Pezzoli and Cereda, 2013), with several studies reporting the existence of a dose-dependent relationship (Yan et al., 2018). The herbicides maneb and paraquat have been shown to double the risk of developing PD for individuals living in rural areas who are routinely exposed to these compounds (Costello et al., 2009). Additionally, occupational exposure to solvents such as trichloroethylene (TCE) has been shown to increase PD risk (Gash et al., 2008; Goldman et al., 2012). Perhaps unsurprisingly, exposure to these maneb, paraquat, and TCE have all been shown to induce parkinsonian phenotypes in rodents (Cicchetti et al., 2005; Liu et al., 2010). Despite the clear and present danger these compounds pose, many of these pesticides and toxins are still commercially available and widely used in agriculture and manufacturing.

Investigations into the interaction between toxin exposure and genetic factors have also been an active area of research in recent years (Ahmed et al., 2017), supporting the idea of PD as a multifactorial disease. Indeed, for most patients without a monolithic genetic risk, it is likely that several factors converge to instigate and perpetuate sporadic PD. This has led to the emergence of the “dual-hit” hypothesis, which suggests that PD pathology originates in the olfactory bulb and enteric nervous system. This theory proposes that an unknown neurotrophic pathogen of viral origin enters the brain by either: 1) traveling directly through the nasal passage to the temporal lobe, or 2) migrating from the gastrointestinal system to the medulla, pons, and midbrain via the motor neurons of the vagus nerve (Hawkes et al., 2007). While the dual-hit hypothesis has gained traction in recent years, widespread acceptance of this theory will require additional clinical and preclinical support.

Meta-analyses of PD patients and healthy controls have helped researchers identify several additional factors conferring risk for or protection from PD. Head injuries (Gao et al., 2015; Taylor et al., 2016) and chronic life stress (Metz, 2007) increase PD risk. On the other hand, moderate exercise (Xu et al., 2010; Fang et al., 2018), caffeine intake (Hernan et al., 2002), and even smoking (Hernan et al., 2002) serve as protective factors. These “lifestyle” contributions do not directly cause or prevent PD, but perform a delicate balancing act throughout our lives, working together or in opposition to culminate in each individual’s overall risk.

1.3.2 CLINICAL PRESENTATION

Motor Symptoms

The classical motor symptoms of PD include resting tremor, rigidity, akinesia or bradykinesia, and postural instability. Many of these symptoms also emerge through the course of normal aging, making it difficult for patients to detect a problem when it first begins. Furthermore, these symptoms are highly heterogenous between patients, varying in both severity and rate of progression (Fritsch et al., 2012). While one subtype of PD is characterized by dominating tremor, rigidity, and instability, other patients may experience only subtle motor impairments that remain relatively stable. In addition to these cardinal symptoms, more subtle motor abnormalities also manifest in some patients. These secondary symptoms may include ocular deficits, dystonia, shuffling, stooped posture, speech impairments such as hypophonia (speaking with a soft voice) or palilalia (repetition of words or phrases), and masked facial expression (Beitz, 2014). It is well appreciated that these motor symptoms arise as a direct result of SN degeneration, occurring once most of the DA neurons have been lost.

Non-Motor Symptoms

In addition to the classical motor symptoms, a host of non-motor features are also seen in up to 90% of PD patients (Lohle et al., 2009). Like motor impairments, non-motor symptoms also vary widely between patients. These symptoms may include autonomic dysfunction (Senard et al., 1997; Pursiainen et al., 2007), sensory disorders (Zhu et al., 2016), neurobehavioral issues (Trojano and Papagno, 2018), and/or sleep disturbances (Arnulf and Leu-Semenescu, 2009; Rothman and Mattson, 2012). Importantly, many of these non-motor symptoms precede the motor symptoms, emerging years or decades before a clinical diagnosis (Kalia and Lang, 2015). While motor symptoms are explained by the loss of SN-DA neurons, many of these non-motor symptoms are more closely associated with dysfunction and degeneration of the LC-NE system (Zweig et al., 1993; Remy et al., 2005; Del Tredici and Braak, 2013; Weinshenker, 2018).

Unlike the motor features of PD, there are currently no therapeutic treatments for the non-motor symptoms. In fact, leading PD pharmacotherapies may exacerbate non-motor symptoms such as psychosis, orthostatic hypotension, and sleep issues (Lim and Lang, 2010). Due to this lack of treatment options, patients often report the non-motor symptoms to be among the most troublesome aspects of their disease, necessitating further research and development efforts.

Therapeutic Treatments

There are currently no disease-modifying therapies to slow or stop the progression of PD. Thus, all current FDA-approved treatments are useful only in targeting the disease symptoms and not the pathology itself. Nonetheless, pharmacotherapies and other interventions have proven beneficial to patient autonomy and quality of life.

As PD is a heterogeneous disorder, therapeutic intervention varies widely and depends on several factors including the patient's age, disease stage, and symptoms (Ferreira et al., 2013). The first-line treatment for PD is DA replacement therapy with levodopa (L-DOPA). Response to this drug is even used to confirm a clinical diagnosis in some patients (Samii et al., 2004). For most patients, this kind of dopamine compensation therapy alleviates the motor symptoms of the disease and allows them to retain functional independence for longer. Similar pharmacological approaches used in conjunction with or instead of levodopa include dopamine agonists, MAO-B inhibitors, and anti-cholinergic drugs (Gazewood et al., 2013).

Unfortunately, DA replacement therapies are known to decline in effectiveness over time due to the relatively short half-life of levodopa, as well as fluctuations in receptor expression and DA reuptake by terminals (Beitz, 2014). Patients experiencing continued motor symptoms are often ideal candidates for deep brain stimulation (DBS), which was developed to treat the motor symptoms of PD when traditional pharmacotherapies fail. This surgical implant electrically stimulates the subthalamic nucleus (STN) or globus pallidum (GP), resulting in reduced tremor, stiffness, and bradykinesia for most patients. DBS does not destroy brain tissue and can be reversed or adjusted based on each patient's disease progression.

While the canonical motor symptoms of PD are usually well managed with DA replacement therapies and DBS, the non-motor symptoms remain difficult to treat. Physicians often must decide which individual symptoms to address based on each patient's individual needs. Medications such as clozapine and quetiapine can treat psychotic behaviors, but often have harmful side effects (Beitz, 2014). Additionally, anxiolytic and antidepressant drugs can be prescribed to treat the affective symptoms of PD. Similarly, drugs such as melatonin and

clonazepam can address the sleep disruptions patients experience (Aurora et al., 2010; McCarter et al., 2013).

Holistic treatment options are also available to patients and their families. These interventions range from providing educational resources and access to support groups, to physical therapy, exercise, and speech therapy to address specific issues. Ultimately, it is up to the patient and their physician to decide which treatment options will best target their most troublesome symptoms.

1.3.3 PATHOLOGY

PD is pathologically is defined as a loss of DA-SN neurons concurrent with the presence of hallmark Lewy bodies (Gazewood et al., 2013). Lewy bodies are large proteinaceous inclusions comprised primarily of misfolded α -syn (Sian-Hulsmann et al., 2015). The accumulation of Lewy bodies within vulnerable neurons contributes to the dysfunction and eventual cell death characteristic of PD. There is evidence to suggest that α -syn fibrils spread throughout the brain in a prion-like fashion (Brundin and Melki, 2017), providing a potential mechanism for how PD pathology advances through the brain.

Postmortem analyses support a staging hypothesis of PD pathology that begins in the brainstem and olfactory bulbs, progresses through the amygdala, basal forebrain, and SN, and finally reaches the forebrain and neocortex in late-stage disease (Braak and Braak, 2000). This entire process can take several decades, with symptoms only emerging once the pathological burden becomes severe enough to degenerate neurons.

1.3.4 ROLE OF THE LOCUS COERULEUS

The LC is among the first brain regions to display Lewy pathology in PD, even before the SN (Braak and Braak, 2000). Accordingly, dysfunction of the LC is closely associated with the prodromal, non-motor symptoms of PD, including sleep disturbances, mood disorders, and cognitive impairment (Zweig et al., 1993; Del Tredici and Braak, 2013). Studies have also implicated the LC in PD-related autonomic dysfunction (Oliveira et al., 2017).

REM sleep behavior disorder (RBD) is a condition characterized by movements during REM sleep when the body would ordinarily be paralyzed. Interestingly, this sleep disorder is up to 80% predictive of an eventual PD diagnosis (Iranzo et al., 2013; Schenck et al., 2013). RBD is linked with LC dysfunction, implicating LC pathology as a potential cause of sleep disturbances in PD, or at least a precipitating factor (Stiasny-Kolster et al., 2005).

Mood disorders such as anxiety and depression are other common non-motor features of PD. These psychiatric symptoms often emerge before a diagnosis, indicating that they are isolated symptoms, rather than emotional responses to the knowledge of their disease. Both anxiety and depression have been linked to LC dysfunction in the general population (Roy, 1988; Bissette et al., 2003), and also specifically in PD patients (Prediger et al., 2012). Issues with impulse control are also linked to LC dysfunction in PD (Kehagia et al., 2014).

As the noradrenergic system is known to play an important role in normal cognitive functioning, it is unsurprising that LC dysfunction in PD leads to cognitive impairments (Chan-Palay, 1991a; Hinson et al., 2017; Li et al., 2019). Mild cognitive impairment (MCI) can arise around the time of a clinical diagnosis (Kalia and Lang, 2015). For some patients, MCI does not progress at the same rate as other disease symptoms, and instead remains relatively stable (Vazey and Aston-Jones, 2012). For other patients, cognition deteriorates into severe dementia or psychosis in late-stage PD (Schneider et al., 2017).

Although pathology in the LC is present early in PD, these noradrenergic neurons are remarkably resilient to outright neurodegeneration. In fact, many of these LC-associated non-motor symptoms align more closely with noradrenergic hyperactivity rather than cell loss (Weinshenker, 2018). However, these neurons do eventually degenerate as PD progresses, likely as a result of pathological burden (perhaps in combination with other characteristics which confer specific vulnerability, discussed in detail below). Evidence for the loss of noradrenergic neurons *in vivo* is found in the diminished LC NM-MRI signal in PD patients (Wang et al., 2018; Kelberman et al., 2020), which compliments postmortem histological data showing LC deterioration in PD (Sulzer and Surmeier, 2013). A comprehensive understanding of noradrenergic dysfunction and degeneration in PD will provide insights into early disease pathology and progression and will aid in the development of novel therapeutic targets for early intervention.

1.3.5 ANIMAL MODELS

Several animal models of PD have recapitulated LC dysfunction in PD. Some of these approaches are transgenic, while others rely on the delivery of viral vectors or specific neurotoxins. Numerous studies have reported an important interaction between LC functioning and SN degeneration, suggesting that noradrenergic health plays a vital role in the progression of PD pathology throughout the brain.

Transgenic Model

Recently, a transgenic rodent model was developed to specifically study the effects of α -syn in the LC. This mouse expresses human wild-type α -syn under the noradrenergic-specific DBH promoter, which results in the development of oligomeric and conformation-specific α -syn

pathology in the LC (Butkovich et al., 2020). By 24-months, these transgenic mice display degeneration of LC terminals but not cell bodies, recapitulating the early noradrenergic dysfunction in PD patients (Weinshenker, 2018; Butkovich et al., 2020). In line with their neuropathology, the transgenic mice also display age-dependent behaviors reminiscent of noradrenergic hyperactivity and the non-motor symptoms of PD, which were rescued by adrenergic receptor antagonists (Butkovich et al., 2020). Additionally, transgenic models that lack noradrenergic specificity also show alterations in LC functioning. The targeted deletion of genes known to be implicated in familial PD, such as *PARK2*, results in loss of LC-NE neurons, loss of NE in projection regions, and a reduced startle response, without any noticeable impairments of the DA system (Von Coelln et al., 2004). Rats with global *Pink1* knockout also display LC dysfunction in the form of increased anxiety-like behavior and decreased TH and adrenoceptor immunoreactivity (Hoffmeister et al., 2021).

Viral Vector Models

Another method for investigating noradrenergic dysfunction and degeneration in PD is through the intracranial delivery of viral vectors to manipulate the LC in rodent models. One such model overexpressed α -syn in the LC, which led to an increase in the pacemaker activity of these neurons coupled with an altered afterhyperpolarization amplitude (Matschke et al., 2022). Additionally, overexpression of human mutant α -syn in the LC results in progressive neurodegeneration and subsequent neuroinflammation (Henrich et al., 2018). These targeted strategies allow for the specific manipulation and investigation of LC dysfunction in PD.

Neurotoxin Models

A subfield of research regarding noradrenergic dysfunction in PD is focused on the administration of compounds to selectively target the LC. One such model is the LC-specific neurotoxin DSP-4, discussed previously as a tool for studying noradrenergic dysfunction in AD. At low doses, DSP-4 harms LC terminals while leaving cell bodies intact. Thus, this model is useful for assessing the early, prodromal aspects of noradrenergic dysfunction in PD.

To model mid- and late-stage, methods degenerating cell bodies are employed. One such neurotoxin is the catecholamine analog 6-Hydroxydopamine (6-OHDA). 6-OHDA is taken up by catecholamine neurons via DA or NE transporters (DAT and NET, respectively). Once inside neurons, 6-OHDA is enzymatically degraded by MAO-A, forming cytotoxic metabolites that induce neuronal damage and death (Simola et al., 2007). When injected into the LC, 6-OHDA results in loss of cell bodies coupled with near-total fiber loss in projection regions after several weeks (Szot et al., 2012), allowing for the assessment of LC neurons neurodegeneration.

Emerging research has also implicated inflammation in the neurodegenerative process. A recent study modeled systemic inflammation and subsequent neurodegeneration in a rodent model by administering lipopolysaccharide (LPS). Researchers found that just one administration of LPS is sufficient to induce neurodegeneration in the LC before other brain regions, such as the SN (Song et al., 2019a). Furthermore, facilitating noradrenergic dysfunction with DSP-4 prior to LPS administration exacerbated neurodegeneration in the SN (Song et al., 2019b), implicating the important role the LC plays in maintaining SN health.

This work aligns with decades of prior research regarding the relationship between LC and SN neurons. Studies have shown that loss of LC neurons exacerbates SN deterioration in MPTP and 6-OHDA models of PD (Mavridis et al., 1991; Srinivasan and Schmidt, 2003). However, there

is also evidence to suggest that loss of LC-NE alone is sufficient to induce similar SN damage and resulting motor impairments (Rommelfanger et al., 2007). It has even been proposed that NE itself has neuroprotective properties, promoting neuronal health (Troadek et al., 2001).

Taken together, these findings demonstrate the importance of LC integrity both in normal brain functioning and also in disease. Losing these noradrenergic neurons can have a cascading effect on the catecholamine system, exacerbating or potentially even causing PD symptoms.

1.4 LOCUS COERULEUS SUSCEPTIBILITY

Noradrenergic neurons are affected early and severely in neurodegenerative diseases, most notably AD and PD. Some reports suggest that degeneration of the LC is even more severe than in other notoriously impacted brain regions, such as the nucleus basalis in AD and the SN in PD (Zarow et al., 2003). Several factors may contribute to the selective vulnerability of these noradrenergic neurons, such as their long and diffuse axonal projections, intrinsic pacemaker activity and high metabolic demand, a unique neuroimmune profile, and the presence of intracellular pigment deposits (Oertel et al., 2019).

Axonal Projections

The LC possesses long and highly branched axonal projections distributed widely throughout the brain (Foote et al., 1983). These axons are unmyelinated, and thus more vulnerable to damage. Axon terminals are lost first when neurons degenerate (Doppler et al., 2021), making this feature an appealing candidate for LC vulnerability. However, the cell bodies of these neurons are remarkably resilient, even after fiber loss (Weinshenker, 2018). This suggests that axonal damage is just one component of LC dysfunction in neurodegenerative disease.

Metabolic Demand

Noradrenergic neurons also display intrinsic pacemaker activity, firing regularly under basal conditions. This tonic pattern of activation is critical for LC functioning but is metabolically demanding. This can compound cellular strain, leading to high levels of oxidant stress (Wang and Michaelis, 2010) and mitochondrial dysfunction (Sanchez-Padilla et al., 2014). Importantly, these factors are well-appreciated for the harmful role they play in neurodegeneration (Nicholls, 2008; Surmeier et al., 2010). High activity levels also lead to increased production of catecholamine metabolites, some of which can be toxic to neurons. For example, elevated production of the NE metabolite DOPEGAL has been linked to increased levels of asparagine endopeptidase and subsequent tau aggregation in LC neurons *in vitro* and *in vivo* (Kang et al., 2020; Kang et al., 2022).

Neuroimmune Contributions

An additional factor contributing to the selective vulnerability of LC neurons is their unique neuroimmune profile. Catecholamine neurons of the SN and LC express high levels of major histocompatibility complex (MHC) class I molecules (Cebrian et al., 2014). MHCs are found on the surface of all nucleated cells and aid in antigen presentation. While MHC-II proteins display exogenous antigens, MCH-I aids in the expression of peptide fragments from within the cell. Importantly, MHC-I presents antigens to cytotoxic T cells, triggering cell death. Indeed, cytotoxic CD8⁺ cells have been observed near catecholamine neurons, suggesting the expression of MHC-I may render these neurons vulnerable to T-cell-mediated degeneration (Cebrian et al., 2014).

It may seem maladaptive for LC neurons to trigger their death, especially by presenting antigens from within the cell. However, the last unique feature of catecholamine neurons may account for this behavior: the presence of intracellular granules called neuromelanin.

1.5 NEUROMELANIN

1.5.1 CHARACTERISTICS OF NEUROMELANIN

Neuromelanin (NM) is comprised of pheomelanin and eumelanin pigments which reside in the cytoplasm of SN-DA and LC-NE neurons. The pigmentation of catecholamine neurons in the SN and the LC is so robust that it can be appreciated by gross anatomical inspection, a finding first described centuries ago which led to the unique nomenclature of these regions, translating from Latin to “black substance” and “blue spot”, respectively. While trace amounts of NM have also been found in non-catecholaminergic brain regions, including the cerebellum and cortex, its presence is less robust and structurally different from SN-NM and LC-NM (Zecca et al., 2008b). Interestingly, this neuronal pigmentation is found only in the brains of humans and non-human primates, and to a lesser extent in a few other long-living animals, such as horses. Although NM is a defining characteristic of SN and LC catecholamine neurons, very little is known about the formation and function of these granules *in vivo*.

1.5.2 NEUROMELANIN FORMATION

Biosynthesis

NM is a byproduct of the catecholamine synthesis pathway (**Fig. 1.1**). Leading thought in the field suggests that NM formation evolved from a necessity to sequester intracellular DA and NE in

highly active neurons (Sulzer et al., 2000). Normally, DA is packaged in synaptic vesicles by VMAT2, where it is then converted into NE by the enzyme DBH. Due to the intrinsic pacemaker activity of the LC, noradrenergic neurons are prone to sustained periods of activation, leading to rapid DA and NE production and turnover. When these neurotransmitters cannot be packaged into synaptic vesicles by VMAT2 as quickly as they are formed, increased cytosolic catecholamine levels become available for metabolism by MAO-A. Importantly, metabolites of DA (e.g. DOPAL) and NE (e.g. DOPEGAL) are highly reactive and toxic to neurons (Kang et al., 2018; Kang et al., 2020). Taken together, the characteristic persistent firing rate and subsequent catecholamine load of LC neurons support the hypothesis of NM production as a mechanism of sequestering these compounds to protect the neurons from damage. Additionally, this theory also provides a compelling rationale for the specificity of this pigmentation for catecholamine neurons.

Despite this theoretical understanding of the cellular requirements driving NM production, the precise biosynthetic pathway is still unclear. Current convention suggests that the process is initiated when DA is oxidized by iron, which is found in high concentrations in catecholamine neurons (Monzani et al., 2019). This reaction forms DA-quinones, which are subsequently converted into pheomelanin and eumelanin through similar but distinct pathways (Bush et al., 2006; Krainc et al., 2022). In the periphery, these pigments lead to the coloration of hair and skin through enzymatic processes, while neuronal pigmentation is believed to be auto-oxidative (Bush et al., 2006). Once synthesized, pheomelanin makes up the core component of NM, while eumelanin comprises the surrounding “shell” (Greco, 2014). These pigments bind additional compounds in the cell to form complete NM granules that can measure up to 30 nm in size.

Additional Components

Most notably, NM chelates metal cations including iron, zinc, copper, manganese, chromium, cobalt, mercury, lead, and cadmium (Liu et al. 2004; Zecca and Swartz, 1993; Zecca et al. 2002). Additionally, catecholamine metabolites such as DOPAC and DOPEG have been identified as elements of SN-NM and LC-NM, respectively (Wakamatsu et al., 2015). These pigmented granules can also bind various psychotropic drugs such as chlorpromazine, haloperidol, and imipramine (Salazar et al., 1978), pesticides, and other toxic compounds (D'Amato et al., 1986). Large lipid droplets are another substantial element of these granules. The major lipid component of NM was found to be the polyisoprenoid dolichol, accounting for 14% of the mass of the isolated pigment (Fedorow et al., 2005).

Following the formation of these granular masses, a proposed fusion with autophagosomes encloses all of the components with a double-layered membrane (Zucca et al., 2018). While this barrier successfully separates toxic NM compounds from the intracellular space, it also makes the breakdown of these pigment granules all but impossible once they are formed. Thus, the concentration of pigmentation in the LC increases over time, beginning at around 3 years of age (Zecca et al., 2004a), potentially conferring a lifetime of protection from harmful compounds. This timeline of accumulation may also explain why NM is not evident in rodent neurons, as rats and mice only live ~2 years.

1.5.3 NEUROTOXICITY OF NEUROMELANIN

Despite the compelling case for NM as an adaptive mechanism protecting neurons from the necessity of producing catecholamines for neuromodulation, certain conditions may lead to an

inadvertent toxic role of these granules. While NM is largely protective across the lifetime, its presence may become detrimental when cells die prematurely in neurodegenerative disease. This issue is two-fold, as LC cells are not only losing a vital neuroprotective mechanism, but as these toxic granules are released, they have detrimental effects on intracellular functioning, and may also affect surrounding neurons once they reach the extracellular space.

Intracellular Toxicity

Because there is no way to safely dispose of NM once the granules are formed, LC neurons eventually become full of pigmentation, which could interfere with other cellular machinery and function. This issue may be exacerbated when the neurons are under stress. Dysregulation of calcium, which can result from excitotoxicity, leads to the production of reactive oxygen species (ROS). These harmful free radicals can degrade NM in the cytosol, leading to the release the iron and other toxic metals that were previously bound in the granules (Zecca et al., 2004a). NM has also been reported to inhibit the 26S proteasome, which could disrupt normal protein degradation, leading to an accumulation of abnormal proteins such as a-syn (Shamoto-Nagai et al., 2004).

Extracellular Toxicity

Additionally, it can be reasoned that as LC neurons die, the NM granules and their previously-bound toxins are released and have the potential to damage neighboring cells. NM released from the neurons is subsequently phagocytosed by microglia, leading to microglia activation and production of reactive oxygen species (ROS) and nitrogen species (RNS), in addition to other proinflammatory factors (Zhang et al., 2011).

1.5.4 PREVIOUS WORK IN THE FIELD

Postmortem Human Tissue

Postmortem human samples have provided insight into the link between NM-expressing neuronal populations and PD. We now know that total NM concentration decreases as SN and LC neurons degenerate in PD (Zecca et al., 2002), and that heavily-pigmented SN neurons show far greater degeneration than other nearby dopaminergic regions, such as nuclei A8 and A10 (Hirsch et al., 1988), and nearly all PD patients exhibit substantial loss of NM-containing neurons in the LC (Sulzer and Surmeier, 2013). Furthermore, it has been reported that the most heavily pigmented neurons are lost first in neurodegeneration (Mann and Yates, 1983). The deterioration of pigmented neurons and subsequent decrease in NM abundance within these brain structures has provided an interesting target for clinical diagnosis through NM-MRI (Kelberman et al., 2020). However, to ensure that NM-MRI is an appropriate readout of neuronal integrity, the presence of NM must be definitively linked to living neurons. As a majority of prior research in the field has been limited to postmortem samples and imaging, we do not know definitely whether or for how long NM can persist in the extracellular space after its host cells are gone. If true, using NM-MRI as a proxy for SN and LC neurons might be misleading, as it would not be a direct readout of neuronal integrity and thus a more complex clinical measurement of disease progression.

In vitro and in vivo Studies

The absence of NM from the brains of typical model organisms, such as mice and rats, has limited research regarding the role that NM plays in PD onset and progression, but some prior work has

studied NM in cultured catecholaminergic cells. For example, NM has been induced in rat SN and PC12 cell cultures through the administration of L-DOPA, which is converted to DA by aromatic acid decarboxylase in the cytosol (Sulzer et al., 2000). Other studies have introduced synthetic NM to these cells to investigate the extracellular impact and uptake of this pigment by dopaminergic neurons (Ostergren et al., 2005). These *in vitro* studies are complimented by work demonstrating that isolated NM granules can be injected into the rat SN, leading to neuroinflammation and neurodegeneration (Zecca et al., 2008a). While cell culture does allow for experimental manipulation, this technique is not well-suited for answering systematic questions regarding the protective vs the toxic role of NM over time *in vivo*.

Enzymatically-Driven Pigmentation in Rodents

Recently, a viral vector-mediated approach for expressing pigmentation in the SN of rodents was developed through the introduction of human tyrosinase (hTyr), the enzyme responsible for peripheral melanin production (Carballo-Carbajal et al., 2019). Although endogenous NM production is thought to be an auto-oxidative process, the introduction of hTyr effectively drives pigmentation in catecholamine neurons of both rats and mice. Importantly, this pigmentation was found to mimic the structure of endogenous NM from humans, as it contains both pheomelanin and eumelanin, lipid droplets, and a membrane encasement visible by electron microscopy (Carballo-Carbajal et al., 2019). Perhaps the most striking finding of this study is that prolonged pigment expression in rodent SN neurons eventually leads to neuron degeneration and subsequent motor impairments (Carballo-Carbajal et al., 2019). Furthermore, this work found that enhancing lysosomal proteostasis was sufficient to reduce intracellular NM levels, mitigating neurodegeneration in hTyr-expressing mice (Carballo-Carbajal et al., 2019).

1.6 DISSERTATION AIMS

The overall goal of this dissertation is to understand noradrenergic dysfunction in the context of neurodegenerative diseases. To accomplish this, I employed two rodent models of LC dysfunction that recapitulate critical aspects of neurodegeneration. We assessed both models on a molecular, cellular, and behavioral level to fully characterize the impact these insults have on LC survival and functioning. The first model – the LC-specific neurotoxin DSP-4 – induces noradrenergic fiber damage, which precedes outright cell loss and mimics prodromal aspects of both AD and PD. DSP-4 administration has a profound effect on the transcriptional profile and cellular functioning of the LC, which leads to behavioral changes reminiscent of the prodromal aspects of neurodegenerative diseases. The other model we utilized is a novel adaptation of hTyr expression, which leads to pigmentation in the LC of mice. We found that hTyr-induced pigmentation led to significant LC neurodegeneration, coupled molecular, cellular, and behavioral changes and a dramatic neuroinflammatory response.

Collectively, these data provide critical insights into LC dysfunction in neurodegenerative disease. Ultimately, we believe that these features contribute to the early, prodromal symptoms patients experience in both AD and PD.

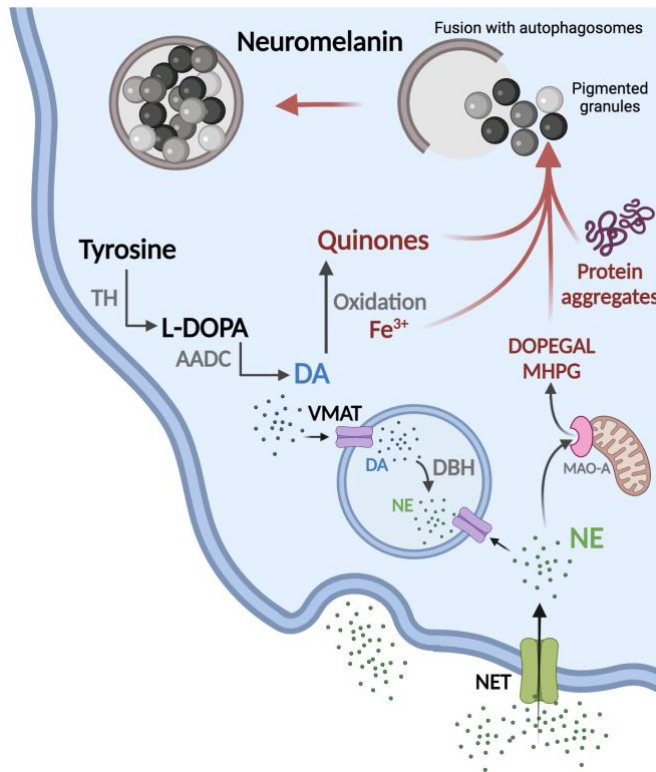


Fig. 1.1. Formation of endogenous neuromelanin granules. Neuromelanin (NM) is formed as a byproduct of the catecholamine synthesis pathway. This pathway begins with the conversion of tyrosine to L-DOPA, which is then synthesized further to form the neurotransmitter dopamine (DA). This process releases iron (Fe^{3+}) and dopaquinones, which are toxic to neurons. The auto-oxidation of dopaquinones is believed to contribute directly to the formation of pigment in catecholamine neurons. The conversion of DA to norepinephrine (NE) precedes neurotransmission in noradrenergic neurons. Extracellular NE is taken up by the NE transporter (NET), and converted into metabolites MHPG and DOPEGAL by the mitochondrial enzyme monoamine oxidase A (MAO-A). These heavy metal, pigment, and metabolite byproducts bind with protein aggregates in the cell, and are collected for degradation by autophagosomes. If the components cannot be degraded fully, the phagosome encloses the components into a membrane, forming the final NM granule.

**CHAPTER 2: THE NEUROTOXIN DSP-4 DYSREGULATES THE LOCUS
COERULEUS-NOREPINEPHRINE SYSTEM AND RECAPITULATES MOLECULAR
AND BEHAVIORAL ASPECTS OF PRODROMAL NEURODEGENERATIVE
DISEASE**

Portions of this chapter were used verbatim, with permission, from the following publication:

Iannitelli AF, Kelberman MA, Lustberg DJ, Korukonda A, McCann KE, Mulvey B, Segal A, Liles C, Sloan SA, Dougherty JD, Weinshenker D. The Neurotoxin DSP-4 Dysregulates the Locus Coeruleus-Norepinephrine System and Recapitulates Molecular and Behavioral Aspects of Prodromal Neurodegenerative Disease. bioRxiv 2022.09.27.509797; doi:

<https://doi.org/10.1101/2022.09.27.509797>

2.1 ABSTRACT

The noradrenergic locus coeruleus (LC) is among the earliest sites of tau and alpha-synuclein pathology in Alzheimer's disease (AD) and Parkinson's disease (PD), respectively. The onset of these pathologies coincides with loss of noradrenergic fibers in LC target regions and the emergence of prodromal symptoms including sleep disturbances and anxiety. Paradoxically, these prodromal symptoms are indicative of a noradrenergic hyperactivity phenotype, rather than the predicted loss of norepinephrine (NE) transmission following LC damage, suggesting the engagement of complex compensatory mechanisms. Because current therapeutic efforts are targeting early disease, interest in the LC has grown, and it is critical to identify the links between pathology and dysfunction. We employed the LC-specific neurotoxin DSP-4, which preferentially damages LC axons, to model early changes in the LC-NE system pertinent to AD and PD in male and female mice. DSP-4 (2 doses of 50 mg/kg, 1 week apart) induced LC axon degeneration, triggered neuroinflammation and oxidative stress, and reduced tissue NE levels. There was no LC cell death or changes to LC firing, but transcriptomics revealed reduced expression of genes that define noradrenergic identity and other changes relevant to neurodegenerative disease. Despite the dramatic loss of LC fibers, NE turnover and signaling were elevated in terminal regions and were associated with anxiogenic phenotypes in multiple behavioral tests. These results represent a comprehensive analysis of how the LC-NE system responds to axon/terminal damage reminiscent of early AD and PD at the molecular, cellular, systems, and behavioral levels, and provides potential mechanisms underlying prodromal neuropsychiatric symptoms.

2.2 INTRODUCTION

Alzheimer's disease (AD) and Parkinson's disease (PD) are the most common cognitive and motor neurodegenerative disorders, respectively. Both conditions are characterized by abnormal protein accumulation in neurons leading to cellular dysfunction and death. While these disorders differ in their etiology and clinical presentation, early pathology in the brainstem locus coeruleus (LC) is a hallmark of both AD and PD (Weinshenker, 2018). The LC is the primary source of central norepinephrine (NE) and projects to nearly every other brain region (Foote et al., 1983; Berridge and Foote, 1996; Aston-Jones et al., 1999; Poe et al., 2020). LC neurons are the first to accumulate hyperphosphorylated tau in AD (Braak et al., 2011) and they develop aberrant alpha-synuclein before dopamine neurons of the substantia nigra (SN) in PD (Del Tredici et al., 2002). Although the LC eventually undergoes catastrophic degeneration in both diseases, these neurons can harbor pathology for years before cell death, displaying axon and dendrite loss in initial stages of AD and PD (Halliday et al., 1990; Busch et al., 1997; Theofilas et al., 2017; Doppler et al., 2021; Gilvesy et al., 2022). Combined, these data suggest that LC-NE deficiency contributes to AD and PD. Indeed, experimental lesions of the LC exacerbate neurodegeneration and cognitive deficits in rodent models, and loss of LC integrity correlates with cognitive decline in humans (Weinshenker, 2018; Jacobs et al., 2021b). However, this simplistic view is inconsistent with other data indicating excessive noradrenergic transmission, particularly early in disease. For example, increased levels and turnover of NE have been reported in the cerebrospinal fluid of AD patients (Palmer et al., 1987; Hoogendijk et al., 1999; Henjum et al., 2022). Moreover, because LC activity promotes arousal and stress responses, increased, rather than decreased, NE signaling is consistent with many of the prodromal symptoms of AD and PD including anxiety, depression, agitation, and sleep disturbances (Weinshenker, 2018).

Animal models of AD (Goodman et al., 2021; Kelly et al., 2021; Kelberman et al., 2022) and PD (Butkovich, 2019; Matschke et al., 2022) that recapitulate early LC pathology but lack outright noradrenergic cell death exhibit LC-NE hyperactivity, anxiety-like behavior, and hyperarousal, which can be alleviated with the administration of adrenergic antagonists. Likewise, neuropsychiatric symptoms in AD correlate with high LC signal contrast and respond to blockade of adrenergic receptors (Peskind et al., 2005; Cassidy et al., 2022). We have proposed a more complex model in which damaged LC neurons engage compensatory mechanisms that lead to noradrenergic hyperactivity and contribute to prodromal behavioral phenotypes, followed later by frank LC cell death and NE deficiency that accelerates cognitive decline (Weinshenker, 2018). However, causal relationships between LC damage, cellular and molecular compensatory mechanisms, and prodromal symptoms remain to be investigated and established.

To better understand noradrenergic dysfunction in early neurodegenerative disease and its links to compensatory mechanisms and behavioral abnormalities, we employed the LC-specific neurotoxin N-(2-chloroethyl)-N-ethyl-2-bromobenzylamine (DSP-4), which preferentially damages noradrenergic axons compared to cell bodies (Grzanna et al., 1989; Fritschy and Grzanna, 1991; Zhang et al., 1995). While many groups have reported depletion of NE following DSP-4 administration (Grzanna et al., 1989; Theron et al., 1993; Wolfman et al., 1994; Harro et al., 1999; Szot et al., 2010), it is important to acknowledge some limitations: (1) the effects of DSP-4 are often interpreted as noradrenergic ablation without taking potential compensatory mechanisms into account; (2) most have focused on only a single (or a few) aspect of LC function (e.g. NE abundance *or* axon integrity *or* LC-sensitive behaviors); and (3) many different dosing regimens and species have been used, limiting our ability to integrate the findings into a comprehensive picture of how the LC-NE system responds to damage. Here, we assessed the consequences of

DSP-4 administration on molecular, cellular, and behavioral responses of the LC-NE system in parallel. Our results are critical for understanding LC dysfunction in AD and PD, and may provide a foundation for early diagnostic and intervention strategies for these disorders.

2.3 MATERIALS AND METHODS

Animals. Adult male and female C57BL/6 mice were used for all behavioral, electrophysiological, and immunohistochemical experiments. No statistically significant differences between male and female mice were found in any of the data analyzed. For translating ribosome affinity purification (TRAP) RNA-sequencing experiments, we used male and female transgenic *Slc6a2-eGFP/Rpl10a* mice (B6;FVB-Tg(*Slc6a2-eGFP/Rpl10a*)JD1538Htz/J, The Jackson Laboratory, #031151), which incorporate an EGFP/Rpl10a ribosomal fusion protein into a bacterial artificial chromosome under the *Slc6a2* (NE transporter; NET) promoter to allow for the isolation of polysomes and translating mRNAs specifically from noradrenergic neurons. *Slc6a2-eGFP/Rpl10a* mice were purchased and maintained as hemizygotes on a C57BL/6 background. Mice were group housed with sex- and age-matched conspecifics (maximum of 5 animals per cage) until one week prior to behavioral testing, and then individually housed for the subsequent week of experimentation until sacrifice. Animals were maintained on a 12:12 light:dark cycle (lights on at 0700), and food and water were available *ad libitum*, unless otherwise specified. All experiments were conducted at Emory University in accordance with the National Institutes of Health *Guideline for the Care and Use of Laboratory Animals* and approved by the Emory Institutional Animal Care and Use Committee. Mice were treated with DSP-4 (50 mg/kg, i.p.; Sigma-Aldrich, St. Louis, MO) or vehicle (0.9% NaCl) on days 1 and 7. Electrophysiology and TRAP were conducted on day 14, and behavioral testing commenced on day 14 and ended on day 18.

HPLC. Mice were anesthetized with isoflurane and euthanized by rapid decapitation. The pons, prefrontal cortex, and hippocampus were rapidly dissected on ice and flash-frozen in isopentane (2-Methylbutane) on dry ice. The samples were weighed and stored at -80°C until processing for HPLC. As previously described (Lustberg et al., 2022), tissue was thawed on ice and sonicated in 0.1 N perchloric acid ($10\ \mu\text{l}/\text{mg}$ tissue) for 12 s with 0.5 s pulses. Sonicated samples were centrifuged (16,100 rcf) for 30 min at 4°C , and the supernatant was then centrifuged through $0.45\ \mu\text{m}$ filters at 4000 rcf for 10 min at 4°C . For HPLC, an ESA 5600A CoulArray detection system, equipped with an ESA Model 584 pump and an ESA 542 refrigerated autosampler was used. Separations were performed using an MD-150 \times 3.2 mm C18, $3\ \mu\text{m}$ column (Thermo Scientific) at 30°C . The mobile phase consisted of 8% acetonitrile, 75 mM NaH_2PO_4 , 1.7 mM 1-octanesulfonic acid sodium and 0.025% trimethylamine at pH 2.9. A $20\ \mu\text{L}$ of sample was injected. The samples were eluted isocratically at 0.4 mL/min and detected using a 6210 electrochemical cell (ESA, Bedford, MA) equipped with 5020 guard cell. Guard cell potential was set at 475 mV, while analytical cell potentials were -175 , 100, 350 and 425 mV. The analytes were identified by the matching criteria of retention time measures to known standards (Sigma Chemical Co., St. Louis MO). Compounds were quantified by comparing peak areas to those of standards on the dominant sensor.

Immunohistochemistry. Mice were euthanized with an overdose of sodium pentobarbital (Fatal Plus, 150 mg/kg, i.p.; Med-Vet International, Mettawa, IL) and were transcardially perfused with cold 4% PFA in 0.01 M PBS. After extraction, brains were post-fixed overnight in 4% PFA at 4°C and then transferred to a 30% sucrose/PBS solution for 72 h at 4°C . Brains were embedded in OCT

medium (Tissue-Tek) and sectioned by cryostat into 40- μ m-thick coronal sections at the level of the LC, ACC, and hippocampus. Sections were blocked in 5% normal goat serum (NGS) in 0.01 M PBS/0.1% Triton-X permeabilization buffer and then incubated for 24 h at 4°C in NGS blocking buffer with primary antibodies listed in Table 2. Following washes in 0.01 M PBS, sections were incubated for 2 h in blocking buffer, including secondary antibodies described in Table 2. After washing, sections were mounted onto Superfrost Plus slides and coverslipped with Fluoromount-G plus DAPI (Southern Biotech, Birmingham, AL).

Quantification. For the catecholaminergic markers NE transporter (NET) and tyrosine hydroxylase (TH), the activity marker activity-regulated cytoskeletal gene (Arc), and the oxidative stress marker 3-nitrotyrosine (3-NT), immunofluorescent micrographs were acquired on a Leica DM6000B epifluorescent upright microscope at 20x magnification with uniform exposure parameters for each stain and region imaged. Following convention, these images are oriented with the dorsal direction up and the ventral direction down. For glial markers, immunofluorescent images were acquired as z-stack images (10 z-stacks; pitch: 0.1 μ m) at 20x magnification and compressed on a Keyence BZ-X700 microscope system. One representative atlas-matched section was selected from each animal and a standard region of interest was drawn for each image to delineate the LC, ACC, and hippocampus. For catecholaminergic and glial markers, image processing and analysis were conducted using the FIJI/ImageJ software. The analysis pipeline included standardized background subtraction, intensity thresholding (Otsu method), and pixel intensity measurements within defined ROIs of the same size (Lustberg et al., 2020b). Furthermore, *GFAP*⁺, *IBAI*⁺ and *SI00B*⁺ cells were quantified based on size and shape for glia (50-1000 μ m², circularity 0.15-1.0) (Rorabaugh et al., 2017).

Silver staining. Assessment of degenerating neuronal processes and cell bodies was performed using the NeuroSilver Staining Kit II (FD NeuroTechnologies, Inc., Columbia, MD) on fixed, free-floating sections from saline and DSP-4 treated mice (n = 3-4 per treatment group). Brain sections (40 μ m) were collected by cryostat (Leica) at the level of the LC, ACC, and DG. Staining was performed according to the manufacturer's instructions (Kolisnyk et al., 2017; Kumbhare et al., 2017), after which tissue sections were allowed to air-dry overnight on SuperFrost Plus slides (Fisher Scientific, Hampton, NH). Once dry, sections were cleared for 2 min in CitriSolv xylene substitute (Fisher Scientific) and coverslipped with DPX non-aqueous mounting media (MilliporeSigma, Burlington, MA). Brightfield micrographs of silver-stained sections were acquired at 20x magnification using a Keyence BZ-X700 at 20x magnification with uniform light exposure parameters throughout image acquisition.

Cell counts. Coronal tissue sections were processed as described above (*Immunohistochemistry*) and images were acquired as described for glial markers (*Quantification*). Using TH as a guide for anatomical LC borders and DAPI as a marker for individual nuclei, sections were atlas-matched and quantified using HALO imaging software (Indica Labs, v3.3.2541.420, FISH/IF v2.1.4). Nine sections were analyzed for each animal (n=3/group), covering most of the LC. The total area analyzed did not differ between the saline and DSP-4 treated groups. Within HALO, nuclei were defined using DAPI, and TH-positive and Nissl-positive nuclei cells were counted and summed across all nine sections for each animal. Comparisons were made between the number of Nissl+ and TH+ nuclei cells in the saline and DSP-4 treated groups.

Translating Ribosome Affinity Purification (TRAP). To obtain adequate quantities of RNA for sequencing, samples from two 6-8 month-old, same-sex and treatment *Slc6a2-eGFP/Rpl10a* mice were pooled to form a biological replicate by dissecting out the hindbrain posterior to the pontine/hypothalamic junction (cerebellum was discarded). Six biological replicates were collected per treatment group. Each replicate was homogenized and TRAP was performed as described (Mulvey et al., 2018), resulting in LC-enriched “TRAP” samples and whole-hindbrain “input” samples. RNA was extracted using Zymo RNA Clean & Concentrator-5 kit, and subsequently sent for library preparation and Illumina sequencing by NovoGene to a minimum depth of 20 million fragments per sample. Forward and reverse sequencing files from each replicate were aligned to the mouse genome (mm10) using STAR alignment, and counts were obtained using FeatureCounts in R Bioconductor. Two samples from saline-treated mice were removed from analysis because the TRAP protocol failed to enrich *Slc6a2* above a 10-fold change, a quality control threshold observed in all other saline-treated samples. All subsequent analysis utilized R Bioconductor packages. Sequencing data will be available on NCBI GEO at the time of publication.

To further characterize the gene expression changes, we performed a Weighted Gene Coexpression Network Analysis (WGCNA), as described previously (Zhang and Horvath, 2005; Langfelder et al., 2008). All samples that survived quality control parameters were used to create the co-expression network. Default parameters were primarily used throughout the analysis. The soft threshold power was set at 10, the point in which the scale free topology fit index was above 0.80. Minimum module size was set to 30 genes and modules with >95% similarity were merged, resulting in 159 modules which were then correlated with treatment. We also compared gene expression patterns in our dataset with a repository of gene sets using Gene Set Enrichment

Analysis (GSEA 4.2.3) (Mootha et al., 2003; Subramanian et al., 2005). Gene set permutation was used, as recommended by GSEA documentation for experiments with fewer than 7 samples per group. Other parameters were set to default settings using 1000 gene set permutations and signal to noise ranking metric. We downloaded KEGG Pathways from the Molecular Signatures Database, which has 186 gene sets. After filtering for the recommended minimum (15) and maximum (500) gene set size, the remaining 145 gene sets were compared to the expression data from our dataset to calculate the GSEA enrichment score and to compute significant enrichment.

Electrophysiology. Mice were anesthetized with chloral hydrate (400 mg/kg i.p.) and placed into a stereotaxic frame. Fur was plucked and an incision was made to expose the skull. Burr holes were drilled over the approximate location of the LC (from bregma, AP: 5.2-5.4, ML: 0.7-1.1).

Recordings were made using 16 channel silicone probes (A1x16-Poly2-5mm-50s-177-CM16LP, NeuroNexus) that were connected to a μ -series Cereplex headstage (Blackrock Microsystems). Digitized signals were acquired with a 16 channel Cereplex Direct system (Blackrock Microsystems) using a 250 Hz-5 kHz bandpass filter and a sampling rate of 10 kS/s. Probes were lowered to the approximate location of the LC (DV: -2.7-4.3).

LC units were identified based on standard criteria, including stereotaxic coordinates, biphasic response to foot-pinch/shock, and reduction/cessation of spontaneous activity following injection of the alpha-2 adrenergic receptor agonist clonidine (0.1 mg/kg, i.p.). For each set of recordings, a 5-min baseline period was collected, and was immediately followed by 10 applications of a contralateral foot-pinch separated by 10 s. Afterwards, 0.5 ms 1 mA footshocks were applied to the contralateral hindpaw separated by 10 s for 5.5 min to assess response to

salient/aversive stimuli. LC spikes were manually sorted offline using Blackrock Offline Spike Sorting software.

Electrophysiology data was analyzed using Neuroexplorer. To ensure that recordings were from single units, neurons that had greater than 2% of recorded spikes within a predefined 3 ms refractory period were eliminated from the analysis. Basal firing rate and interspike intervals were calculated based on spikes collected within the 5-min baseline period. Spontaneous burst characteristics (number of bursts, percentage of spikes in a burst, burst duration, spikes per burst, interspike interval within a burst, burst rate, and interburst interval) during baseline was characterized using previously defined criteria derived from dopamine neurons (Grace and Bunney, 1983; Iro et al., 2021). Finally, response to footshock was analyzed in three time windows: immediate (0-60 ms), intermediate (60-100 ms), and long (200-400 ms), as previously described (Hirata and Aston-Jones, 1994).

Behavioral assays. Behavioral assays were performed in the following order, from least to most stressful.

Novelty-induced and circadian locomotion: Individual mice were placed in a plexiglass arena (10" × 18" × 10") surrounded by a 4 × 8 photobeam grid that records infrared beam breaks (Photobeam Activity System, San Diego Instruments, San Diego, CA; Lustberg et al. 2020). Two consecutive beam breaks were recorded as an ambulation, and total ambulatory activity was recorded. Mice were left undisturbed in the arena for 23 h. The first hour of the test reflected novelty responses while the remainder of the testing period showed changes in locomotion as a function of circadian cycle. The number and location of ambulations were recorded in 5-min intervals.

Novelty suppressed feeding: Chow was removed from individual home cages 24 h prior to behavioral testing. Mice were moved to the test room under red light and allowed to habituate for 2 h prior to the start of the test. Individual mice were placed in a novel arena (10" × 18" × 10") with a single pellet of standard mouse chow located in the center. The latency to feed, operationally defined as grasping and biting the food pellet, was recorded using a stopwatch. Mice that did not feed within the 15-min period were assigned a latency score of 900s (Tillage et al., 2020b).

Marble burying: Individual mice were placed in a novel arena (10" × 18" × 10") containing 20 marbles of uniform size and color arranged in a 4 × 5 grid, each on top of 2" of lightly pressed cobb bedding. Mice were left undisturbed for 30 min in a brightly lit room. At the end of testing, the mice were placed back into home cages, and the number of marbles buried were counted by two independent observers. If different scores were reported between observers, the average was taken. A marble was considered buried if at least two-thirds of its height was submerged in the bedding. For each test cage, digital photographs were obtained at uniform angles and distances.

Statistical analyses. Immunohistochemical quantification, stereological cell counting, and HPLC measurements of catechol concentrations were compared between saline and DSP-4 treated groups using a student's t-test in GraphPad Prism. Similarly, behavioral assessment relied on t-test comparison between groups for total ambulations in the novelty-induced locomotion assay, latency to feed in the novelty-suppressed feeding task, and number of marbles buried in the marble-burying test. R Bioconductor packages were utilized for statistical analyses of RNA sequencing data, including differential gene expression (DGE). For electrophysiological recordings, students t-tests or Mann-Whitney tests were used for comparison of basal firing rates and spontaneous bursting properties between treatment conditions for normally and non-normally distributed data,

respectively. A two-way repeated measures ANOVA, with response period as the within subject factor and treatment as the between subject factor, was used to analyze LC response to footshock.

2.4 RESULTS

DSP-4 reduces NE content and dysregulates NE turnover in the pons and LC projection fields. To confirm the efficacy and specificity of DSP-4 (two injections of 50 mg/kg, administered one week apart), we assessed tissue levels of catecholamines and their metabolites (**Fig. 2.1**). DSP-4 dramatically reduced NE in the pons, where LC cell bodies reside ($t_{(6)} = 17.73$, $p < 0.0001$), as well as in the hippocampus ($t_{(14)} = 3.27$, $p = 0.0056$) and prefrontal cortex (PFC; $t_{(14)} = 3.347$, $p = 0.0048$), two of the primary projection regions of the LC. (**Fig. 2.1a**). DSP-4 treatment similarly decreased levels of MHPG, the primary catecholamine metabolite, in the pons ($t_{(6)} = 5.205$, $p = 0.002$), PFC ($t_{(14)} = 2.978$, $p = 0.01$) and hippocampus ($t_{(14)} = 3.140$, $p = 0.0072$) (**Fig. 2.1b**). Despite the reduction of NE, the rate of turnover (MHPG:NE ratio) was significantly increased in the pons ($t_{(6)} = 2.685$, $p = 0.0363$) and PFC ($t_{(14)} = 2.499$, $p = 0.0255$) compared to saline controls, with a similar trend seen in the hippocampus ($t_{(14)} = 2.049$, $p = 0.0596$), suggesting adaptations in the LC-NE system (**Fig. 2.1c**). By contrast, levels of other amine neuromodulators, including dopamine, serotonin, and their respective metabolites, were unchanged in all regions assessed (data not shown), confirming the specificity of this neurotoxin for noradrenergic neurons.

DSP-4 triggers loss of LC fibers and neuroinflammation but not frank cell body degeneration. Consistent with the depletion of tissue NE and canonical findings of LC fiber damage following DSP-4 treatment (Grzanna et al., 1989; Theron et al., 1993; Wolfman et al., 1994; Harro et al., 1999), NET immunoreactivity, a marker of LC axon, dendrite, and terminal

integrity, was reduced in the LC ($t_{(6)} = 6.003$, $p = 0.001$), ACC ($t_{(6)} = 13.76$, $p < 0.0001$), and dentate gyrus (DG) region of the hippocampus ($t_{(6)} = 10.23$, $p < 0.0001$) in DSP-4 treated mice compared to controls (**Fig. 2.2a**). In contrast, we found that NET immunoreactivity in the bed nucleus of the stria terminalis (BNST), which receives noradrenergic innervation from brainstem A1 and A2 instead of the LC (Aston-Jones et al., 1999), was intact in DSP-4 treated mice (data not shown), indicating sparing of the ventral noradrenergic bundle and highlighting the specificity of DSP-4 induced damage to LC neurons.

Next, we used silver staining to verify that the loss of NET immunoreactivity reflected LC fiber degeneration and not just a downregulation of NET. Robust silver staining in the LC, ACC, and DG indicated the presence of degenerative processes in the LC and projection regions (**Fig. 2.2b**). Finally, we assessed levels of oxidative stress marker 3-NT in the LC and projection regions and found that it was significantly decreased in the LC following DSP-4 administration ($t_{(6)} = 4.746$, $p = 0.0032$), but was increased in the ACC ($t_{(6)} = 4.397$, $p = 0.0046$) and DG ($t_{(6)} = 6.558$, $p = 0.0006$) (**Fig. 2.2c**).

To determine whether damage resulting from DSP-4 impacted cell body integrity, we performed a count of LC neurons. We quantified DAPI+ cells also positive for TH or NeuroTrace Nissl in the LC. We found no differences in the number of LC neurons in DSP-4 treated mice compared to controls in either analysis (**Fig. 2.2d**).

Because neuroinflammation often occurs in response to damage and is a key component of AD and PD pathology (Tansey et al., 2022; Thakur et al., 2022), and glial activation can be impeded by NE signaling (Liu et al. 2019), we assessed immunoreactivity of the astrocyte marker GFAP and the microglial marker Iba-1 in the LC and target regions. We observed robust astrocytic ($t_{(4)} = 6.969$, $p = 0.0022$) and microglial ($t_{(4)} = 3.642$, $p = 0.0219$) responses in and around the LC

of DSP-4 treated mice compared to controls (**Fig. 2.3**). GFAP immunoreactivity was elevated in the DG ($t_{(6)} = 2.227$, $p = 0.0675$), but decreased in the ACC ($t_{(6)} = 2.480$, $p = 0.0478$), and Iba-1 was increased in both the ACC ($t_{(6)} = 3.351$, $p = 0.0154$) and the DG ($t_{(6)} = 4.118$, $p = 0.0062$). These results reveal that damage to the LC and its projections recapitulates key aspects of neuroinflammation and neurodegeneration in AD and PD.

DSP-4 treatment leads to molecular but not cellular dysfunction in LC cell bodies. The marked reduction in NET immunoreactivity (**Fig. 2.2a**) in the LC without the loss of cell bodies (**Fig. 2.2d**) suggested that dysregulation of noradrenergic markers may be occurring first on a molecular level. To assess this, we expanded our analysis to the entire LC transcriptome as a complement to our immunohistochemical staining of specific protein markers. We employed a *Slc2a6-Rpl110-eGFP* line for specific targeting of noradrenergic neurons through TRAP (Mulvey et al., 2018). We observed robust enrichment of LC genes in our TRAP samples compared to input (**Fig. 2.4a and data not shown**), indicating the successful implementation of this technique. Next, we assessed differentially expressed genes (DEGs) between replicate samples from the DSP-4 treatment and saline control groups. Most notably, we saw a marked downregulation of multiple noradrenergic function and specification genes, including *Slc6a2* (NET; $\logFC = -1.5032$, $p < 0.0001$), *Th* ($\logFC = -0.7850$, $p = 0.0006$), *Dbh* ($\logFC = -1.2642$, $p < 0.0001$), and *Phox2a* ($\logFC = -1.0292$, $p = 0.0054$), and the LC-enriched neuropeptide *Gal* ($\logFC = -1.1636$, $p < 0.0001$), which is reflective of a loss of LC neuron “identity” following DSP-4 administration (**Fig. 2.4b and 2.4c**). While only three DEGs reached stringent statistical significance with a false discovery rate (FDR) < 0.1 (*Slc6a2*, *Dbh*, *Gal*), this experiment yielded a substantial list of biologically informative transcripts (**Figure 2.4c**). Further analysis of gene expression networks using

WGCNA revealed four modules that were significantly correlated with treatment, one of which included *Dbh*, *Gal*, and *Slc6a2* (**Fig 2.4d**). This module contained 72 genes, including several that are implicated in neurodegenerative diseases, suggesting that critical LC genes (*Dbh*, *Gal*, *Slc6a2*) are clustering with neurodegeneration genes in their expression patterns after treatment with DSP-4. Finally, using GSEA to compare the gene expression patterns in our dataset with repositories of known gene sets, we identified 17 KEGG pathways that were significantly enriched in our dataset, including oxidative phosphorylation (enrichment score (ES)=-0.53, $p<0.001$), lysosome (ES=0.41, $p=0.006$), pathways in cancer (ES=0.35, $p=0.004$), melanogenesis (ES=0.44, $p=0.023$), and cytokine-cytokine receptor interaction (ES=0.45, $p=0.025$). Notably, the pathways for PD (ES=-0.49, $p<0.001$), AD (ES=-0.37, $p=0.037$), and Huntington's disease (ES=-0.45, $p=0.002$) were significantly negatively correlated with treatment, and further investigation revealed that many of the core enrichment genes in these pathways are similarly downregulated in clinical neurodegenerative diseases and after DSP-4 treatment in mice (**Fig. 2.4e**).

Next, we investigated whether these molecular changes in LC neurons after DSP-4 treatment were accompanied by cellular changes. LC neurons are tonically active, show elevated tonic activity during stress, and exhibit “bursting” activity in response to salient and novel stimuli (Valentino, 1988; Vankov et al., 1995; Curtis et al., 1997; McCall et al., 2015). To determine whether DSP-4-induced molecular dysregulation impacted cellular activity, *in vivo* electrophysiology under anesthesia was conducted to measure baseline and footshock-evoked firing of LC neurons. There were no differences in the baseline firing rate of LC neurons between treatments (Mann-Whitney $U = 1072$, $p = 0.2312$) (**Fig. 2.5**), with interspike intervals and spontaneous bursting properties also remaining unchanged (data not shown). There was a main effect of time period in response to footshock such that firing rate of LC neurons decreased in each

successive response phase ($F_{2,176} = 17.09$, $p < 0.0001$). However, there was no main effect of treatment ($F_{1,188} = 2.408$, $p = 0.1243$) or a treatment x time period interaction ($F_{2,176} = 0.2655$, $p = 0.7671$) on response to footshock. We conclude that the molecular changes occurring following DSP-4 do not significantly affect LC neuron firing under these conditions.

DSP-4 treatment results in a novelty-induced anxiety phenotype, implying compensatory hyperactivity of LC-NE transmission. AD and PD share several prodromal behavioral symptoms related to affect and arousal, processes known to be regulated by the LC-NE system and sensitive to LC integrity (Weinshenker, 2018). Moreover, cognitive impairment is a diagnostic criterion for AD and is common in later stage PD; thus, we assessed the consequences of DSP-4 on LC/NE-sensitive behaviors that reflect prodromal and cognitive abnormalities in AD and PD. We found that lesioned mice were profoundly more reactive in novelty-induced stress paradigms, which are commonly used to model anxiety and are bidirectionally modulated by NE (Lustberg et al., 2020a). DSP-4 treated mice took significantly longer to consume food in the novelty-suppressed feeding test ($t_{(20)} = 3.158$, $p = 0.0048$), buried more marbles ($t_{(14)} = 4.290$, $p = 0.0007$), and ambulated less during the first hour in a novel cage ($t_{(14)} = 2.999$, $p = 0.0096$) compared to saline-treated controls (**Fig. 2.6**). Importantly, DSP-4 treatment had no effect on latency to eat in the home cage or in total ambulations across a 23-h period, suggesting increased anxiety-like behavior rather than a decrease in hunger or general locomotion. Arousal (as assessed by latency to fall asleep following gentle handling) and associative memory (as measured by freezing in a footshock-associated context) did not differ between treatment groups (data not shown).

Elevated novelty-induced anxiety-like behavior is consistent with increased noradrenergic activity (Lustberg et al., 2020b), which was surprising given the profound loss of noradrenergic

fibers and NE in LC terminal fields. Our HPLC data indicated increased NE turnover from surviving terminals, and adrenergic receptor supersensitivity has been reported in DSP-4 lesioned animals (Wolfman et al., 1994; Szot et al., 2010). To investigate whether these adaptations are sufficient to boost downstream signaling mechanisms that underlie behavioral reactivity, immunostaining for Arc was quantified following cage change, a mild stressor that is resistant to habituation and sensitive to NE transmission (Vankov et al., 1995; McCall et al., 2015; Takeuchi et al., 2016; Grella et al., 2019; Lustberg et al., 2020a; Lustberg et al., 2020b; Prokopiou et al., 2022). Arc is an immediate early gene and neural activity marker that is induced following adrenergic receptor stimulation, and acts as a readout of postsynaptic LC-NE transmission (McIntyre et al., 2005; McReynolds et al., 2014). After cage change, a marked increase in Arc immunoreactivity was observed in the LC ($t_{(6)} = 4.258$, $p = 0.0053$), ACC ($t_{(6)} = 2.755$, $p = 0.0331$), and DG ($t_{(6)} = 5.099$, $p = 0.0022$) of DSP-4 treated mice compared to saline-treated mice (**Fig. 2.6**).

2.5 DISCUSSION

The present study characterized the impact of DSP-4 on the molecular, cellular, and behavioral levels in mice to comprehensively assess the consequences of damage to LC neurons reminiscent of early stages of AD and PD. The depletion of NE and its metabolite MHPG, as well as the elevated MHPG:NE ratio, by DSP-4 are consistent with decades of previous research and indicate reduced total NE but increased NE turnover (Jonsson et al., 1981; Logue et al., 1985; Harro et al., 1999; Szot et al., 2010). Immunohistochemical staining following DSP-4 treatment revealed a dramatic reduction of NET in the PFC and hippocampus, which could mean a loss of noradrenergic terminals and/or a downregulation of NET expression. We found evidence for both. NET mRNA

in LC neurons was significantly reduced by DSP-4, and silver staining provided evidence for degeneration of axons/terminals in projection regions. Diminished NET immunoreactivity was also observed in the LC of DSP-4 treated mice. To determine whether this was due to a loss of neurons, we counted LC cell bodies (i.e. positive for DAPI and TH or Nissl) and found no effect of DSP-4, which is typical for similar dosing regimens (Lyons et al., 1989; Matsukawa et al., 2003; Szot et al., 2010). Taken together, the loss of NE and NET in terminal regions and pons is indicative of LC axon, terminal, and dendrite degeneration, with the increased MHPG:NE ratio potentially signifying compensatory elevation of NE release from surviving fibers (Jacobs, 2019; van Hooren et al., 2021; Gilvesy et al., 2022).

DSP-4 provoked oxidative stress in the forebrain and a robust neuroimmune response in the both the LC and its projection regions. 3-NT immunoreactivity was elevated in the ACC and DG following DSP-4 administration, providing a link to AD, as LC lesions also increased 3-NT in the cortex of mice that overexpress mutant amyloid precursor protein (Heneka et al., 2006). Paradoxically, the abundance of 3-NT in control LCs was high at baseline relative to the other brain regions and decreased by DSP-4. Catecholamine synthesis and metabolism generate oxidative stress, which could contribute to the high baseline levels of 3-NT in the LC, while the DSP-4 induced reduction may reflect the loss of catecholamine synthetic capacity. Interestingly, lipopolysaccharide-induced 3-NT oxidative stress in the dopaminergic SN that is reminiscent of PD pathology was also attenuated by DSP-4 lesions of the LC (Iravani et al., 2014).

Microglial activation as measured by Iba-1 immunoreactivity was elevated in the LC, ACC, and DG of DSP-4 treated mice compared to controls. GFAP+ reactive astrocytes were increased in the LC and DG of DSP-4 tissue but were suppressed in the ACC. The interplay between neuroinflammation and neurodegeneration is bidirectional, and our experiments with

NeuroSilver staining revealed active degenerative processes in both fibers and cell bodies of the LC and its projection regions. Because our analysis was restricted to a single timepoint when both processes were evident, we cannot know whether one triggered the other. Neuroinflammation and neurodegeneration are key components of AD and PD, and both are exacerbated by ablation of LC-NE in animal models of these disorders and can be ameliorated by pro-noradrenergic therapies in clinical populations (Rommelfanger et al., 2004; Heneka et al., 2006; Rommelfanger et al., 2007; Heneka et al., 2010; Chalermphanupap et al., 2018; Song et al., 2019a; Song et al., 2019b; Levey et al., 2022). Given that we observed no difference in LC cell body number, our DSP-4 dosing regimen appears to represent an early phase of neurodegeneration, which is characterized by initial loss of noradrenergic innervation prior to frank LC degeneration in AD and PD (Fritschy et al., 1990; Doppler et al., 2021; Gilvesy et al., 2022).

In AD and PD, LC neurons become dysfunctional early on but persist for many years prior to cell death. However, almost nothing is known about the molecular changes that drive LC dysfunction prior to outright degeneration. Due to its small size and neuron number, selective mRNA profiling of the murine LC transcriptome has historically been challenging. To address this gap, we assessed the effects of DSP-4 treatment on the LC transcriptome using TRAP and obtained enrichment of known LC genes such as *Th*, *Slc6a2* (NET), *Dbh*, *Phox2a*, and *Gal* in saline-treated mice, as previously reported (Mulvey et al., 2018). Remarkably, we found that these same genes were down-regulated in DSP-4 treated mice, suggesting a deterioration of noradrenergic identity prior to LC neuron loss. Differential gene expression and down-regulation of NET, *Dbh*, and *Th* are consistent with *in vitro* studies exposing SH-SY5Y cells to DSP-4 (Wang et al., 2014), but opposite of what has been reported in clinical AD, where *Th* and NET are increased in surviving LC neurons (Szot et al., 2006). We speculate that compensatory increases in noradrenergic markers

are triggered by the cell loss ubiquitous in late-stage AD, which did not occur in our DSP-4 treated mice. In addition to the disruption in noradrenergic gene expression, we also found several genes associated with neurodegeneration and neurotoxicity that were differentially expressed between our treatment groups. Some of these genes, highlighted in Fig. 4 and detailed in Table 3, were also found in the co-expression network module with *Gal*, *Dbh*, and *Slc6a2*. These results were complemented by significant enrichment in gene sets associated with AD, PD, and Huntington's disease, and contribute to the rich array of potential genetic targets for better understanding the early stages of neurodegeneration.

Prodromal AD and PD are characterized by neuropsychiatric abnormalities including anxiety, agitation, depression, and sleep disturbances that appear long before the primary diagnostic symptoms of these diseases (cognitive and motor impairment, respectively). Using a battery of tests to probe these behavioral domains, we found that DSP-4-treated mice displayed increased anxiety-like behavior specific to novelty: they took significantly longer to consume a food pellet, buried more marbles, and had reduced locomotor activity in novel environments. These results are consistent with previous reports that surgical or neurotoxin ablation of the LC in rats induces similar anxiety-like phenotypes that reflect responses to novelty stress (Martin-Iverson et al., 1982; Harro et al., 1995).

LC-NE transmission is triggered by novelty stress, and activation of this system promotes, while inactivation suppresses, novelty-induced anxiety (McCall et al., 2015; Lustberg et al., 2020a; Lustberg et al., 2020b). Thus, the emergence of anxiety-like behavior in DSP-4-treated mice and AD/PD patients where a dramatic *loss* of noradrenergic fibers and NE is evident creates a paradox and suggests that compensatory mechanisms are engaged in response to LC damage that lead to hyperactive NE transmission. We can imagine three potential neuroanatomical/neurobiological

substrates where this compensation may occur: LC cell bodies (e.g. increased neuron firing), LC terminals (e.g. increased NE release), and/or postsynaptic compartments (e.g. receptor/signaling molecules super-sensitivity).

Using *in vivo* electrophysiology, we detected no differences in the baseline (firing rate, interspike interval, spontaneous bursting properties) or footshock-evoked firing rate of LC neurons. This is consistent with previous reports in DSP-4 treated rats (Szot et al., 2010) but distinct from partial 6-OHDA LC lesions, which increased LC activity in mice (Szot et al., 2016). One important difference is that the 6-OHDA-treated mice had LC neuron loss (~30%), while LC cell bodies remained intact in our study. These results suggest that LC neurons are capable of compensatory increases in firing, but that cell body degeneration is required to trigger this response. By contrast, we did find evidence for increased NE release. Although we did not measure this directly, metabolite to parent neurotransmitter ratio is a validated proxy for turnover. We detected elevated MHPG:NE ratio in the LC and terminal regions, which has been previously reported in DSP-4 treated rodents (Hallman and Jonsson, 1984) and consistent with human AD cerebrospinal fluid data (Francis et al., 1985; Hoogendijk et al., 1999; Raskind et al., 1999; Jacobs et al., 2021b). Indeed, high CSF MHPG levels are associated with neuropsychiatric abnormalities in AD (Jacobs et al., 2021a).

Finally, postsynaptic compensatory mechanisms resulting from the loss of LC fibers may be at play. There are many reports of increased adrenergic receptor density following DSP-4 administration (Johnson et al., 1987; Harro et al., 1999), but the consequences on downstream receptor signaling have not been carefully investigated. We performed immunostaining for the immediate early gene *Arc*, which is a marker for neuronal activity and induced by activation of adrenergic receptors (Essali and Sanders, 2016). Following cage-change stress, *Arc*

immunoreactivity was dramatically elevated in DSP-4 treated tissue compared to controls in the LC and its output regions in the forebrain. We conclude that compensatory changes in NE release from surviving LC terminals and/or postsynaptic adrenergic receptor signaling could contribute the anxiogenic effects of DSP-4, while increases in LC firing do not. These results have important implications for AD and PD, where early LC pathology, damage to noradrenergic fibers, and neuropsychiatric symptoms precede frank LC loss in prodromal disease. In addition, these experiments support the notion that DSP-4 dysregulates, rather than simply ablates, the noradrenergic system, and should act as a caution to researchers employing this neurotoxin as they interpret their results.

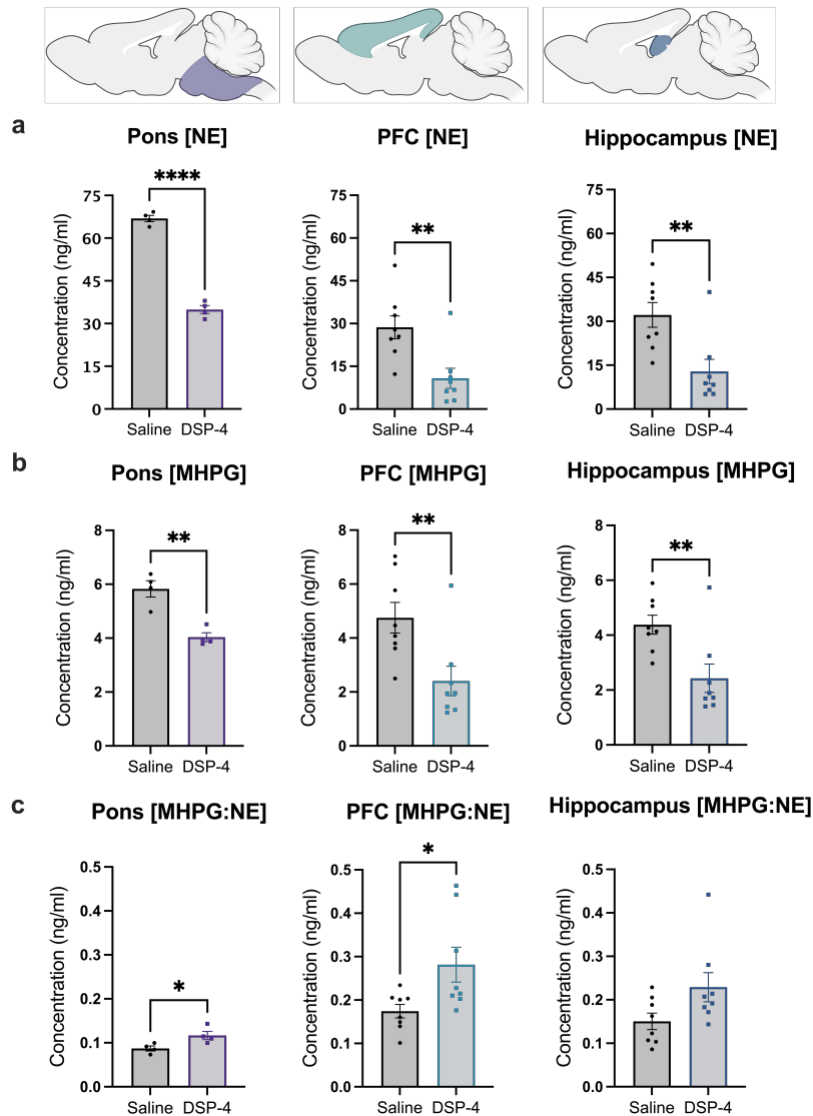


Fig. 2.1. DSP-4 decreases tissue NE and metabolite levels and increases turnover. Mice received saline or DSP-4 (2 x 50 mg/kg, i.p.), and tissue monoamine and metabolite levels were measured 1 week later by HPLC in the pons, prefrontal cortex (PFC), and hippocampus (color shaded images at top represent the approximate regions dissected for analysis). DSP-4 significantly decreased NE (**a**) and its primary metabolite MHPG (**b**) in all 3 brain regions. (**c**) NE turnover, defined as the MHPG:NE ratio, was increased in the pons and PFC by DSP-4, with a similar trend in the hippocampus. Data shown as mean \pm SEM. N=8 per group. * $p<0.05$, ** $p<0.01$, **** $p<0.0001$.

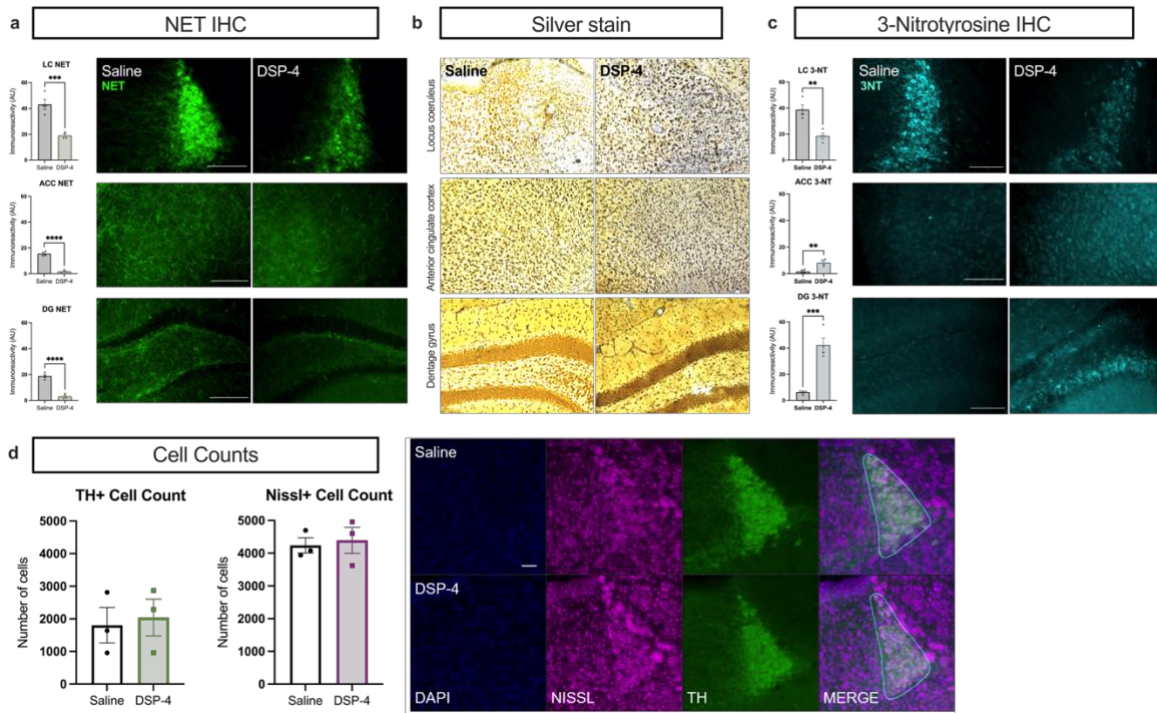


Fig. 2.2. DSP-4 induces degeneration of noradrenergic terminals and oxidative stress but leaves LC cell bodies intact. Mice received saline or DSP-4 (2 x 50 mg/kg, i.p.) and assessed for locus coeruleus (LC) neuron damage 1 week later. **(a)** DSP-4 results in substantial loss of axon terminals as measured by norepinephrine transporter (NET) immunoreactivity in the dentate gyrus (DG) and anterior cingulate cortex (ACC), with a similar decrease in NET also present in the LC itself. **(b)** Representative images of silver stained brain tissue indicates neurodegenerative processes in the LC, ACC, and DG following DSP-4. **(c)** The oxidative stress marker 3-nitrotyrosine (3-NT) was increased in the ACC and DG but decreased in the LC by DSP-4. **(d)** Despite NE fiber damage and the evidence of neurodegenerative and oxidative processes following DSP-4, LC cell body number was unaffected as measured by TH and NeuroTrace Nissl immunoreactivity. Images acquired at 20X. Data shown as mean \pm SEM. N=3-4 per group. ** $p < 0.01$, *** $p < 0.001$, **** $p < 0.0001$.

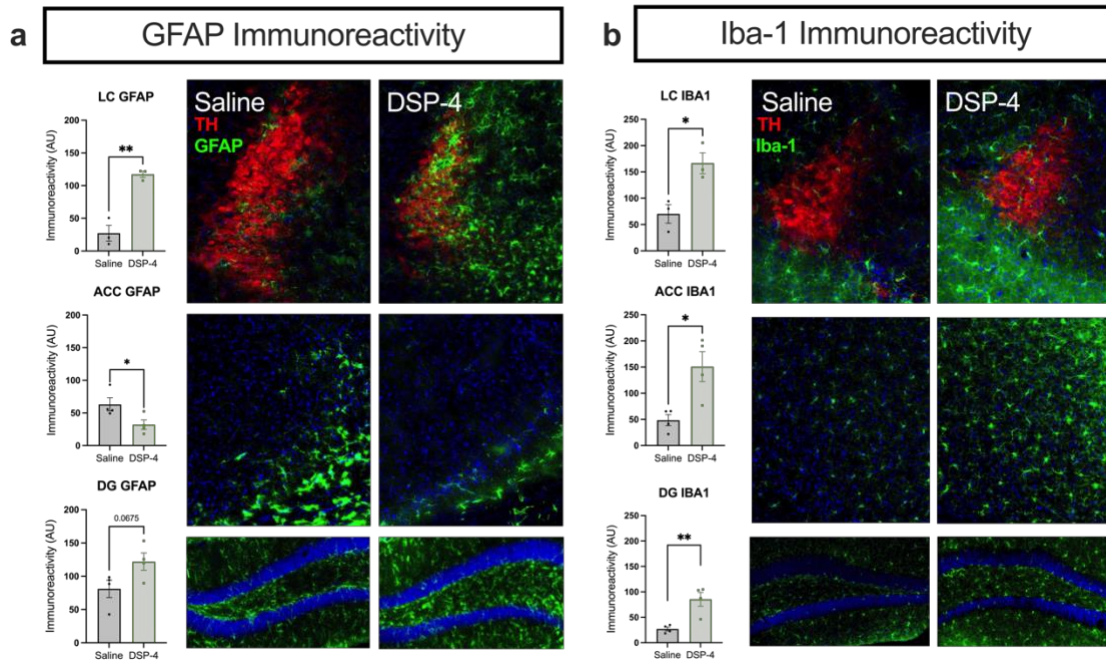
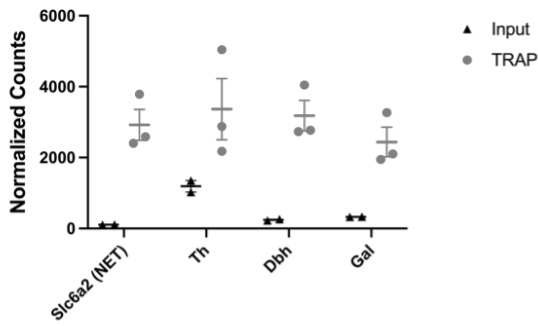
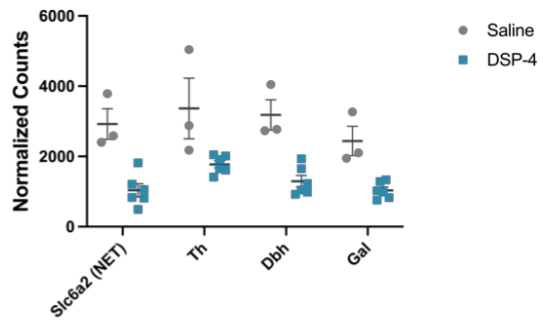


Fig. 2.3: DSP-4 alters astrocyte and microglia activation across the LC-NE system. Mice received saline or DSP-4 (2 x 50 mg/kg, i.p.) and assessed for neuroinflammation 1 week later. **(a)** Astrocyte reactivity, as measured by GFAP immunostaining, was significantly increased in the locus coeruleus (LC) with a trend in the dentate gyrus (DG) following DSP-4 treatment, while the anterior cingulate cortex (ACC) showed a decreased astrocytic response. **(b)** Microglial response, indicated by Iba-1 immunoreactivity, was increased across all regions assessed. Images acquired at 20X. Data shown as mean \pm SEM. N=3-4 per group. * p <0.05, ** p <0.01.

a TRAP Enriches for LC-mRNA



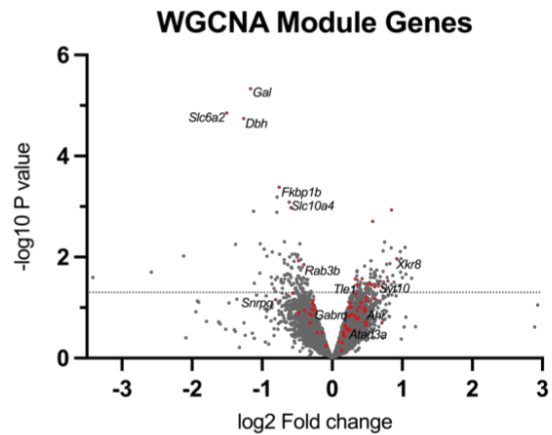
b Downregulation of LC Genes with DSP-4



c

Top 15 Downregulated Genes			Top 15 Upregulated Genes		
geneID	logFC	P.Value	geneID	logFC	P.Value
Gm16677	-3.41618	0.02515	Tmem181b-ps	0.84182	0.00654
LOC108168645	-2.57934	0.01984	Tll1	0.84390	0.03513
G530011006Rik	-2.12039	0.00951	Mitf	0.84777	0.00117
Slc6a2	-1.50317	0.00001	Ppwd1	0.86541	0.02303
Calr3	-1.37721	0.00557	Sema3b	0.88365	0.03161
Dbh	-1.26418	0.00002	Rasa1	0.91005	0.04723
Gal	-1.16362	0.00000	Xkr8	0.92298	0.01075
Ppp2r3d	-1.12240	0.00124	Six3	0.95911	0.03635
Erd1	-1.11240	0.03277	Hspa1l	0.97173	0.00783
Ndufa4l2	-1.03058	0.02075	Fut10	0.97753	0.01994
Phox2a	-1.02918	0.00544	Hpgd	0.98270	0.01075
Tspan18	-0.97218	0.00693	Rai14	1.00282	0.02561
Gm5093	-0.93153	0.00964	Slc5a5	1.04108	0.00642
Calcr	-0.86932	0.02485	Foxj1	1.05013	0.02175
Dcx	-0.85743	0.03389	Dctd	1.13396	0.02620

d



e

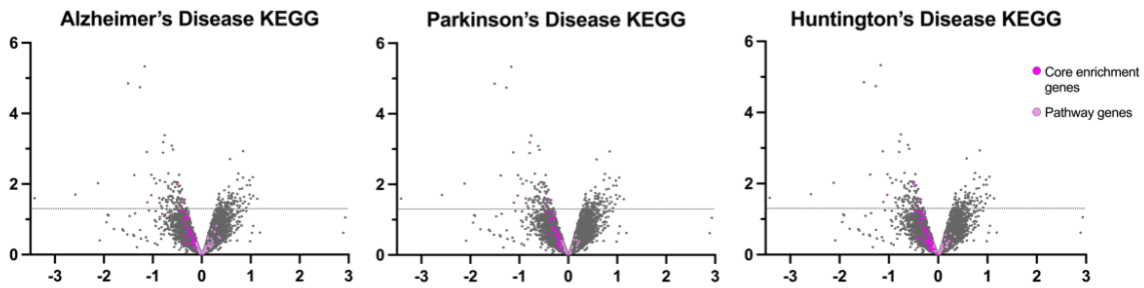


Fig. 2.4. DSP-4 triggers changes in the LC transcriptome. Mice received saline or DSP-4 (2 x 50 mg/kg, i.p.) and LC gene expression was assessed 1 week later. **(a)** TRAP allows for purification of mRNA from LC neurons through immunoprecipitation (TRAP, grey), resulting in enrichment of noradrenergic genes compared with mRNA from the entire hindbrain sample (input, black). **(b)** Differential gene expression (DGE) was assessed between DSP-4 (blue) and saline control (grey) TRAP samples, and revealed that noradrenergic-specific genes, including galanin (*Gal*), norepinephrine transporter (*Slc6a2*), dopamine β -hydroxylase (*Dbh*) and tyrosine hydroxylase (*Th*), were among the most significantly and robustly downregulated transcripts in the LC of DSP-4 treated mice. Data for **a** and **b** shown as mean \pm SEM, N=2-6 per group. **(c)** List of top 15 downregulated and top 15 upregulated DGE, sorted by fold change (logFC) with $p < 0.05$. **(d)** Volcano plot of all filtered, normalized genes (~11,500) with genes from WGCNA-defined module in red. Labeled genes from this module are those of interest based on published connections to neurodegenerative disease. **(e)** Volcano plots (as shown in (d)) highlighting genes from 3 significantly enriched KEGG pathways in our LC data, with GSEA-identified “core enrichment genes” colored magenta, and remaining pathway genes colored light pink.

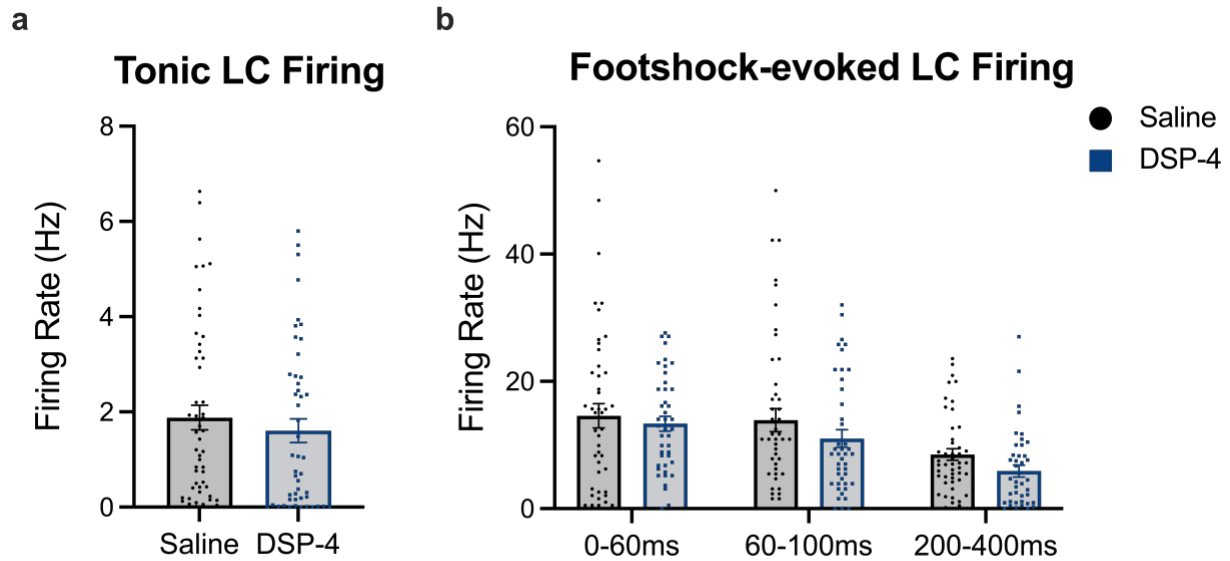


Fig. 2.5. DSP-4 treatment does not alter baseline or footshock-induced LC activity. Mice received saline or DSP-4 (2 x 50 mg/kg, i.p.) and assessed for locus coeruleus (LC) neuron firing under anesthesia 1 week later. No differences were found for **(a)** baseline tonic firing rates (in Hz). **(b)** There was no main effect of treatment on footshock-evoked firing rates of LC neurons 0-60, 60-100, or 200-400 ms following the stimulus. Data shown as mean \pm SEM. N=5 mice per group 42-53 neurons/group. * $p < 0.05$

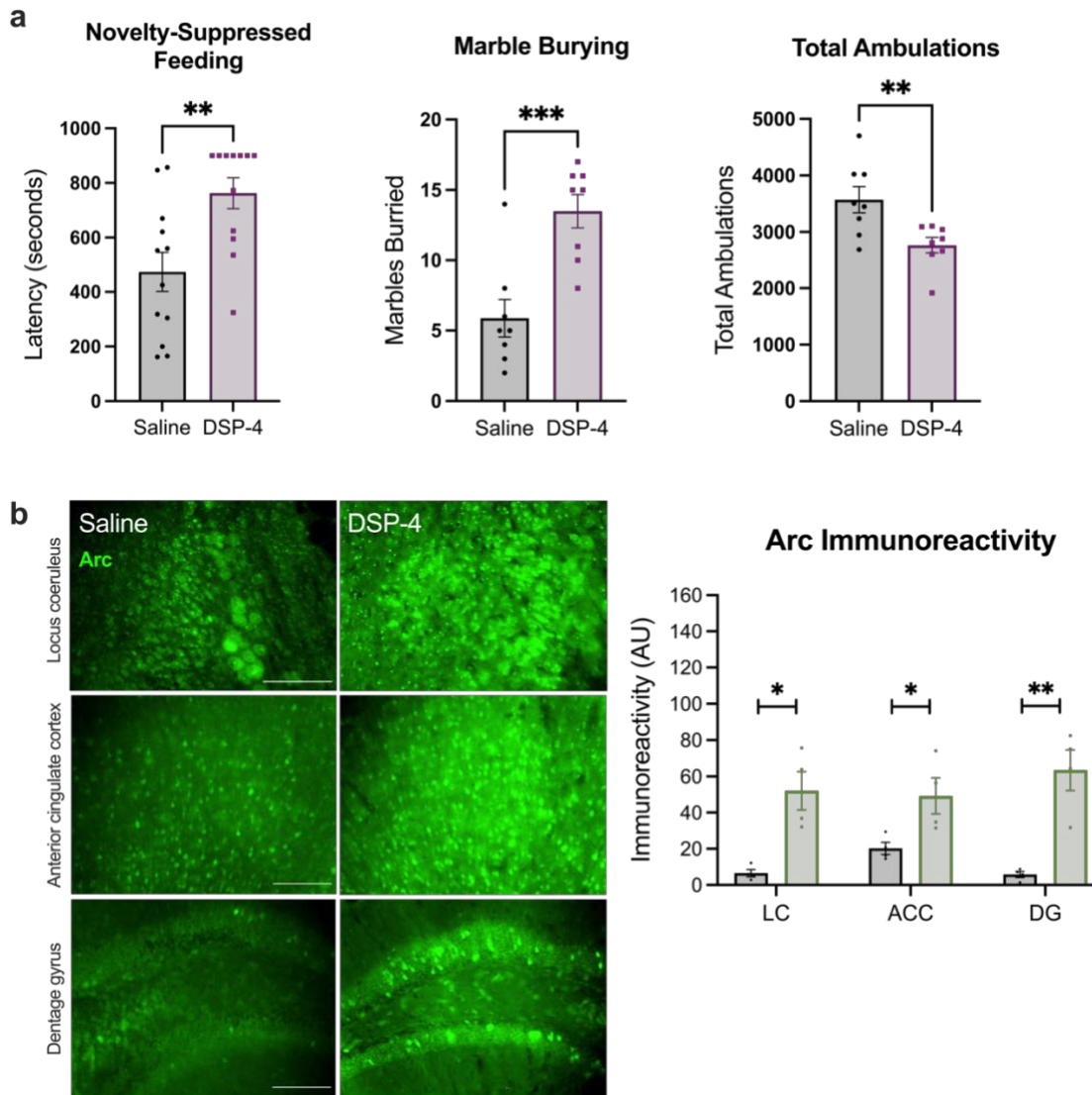


Fig. 2.6. DSP-4 increases novelty-induced anxiety and arc expression. (a) DSP-4-treated mice display increased latency to bite the food pellet in the novelty-suppressed feeding test, buried more marbles, and showed fewer ambulations in response to a novel environment (N=8-12 per group). (b) Immunoreactivity for the immediate early gene Arc following cage change was reduced in the locus coeruleus (LC) and projection regions (anterior cingulate cortex, ACC; dentate gyrus region of the hippocampus, DG) (N=3-4 per group). Images acquired at 20X. Data shown as mean \pm SEM. * p <0.05, ** p <0.01, *** p <0.001.

Table 2.1. Monoamine levels measured by HPLC

	Pons		PFC		Hippocampus	
	Saline	DSP-4	Saline	DSP-4	Saline	DSP-4
NE	66.89 ± 1.28	34.91 ± 1.41 **	28.69 ± 4.02	10.80 ± 3.56 *	32.18 ± 4.23	12.85 ± 4.14 *
MHPG	5.83 ± 0.30	4.04 ± 0.16 *	4.75 ± 0.57	2.40 ± 0.55 *	4.38 ± 0.34	2.42 ± 0.52 *
MHPG:NE	0.09 ± 0.01	0.12 ± 0.01 *	0.17 ± 0.02	0.28 ± 0.04 *	0.15 ± 0.02	0.23 ± 0.03
DA	4.79 ± 0.41	5.27 ± 0.43	52.76 ± 18.95	48.07 ± 22.55	73.84 ± 44.50	92.99 ± 39.37
DOPAC	5.70 ± 0.74	5.94 ± 0.47	27.10 ± 5.67	17.03 ± 4.72	25.50 ± 12.82	28.74 ± 9.26
DOPAC:DA	1.18 ± 0.07	1.15 ± 0.12	0.78 ± 0.12	0.99 ± 0.25	0.98 ± 0.18	0.76 ± 0.19
HVA	6.10 ± 0.39	6.58 ± 0.50	22.35 ± 4.14	16.63 ± 3.25	16.49 ± 7.49	20.44 ± 6.17
5-HT	69.54 ± 8.13	65.91 ± 2.08	42.58 ± 5.87	41.33 ± 4.59	55.86 ± 6.29	51.42 ± 4.22
5-HIAA	64.71 ± 4.47	60.06 ± 2.48	34.01 ± 3.93	26.39 ± 3.06	46.38 ± 5.62	43.25 ± 5.10
5-HIAA:5-HT	1.09 ± 0.15	1.11 ± 0.07	0.86 ± 0.08	0.66 ± 0.06	0.86 ± 0.07	0.87 ± 0.11

Data shown as mean ± SEM. N=4 per group for the pons, and N=8 per group for the PFC and Hippocampus. *p<0.05, **p<0.01.

Table 2.2: IHC antibodies

Antibodies	Host	Manufacturer	Catalog #	Dilution
Tyrosine hydroxylase	Chicken	Abcam	ab76442	1:1000
Tyrosine hydroxylase	Rabbit	Pel-Freez	P40101-0	1:1000
Norepinephrine transporter	Mouse	Mab Technologies	NET05-2	1:1000
GFAP	Guinea Pig	Synaptic Systems	173 004	1:1000
IBA1	Rabbit	FUJIFILM Wako Pure Chemical Corporation	019-19741	1:1000
Nitrotyrosine	Mouse	Abcam	ab125106	1:1000
Arc	Guinea Pig	Synaptic Systems	156 004	1:1000
NeuroTrace 435/455 Blue Fluorescent Nissl Stain	NA	Thermo Fisher Scientific	N21479	1:500
Alexa Fluor 488 Anti-Rabbit	Goat	Thermo Fisher Scientific	A-11008	1:500
Alexa Fluor 488 Anti-Guinea Pig	Goat	Thermo Fisher Scientific	A-11073	1:500
Alexa Fluor 568 Anti-Chicken	Goat	Thermo Fisher Scientific	A-11041	1:500

Table 2.3. Highlighted genes from WGCNA shown in Figure 2.4

Gene ID	logFC	P.Value	Gene name and citations
<i>Slc6a2</i>	-1.5032	1.41E-05	<u>Norepinephrine transporter</u> – LC enriched gene downregulated in DSP-4 mice
<i>Dbh</i>	-1.2642	1.81E-05	<u>Dopamine beta-hydroxylase</u> – LC enriched gene downregulated in DSP-4 mice
<i>Gal</i>	-1.1636	4.67E-06	<u>Galanin</u> – LC enriched gene downregulated in DSP-4 mice
<i>Snrpg</i>	-0.8073	0.0698	<u>Small nuclear ribonucleoprotein polypeptide G</u> – downregulated in DSP-4 mice; potential AD biomarker (Tao et al., 2020; Du et al., 2021)
<i>Fkbp1b</i>	-0.7567	0.0004	<u>FK506 binding protein 1B</u> – downregulated in DSP-4 mice; linked to calcium dysfunction in aging (Gant et al., 2014; Gant et al., 2015)
<i>Slc10a4</i>	-0.613	0.0008	<u>Solute carrier family 10 member 4</u> – downregulated in DSP-4 mice; possible links to AD brain pathology (Popova and Alafuzoff, 2013)
<i>Rab3b</i>	-0.4018	0.0141	Ras-related protein Rab-3B – downregulated in DSP-4 mice; involved in dopamine vesicular intake
<i>Gabrq</i>	-0.2844	0.1076	Gamma-aminobutyric acid type A receptor subunit theta – downregulated in DSP-4 mice; associated with behavioral changes in FTD (Gami-Patel et al., 2022)
<i>Atad3a</i>	0.2154	0.2627	ATPase family AAA domain containing 3A – upregulated in DSP-4 mice; potential AD biomarker (Zhao et al., 2022)
<i>Tle1</i>	0.3581	0.0351	TLE family member 1, transcriptional corepressor – upregulated in DSP-4 mice; potential AD biomarker (Madar et al., 2021)
<i>Ahr</i>	0.4676	0.1082	Aryl hydrocarbon receptor – upregulated in DSP-4 mice; potential PD biomarker (Zhou et al., 2021)
<i>Syt10</i>	0.663	0.0335	Synaptotagmin 10 – upregulated in DSP-4 mice; provides neuroprotection after excitotoxic input (Woitecki et al., 2016)
<i>Xkr8</i>	0.923	0.0107	XK related 8 – upregulated in DSP-4 mice; engulfs apoptotic cells

CHAPTER 3: CONSEQUENCES OF PIGMENTATION ON LOCUS COERULEUS
SURVIVAL AND FUNCTIONING

3.1 ABSTRACT

Parkinson's disease (PD) is the second most common neurodegenerative disorder worldwide, and is characterized by motor and non-motor symptoms. The leading pharmacotherapy, levodopa, is only effective for treating the motor symptoms caused by dopamine (DA) neuron degeneration, while non-motor symptoms associated with noradrenergic dysfunction have grave consequences for the quality of life experienced by PD patients and are not alleviated by any currently available therapies. Thus, new research on PD neuropathology and treatment must consider the locus coeruleus (LC), the major central noradrenergic nucleus. The LC develops α -synuclein pathology prior to DA neurons in PD and is almost completely degenerated in later stage disease, but the molecular mechanisms responsible for its vulnerability are unknown. Along with substantia nigra DA neurons, the LC is the only structure in the brain that produces appreciable amounts of neuromelanin (NM), a dark brown cytoplasmic pigment. It has been proposed that these NM granules initially play a protective role by sequestering toxic catecholamine metabolites and heavy metals, but become harmful during aging and particularly in PD as they overwhelm cellular machinery and get released during neurodegeneration. Because rodents do not naturally produce NM, the study of this pigment has been mostly limited to human postmortem studies, and it has not been possible to establish causal relationships between NM and PD-associated LC pathology. We have adapted a viral-mediated approach for expression of human tyrosinase, the enzyme responsible for peripheral melanin production, to promote pigmentation in rodent LC neurons. We found that pigment expression in the LC recapitulates key features of endogenous NM found in primates, including eumelanin and pheomelanin, lipid droplets, and a double-membrane encasement. Pigment expression results in mild neurodegeneration, altered catecholamine levels, transcriptional changes, and novelty-induced anxiety phenotypes as early as 1 week post-injection.

By 6-weeks, the expression of this pigment results in severe LC neurodegeneration and a robust neuroinflammatory response. These phenotypes are reminiscent of LC dysfunction in PD, validating the utility of this model for studying the consequences of pigment accumulation in the LC as it relates to neurodegenerative disease.

3.2 INTRODUCTION

Parkinson's disease (PD) is a common neurodegenerative condition affecting nearly one million Americans and over 10 million individuals worldwide (Marras et al., 2018). PD is pathologically characterized by α -synuclein protein aggregation and subsequent degeneration of specific populations of catecholamine neurons, most notoriously dopamine (DA) neurons in the substantia nigra (SN) and norepinephrine (NE) neurons in the locus coeruleus (LC). The consequences of losing SN-DA neurons is well understood, as their death directly results in the emergence of motor symptoms, such as rigidity and tremor, which constitute a clinical diagnosis. The first line treatment for PD is DA replacement therapy with the precursor levodopa (L-DOPA), which ameliorates motor symptoms. However, PD is also characterized by early non-motor symptoms such as REM Sleep Behavior Disorder (RBD) (Stiasny-Kolster et al., 2005), anxiety (Prediger et al., 2012), depression (Remy et al., 2005), and cognitive impairment (Chan-Palay, 1991b; Vazey and Aston-Jones, 2012; Hinson et al., 2017; Li et al., 2019) which may be mediated, at least in part, to LC dysfunction and degeneration (Zweig et al., 1993). LC dysfunction is closely associated with these prodromal symptoms in clinical studies (Del Tredici and Braak, 2013), and experimental manipulations of the LC faithfully recapitulate non-motor symptoms in animal models (Mavridis et al., 1991; Srinivasan and Schmidt, 2003; Song et al., 2019b; Iannitelli et al.,

2022). Importantly, these non-motor symptoms are not reversed by L-DOPA, and there are no alternative treatments available. As such, these early, LC-associated, pre-motor symptoms are often reported by PD patients to be detrimental to quality of life and present serious obstacles for maintaining independence.

The specific factors that make catecholamine neurons vulnerable to α -synuclein pathology, dysfunction, and death in PD are not fully understood, although several likely contributors have been identified. One notable feature of LC neurons is their length. As the LC is the primary source of central norepinephrine (NE), it projects to virtually every other region of the brain (Foote et al., 1983), resulting in long, highly branched, unmyelinated axons. The LC neurons have intrinsic pacemaker activity, which leads to high levels of oxidant stress (Wang and Michaelis, 2010) and risk for mitochondrial dysfunction (Sanchez-Padilla et al., 2014), factors which are well-studied in relation to PD etiology (Nicholls, 2008; Surmeier et al., 2010). Additionally, these noradrenergic neurons harbor toxic NE metabolites, including DOPEGAL (Kang et al., 2020). Perhaps the most defining characteristic of these neurons, though, is their unique expression of a dark, cytoplasmic pigment called neuromelanin (NM).

NM is found exclusively in catecholaminergic cells of the SN and LC, the two neuronal populations that are selectively vulnerable in PD (Zecca et al., 2004b; Zecca et al., 2008b). NM is a byproduct of catecholamine synthesis and metabolism, and studies suggest that the formation of NM granules likely results from an overabundance of catecholamines that cannot be sequestered into vesicles quickly enough in active neurons (Sulzer et al., 2000). In addition to catecholamine metabolites, these granules contain melanins such as eumelanin and pheomelanin (Bush et al., 2006), lipid droplets, protein aggregates (Sulzer et al., 2008), and heavy metals, most notably iron (Zecca et al., 2008b). Thus, it has been proposed that the primary function of NM is to bind and

sequester these harmful compounds in the cytoplasm so that they do not harm the neurons (Zecca et al., 2003a). However, because SN-DA and LC-NE neurons do not possess the machinery required to break down these granules, NM accumulates over time, visibly darkening the pigmentation of these brain regions with age. Eventually, this buildup of NM within catecholamine neurons may exacerbate neurodegeneration in PD either by interfering with and overwhelming cellular machinery and/or via release of previously bound toxins as it breaks down during cell death. Indeed, LC neurons containing the highest amounts of NM are disproportionately lost during both normal aging and PD (Mann and Yates, 1983), and increased iron (Sasaki et al., 2006), zinc (Dexter et al., 1992), and copper (Pall et al., 1987) are evident in brain and CSF samples from PD patients, suggesting dysregulation of heavy-metal homeostasis.

Despite the clear link between NM and neurodegeneration in PD, establishing a causal relationship has been difficult because NM is not produced endogenously in rodents, which comprise the majority of animal models for studying PD (Barden and Levine, 1983). The lack of NM in rats and mice is likely not due to fundamental neurobiological differences between primate and rodent LC neurons, but rather reflects their comparatively short life span (~2 years). Indeed, one study did report trace amounts of NM in aged rats (DeMattei et al., 1986), and even humans do not express detectable amounts of NM in LC neurons until they are 3 years old (Mann and Yates, 1974). Thus, despite an ever-growing toolbox of mouse genetic technology that makes them ideal for investigating the molecular mechanisms of disease, *in vivo* studies on NM have been extremely limited. To date, only two rodent models of NM has been reported (Zecca et al., 2008a; Carballo-Carbajal et al., 2019). The first study in rodents relied on purification and injection of human neuromelanin granules (Zecca et al., 2008a), but more recently, researchers were able to drive pigmentation in the SN of mice and rats through viral-mediated expression of human

Tyrosinase (hTyr), the biosynthetic enzyme responsible for melanin production in the skin (Carballo-Carbajal et al., 2019). In this model, NM expression in the SN resulted in neurodegeneration and subsequent motor impairments similar to those seen in other mouse models of PD. We have adapted this strategy to promote NM production in the mouse LC, developing the first rodent model of pigment expression in noradrenergic neurons. Here we present the characterization of this novel mouse model of PD through immunohistochemical and behavioral analyses, revealing neuroinflammatory and neurodegenerative responses coupled with a behavioral phenotype reminiscent of the non-motor features of PD. Additionally, we employed the Translating Ribosome Affinity Purification (TRAP) technique to isolate and sequence mRNA exclusively from these pigmented LC neurons, yielding insight into the molecular mechanisms of NM-mediated adaptations and neurotoxicity in the LC.

3.3 MATERIALS AND METHODS

Animals. Adult male and female mice were used for all behavioral and immunohistochemical experiments. For immunohistochemistry, behavior, and HPLC, TH-Cre mice (B6.Cg-7630403G23RikTg(Th-cre)1Tmd/J, The Jackson Laboratory, # 008601) were used for the specific expression of Cre-dependent viral vectors in the LC. For translating ribosome affinity purification (TRAP) RNA-sequencing experiments, we crossed TH-Cre mice with transgenic *Slc6a2-eGFP/Rpl10a* mice (B6;FVB-Tg(*Slc6a2-eGFP/Rpl10a*)JD1538Htz/J, The Jackson Laboratory, #031151), which incorporate an EGFP/Rpl10a ribosomal fusion protein into a bacterial artificial chromosome under the *Slc6a2* (NE transporter; NET) promoter to allow for the isolation of polysomes and translating mRNAs specifically from noradrenergic neurons. Mice were group housed with sex- and age-matched conspecifics (maximum of 5 animals per cage) until one week

prior to behavioral testing, and then individually housed for the subsequent week of experimentation until sacrifice. Animals were maintained on a 12:12 light:dark cycle (lights on at 0700), and food and water were available *ad libitum*, unless otherwise specified. All experiments were conducted at Emory University in accordance with the National Institutes of Health *Guideline for the Care and Use of Laboratory Animals* and approved by the Emory Institutional Animal Care and Use Committee.

Viral vectors. To express hTyr in the LC, we developed an AAV5-DIO-hTyr construct with assistance from the Emory Custom Cloning and Viral Vector Cores. For some preliminary experiments (immunohistochemistry for viral confirmation and gliosis, stereology), all mice were injected with AAV5-DIO-hTyr, and TH-Cre⁺ animals were used as the experimental group while TH-Cre⁻ littermates served as the controls. For the remaining experiments (behavior, TRAP, and HPLC), only TH-Cre⁺ mice were used, and mice were injected with either the AAV5-DIO-hTyr experimental virus or a comparable AAV5-DIO-EYFP control virus (Addgene, plasmid #27056). Due to the volume of virus required for these experiments, several batches of AAV5-DIO-hTyr were produced. Despite our best efforts to control for titer and delivery, inherent variability was evident between batches. For this reason, some of the time courses varied between experiments. We are specific in our language characterizing the timeline of each individual experiment. For the purposes of consistency, the 1-2 week cohorts represent a time when NM is expressed by the LC, but has not led to widespread cell body death, while a 6-8 week cohort is used to illustrate considerable LC degeneration. The 4-week cohort presented in the discussion of astrocytic responding of the LC should be considered a mid-point of LC pigment accumulation.

Stereotaxic injections. Stereotaxic injections were performed as previously described (Tillage et al., 2020a), in a stereotaxic frame under 2.0% isoflurane anesthesia. Bilateral LC injections were made at a volume of 0.5 μL /hemisphere using a 5 μL Hamilton glass syringe. The virus was injected at a rate of 0.15 $\mu\text{L}/\text{min}$, and the needle was allowed to remain in place for 5 min following the completion of each injection. LC coordinates are AP: - 5.4mm, ML: +/- 1.2mm, and DV: - 4.0mm relative to Bregma.

HPLC. Mice were anesthetized with isoflurane and euthanized by rapid decapitation. The pons, prefrontal cortex, and hippocampus were rapidly dissected on ice and flash-frozen in isopentane (2-Methylbutane) on dry ice. The samples were weighed and stored at -80°C until processing for HPLC by the Emory HPLC Bioanalytical Core. As previously described (Lustberg et al., 2022), tissue was thawed on ice and sonicated in 0.1 N perchloric acid (10 $\mu\text{L}/\text{mg}$ tissue) for 12 s with 0.5 s pulses. Sonicated samples were centrifuged (16,100 rcf) for 30 min at 4°C , and the supernatant was then centrifuged through 0.45 μm filters at 4000 rcf for 10 min at 4°C . For HPLC, an ESA 5600A CoulArray detection system, equipped with an ESA Model 584 pump and an ESA 542 refrigerated autosampler was used. Separations were performed using an MD-150 \times 3.2 mm C18, 3 μm column (Thermo Scientific) at 30°C . The mobile phase consisted of 8% acetonitrile, 75 mM NaH_2PO_4 , 1.7 mM 1-octanesulfonic acid sodium and 0.025% trimethylamine at pH 2.9. A 20 μL of sample was injected. The samples were eluted isocratically at 0.4 mL/min and detected using a 6210 electrochemical cell (ESA, Bedford, MA) equipped with 5020 guard cell. Guard cell potential was set at 475 mV, while analytical cell potentials were -175 , 100, 350 and 425 mV. The analytes were identified by the matching criteria of retention time measures to known standards

(Sigma Chemical Co., St. Louis MO). Compounds were quantified by comparing peak areas to those of standards on the dominant sensor.

Immunohistochemistry. Mice were euthanized with an overdose of sodium pentobarbital (Fatal Plus, 150 mg/kg, i.p.; Med-Vet International, Mettawa, IL) and were transcardially perfused with cold 4% PFA in 0.01 M PBS. After extraction, brains were post-fixed overnight in 4% PFA at 4°C and then transferred to a 30% sucrose/PBS solution for 72 h at 4°C. Brains were embedded in OCT medium (Tissue-Tek) and sectioned by cryostat into 40- μ m-thick coronal sections at the level of the LC, anterior cingulate cortex (ACC), and hippocampus. Sections were blocked in 5% normal goat serum (NGS) in 0.01 M PBS/0.1% Triton-X permeabilization buffer and then incubated for 24 h at 4°C in NGS blocking buffer with primary antibodies listed in Table 2. Following washes in 0.01 M PBS, sections were incubated for 2 h in blocking buffer, including secondary antibodies described in Table 2. After washing, sections were mounted onto Superfrost Plus slides and coverslipped with Fluoromount-G plus DAPI (Southern Biotech, Birmingham, AL).

Microscopy. For the catecholaminergic marker tyrosine hydroxylase (TH) and hTyr, immunofluorescent micrographs were acquired on a Leica DM6000B epifluorescent upright microscope at 20x magnification with uniform exposure parameters for each stain and region imaged. Brightfield images of pigment granules were also obtained on the Leica DM6000B upright microscope at 20x magnification. Following convention, these images are oriented with the dorsal direction up and the ventral direction down. For astrocyte marker glial fibrillary acidic protein (GFAP) and LC terminal marker NE transporter (NET), immunofluorescent images were acquired as z-stack images (10 z-stacks; pitch: 0.1 μ m) at 20x magnification and compressed on a Keyence

BZ-X700 microscope system. One representative atlas-matched section was selected from each animal. Image processing for all images was conducted using the FIJI/ImageJ software.

Electron microscopy. Electron microscopy experiments were conducted by the laboratory of Dr. Yolanda Smith at the Emory National Primate Research Center. Sections that included the locus coeruleus were rinsed in Phosphate buffer (PB; 0.1 M, pH 7.4) and then treated with 0.5% osmium tetroxide (OsO₄) for 10 min (RT) and returned to PB. Sections were then dehydrated with increasing concentrations of ethanol; 1% uranyl acetate was added to the 70% ethanol solution to increase EM contrast (10 min incubation at RT in the dark). Sections were next placed in propylene oxide, followed by tissue embedding with an epoxy resin (Durcupan, Fluka) for at least 12 hr. Resin-embedded sections were then baked at 60°C for at least 48-hr until fully cured. Blocks containing the LC were removed before being cut into ultrathin 60 nm sections (Leica Ultracut T2). These ultrathin sections were mounted onto pioloform-coated grids and stained with lead citrate (5 min, RT) for added contrast. Grids were then examined with an electron microscope (EM; Jeol; Model 1011) coupled with a CCD camera (Gatan; Model 785) controlled with DigitalMicrograph software (Gatan; version 3.11.1).

Cell counts. TH-Cre⁺ animals received a unilateral LC injection of AAV5-DIO-hTyr in the right hemisphere. Coronal tissue sections were processed as described above (*Immunohistochemistry*) and images were acquired as described for glial markers (*Microscopy*). Using TH as a guide for anatomical LC borders and DAPI as a marker for individual nuclei, sections were quantified using HALO imaging software (Indica Labs, v3.3.2541.420, FISH/IF v2.1.4). Nine sections were analyzed for each animal (n=4/group), covering most of the LC. The total area analyzed did not

differ between the hTyr-injected hemisphere and the non-injected hemisphere. Within HALO, nuclei were defined using DAPI, and TH-positive and Nissl-positive nuclei cells were counted and summed across all nine sections for each animal. Comparisons were made between the number of Nissl+ and TH+ nuclei cells in the hTyr-injected hemisphere and the non-injected hemisphere.

Translating Ribosome Affinity Purification (TRAP). To obtain adequate quantities of RNA for sequencing, samples from two 6-8 month-old, same-sex and treatment TH-Cre+, *Slc6a2-eGFP/Rpl10a*+ mice were pooled to form a biological replicate by dissecting out the hindbrain posterior to the pontine/hypothalamic junction (cerebellum was discarded). Six biological replicates were collected per treatment group. Each replicate was homogenized and TRAP was performed as described (Mulvey et al., 2018), resulting in LC-enriched “TRAP” samples and whole-hindbrain “input” samples. RNA was extracted using Zymo RNA Clean & Concentrator-5 kit, and subsequently sent for library preparation and Illumina sequencing by NovoGene to a minimum depth of 20 million fragments per sample. Forward and reverse sequencing files from each replicate were aligned to the mouse genome (mm10) using STAR alignment, and counts were obtained using FeatureCounts in R Bioconductor. Two samples from saline-treated mice were removed from analysis because the TRAP protocol failed to enrich *Slc6a2* above a 10-fold change, a quality control threshold observed in all other saline-treated samples. All subsequent analyses utilized R Bioconductor packages. Sequencing data will be available on NCBI GEO at the time of publication.

To further characterize the gene expression changes, we performed analyses to compare gene expression patterns in our dataset with a repository of gene sets using Gene Set Enrichment Analysis (GSEA 4.2.3) (Mootha et al., 2003; Subramanian et al., 2005). Gene set permutation was

used, as recommended by GSEA documentation for experiments with fewer than 7 samples per group. Other parameters were set to default settings using 1000 gene set permutations and signal to noise ranking metric. We downloaded KEGG Pathways from the Molecular Signatures Database, which has 186 gene sets. After filtering for the recommended minimum (15) and maximum (500) gene set size, the remaining 145 gene sets were compared to the expression data from our dataset to calculate the GSEA enrichment score and to compute significant enrichment.

Behavioral assays. Behavioral assays were performed in the following order, from least to most stressful.

Novelty-suppressed feeding: Chow was removed from individual home cages 24 h prior to behavioral testing. Mice were moved to the test room under red light and allowed to habituate for 2 h prior to the start of the test. Individual mice were placed in a novel arena (10" × 18" × 10") with a single pellet of standard mouse chow located in the center. The latency to feed, operationally defined as grasping and biting the food pellet, was recorded using a stopwatch. Mice that did not feed within the 15-min period were assigned a latency score of 900 s (Tillage et al., 2020b). We have shown that increasing NE promotes anxiety-like behavior in this task reflected by longer latencies to eat in the novel environment, while decreasing attenuates anxiety and reduces latency to eat (Lustberg et al., 2020b).

Fear conditioning and context testing: Fear-conditioning training and subsequent contextual fear testing is a widely-used assessment of associative memory, particularly for an environment in which an aversive stimulus (footshock) was previously administered. This method has been described previously by our group and others and is sensitive to changes in NE (Murchison et al., 2004; Chalermplanupap et al., 2018; Butkovich et al., 2020). Mice were placed in a fear-

conditioning apparatus (7 in. x 7 in. x 12 in.; Coulbourn Instruments) with a metal shock grid floor. Following 3 min of habituation, three conditioned stimulus (CS)-unconditioned stimulus (US) pairings were presented with a 1-minute intertrial interval. The CS was a 20-second, 85 dB tone which co-terminated with the US, a 2-s, 0.5 mA footshock (Precision Animal Shocker, Colbour Instruments). The following day, the context test was conducted by placing animals back into the fear conditioning chamber without the administration of CS-US pairings. Freezing behavior was measured as a readout of memory for the fear-associated context.

Statistical analyses. Stereological cell counting and HPLC measurements of catechol concentrations were compared between hTyr-injected and control groups using a student's t-test in GraphPad Prism. Similarly, behavioral assessment relied on t-test comparison between groups for latency to feed in the novelty-suppressed feeding task and average percent freezing in the contextual fear assay. R Bioconductor packages were utilized for statistical analyses of RNA sequencing data, including differential gene expression (DGE).

3.4 RESULTS

Viral infusion of hTyr induces NM-like pigmentation in the LC of mice. To recapitulate NM found endogenously in the human LC, we adapted a viral vector-mediated approach to drive neuronal pigmentation in rodents. TH-Cre mice were stereotaxically injected with AAV5-DIO-hTyr in the LC to drive viral expression of hTyr (**Fig. 3.1a**), which is known to produce pigment when introduced in rodent SN DA neurons (Carballo-Carbajal et al., 2019). We found that hTyr expression likewise drove pigmentation of the LC in Cre⁺ (**Fig. 3.1b**) but not in Cre⁻ mice (**Fig. 3.1d**) as early as 1 week post-infusion. This pigmentation was visible by gross anatomical

inspection (**Fig. 3.1e**) and brightfield microscopy (**Fig. 3.1b**). Additionally, we confirmed the presence of melanin in this pigment using Fontana-Masson staining (**Fig. 3.1f**). We then utilized electron microscopy to compare the pigment granules in our rodent model (**Fig. 3.1g**) with endogenous NM granules from 16-year-old Rhesus macaque tissue (**Fig. 3.1h**). Ultrastructural inspection revealed that many of the components known to reside in endogenous NM, including pheomelanin and eumelanin pigments, lipid droplets, and a double-membrane, were also present in granules from our rodent model. Together, these results validate the use of hTyr expression to induce NM-like pigmentation in the mouse LC.

Pigmentation results in loss of LC fibers and cell bodies at 1-week. Consistent with other rodent models of LC neurodegeneration (Chalermphanupap et al., 2018; Butkovich et al., 2020), NET immunoreactivity, a marker of LC dendrite, axon, and terminal integrity, was visibly reduced in the LC (**Fig. 3.2a**), as well in the LC projections to the anterior cingulate cortex (ACC) (**Fig. 3.2c**) and dentate gyrus (DG) (**Fig. 3.2d**) of hTyr-injected mice compared to EYFP-injected controls. To determine whether pigmentation impacted cell body integrity at 1 week post-injection, we performed a count of LC neurons. We quantified DAPI+ cells also positive for NeuroTrace Nissl in the LC, and found a 37% reduction of LC neurons in hTyr-injected mice compared to controls (**Fig. 3.2b**).

Pigmentation reduces NE levels throughout the LC network and dysregulates NE turnover in the projection fields at 1-week. Given the loss of LC axons/terminals, we assessed the impact of hTyr-driven pigmentation on tissue levels of catecholamines and their metabolites (**Fig. 3.3**). NE was dramatically reduced in the pons, where LC cell bodies reside ($t_{(10)} = 10.14$, $p < 0.0001$),

as well as in the prefrontal cortex (PFC; $t_{(10)} = 7.607$, $p < 0.0001$) and hippocampus ($t_{(10)} = 9.735$, $p < 0.0001$), two of the primary projection regions of the LC. Additionally, levels of the primary NE metabolite MHPG were also reduced in the pons ($t_{(10)} = 7.532$, $p < 0.0001$), PFC ($t_{(10)} = 5.152$, $p = 0.0004$) and hippocampus ($t_{(10)} = 3.666$, $p = 0.0043$) (**Fig. 3.3**). Despite the reduction of total NE and MHPG, the MHPG:NE ratio, which provides an estimate of NE turnover, was significantly increased in the PFC ($t_{(10)} = 2.905$, $p = 0.0157$) and hippocampus ($t_{(10)} = 4.392$, $p = 0.0014$) compared to controls, suggesting adaptations in the LC-NE system (**Fig. 3.3**). Levels of other amine neuromodulators, including DA, 5-HT, and their respective metabolites, were unchanged with the exception of an increase in DA turnover (metabolite DOPAC:DA) in both the pons ($t_{(10)} = 3.288$, $p = 0.0082$) and PFC ($t_{(10)} = 2.905$, $p = 0.0157$), suggesting that dysfunction resulting from pigmentation of the LC was largely confined to the noradrenergic system at 1 week post-injection.

The presence of LC pigment drives novelty-induced anxiety behavior at 1-week. Several prodromal symptoms of PD are regulated by the LC-NE system, and thus are sensitive to the early LC dysfunction which precedes neurodegeneration (Weinshenker, 2018). We assessed the impact of hTyr-induced pigmentation on LC-associated behaviors, including stress response and cognition. We found that hTyr-injected mice were significantly more reactive in a novelty-induced stress paradigm commonly used to model anxiety (Lustberg et al., 2020a). At 1 week post-injection, hTyr-expressing mice took significantly longer than EYFP controls to consume food in the novelty-suppressed feeding task ($t_{(24)} = 2.359$, $p = 0.0268$) (**Fig. 3.4a**). Five hTyr-injected mice (approximately one third) timed out of the task at 15-min, while only one EYFP control mouse timed out of the task (**Fig. 3.4a**), further illustrating an increase in novelty-induced anxiety-like

behavior resulting from LC pigmentation. Importantly, hTyr- and EYFP-injected mice displayed no differences in latency to eat in the home cage, indicating the experimental group's increased latency to eat during the task resulted from novelty stress behavior rather than changes in satiety state. Associative memory, as measured by freezing in a footshock-associated context, did not differ between treatment groups (**Fig. 3.4b**).

hTyr-induced pigmentation alters LC transcriptome. Following confirmation of LC-mRNA enrichment with TRAP (**Fig. 3.5a**), we performed a gene set enrichment analysis (GSEA) to compare the gene expression patterns of our data with repositories of known gene sets. We identified 10 KEGG pathways that were significantly enriched in the LC of hTyr-expressing animals, including Tyrosine metabolism (enrichment score (ES) = 0.622, $p = 0.008$), Tryptophan metabolism (ES = 0.596, $p = 0.014$), P53 stress signaling (ES = 0.513, $p = 0.018$), and lysosome activity (ES = 0.348, $p = 0.042$) (**Fig. 3.5c**).

Comparing our gene set to the Human Phenotype Ontology pathways, we found that hTyr samples displayed significant upregulation in the gene sets titled “Parkinsonism with favorable response to dopaminergic medication” (ES = 0.538, $p = 0.039$), “startle response” (ES = 0.558, $p = 0.047$), “speech articulation” (ES = 0.581, $p = 0.04$), and “sleep apnea” (ES = 0.591, $p = 0.021$) (**Fig. 3.5**).

The most significant transcriptional differences were seen when comparing our dataset to the Gene Ontology Biological Process gene sets. We found a staggering 140 gene sets significantly enriched in our hTyr group compared to EYFP controls. These pathways fell into four notable categories: apoptotic pathways, immune regulation, endoplasmic reticulum functioning, and heavy metal ion metabolism. A comprehensive list of these pathways can be found in Table 3.2. Of these

many upregulated pathways, we identified several that we believe to be critically important in assessing the impact of NM on LC neurons. Of particular interest were the gene sets titled “antigen processing and presentation via MHC class I” (ES = 0.74, $p < 0.000$), “response to iron ion” (ES = 0.61, $p = 0.018$), “positive regulation of macroautophagy” (ES = 0.47, $p = 0.011$), and “pigment metabolic process” (ES = 0.46, $p = 0.024$) (**Fig. 3.5c**).

Finally, a comparison with the Gene Ontology Cell Component database showed 9 gene sets significantly enriched in the hTyr group compared to controls. The most notable was “pigment granule” (ES = 0.434, $p < 0.000$), with our rodent model displaying 45 core enriched genes of the 88 total present in the gene set (**Fig. 3.5c**).

Pigment accumulation results in neurodegeneration and neuroinflammation.

To assess the consequences of prolonged pigment burden in the LC, we allowed mice to age several weeks following viral infusion. Despite batch-dependent variability, we consistently saw a near-total loss of LC cell bodies by 6- to 8-weeks post-infusion, as measured by TH immunoreactivity (**Fig. 3.6**). Although few LC neurons remain at this time point, pigmented granules remained abundant in the region. In fact, pigment granules after 6-weeks (**Fig. 3.6**) were visibly darker and more robust than at 1-week (**Fig. 3.1**). By 6-weeks, the pigmentation was also visible beyond the confines of the LC. Taken together, these data suggest that pigmented granules persist following the death of their host neurons, and in fact may spread to adjacent tissue. Moreover, it appears that the most densely pigmented sub-regions of the LC display the most profound cell loss (**Fig. 3.7**), a finding which would mimic the patterns of neurodegeneration seen in human patients (Mann and Yates, 1983).

Glial cells help dispose of extracellular waste following neurodegeneration (Heneka et al., 2015). To investigate whether neuroinflammation is a potential mechanism of pigment engulfment and clearance in our model, we assessed glial reactivity in the region throughout the neurodegenerative process. While we found minimal differences in microglial reactivity at 4- or 6-weeks (data not shown), we observed robust GFAP+ astrocyte reactivity in and around the LC of pigment-expressing mice at both 4- and 6-weeks, well beyond the levels seen in controls (**Fig. 3.7a-f**). Furthermore, there was extensive overlap between GFAP immunoreactivity and pigment, suggesting a direct interaction between the astrocytes and pigment granules (**Fig. 3.7g**).

Loss of pigment-bearing noradrenergic neurons depletes catecholamine levels in the LC and projection regions and dysregulates NE turnover.

Following pigment-mediated LC degeneration at 6 weeks post-infusion, we re-assessed tissue catecholamine levels. In line with the 1-week data, we found an even greater decrease in NE (~65%) in the pons ($t_{(9)} = 10.23$, $p < 0.0001$); PFC ($t_{(9)} = 9.745$, $p < 0.0001$), and hippocampus ($t_{(9)} = 12.83$, $p < 0.0001$) of hTyr-injected mice as compared to EYFP controls (**Fig. 3.8**). Similarly, we found a decrease in MHPG in the pons ($t_{(9)} = 9.489$, $p < 0.0001$), PFC ($t_{(9)} = 7.659$, $p < 0.0001$), and hippocampus ($t_{(9)} = 8.207$, $p < 0.0001$) (**Fig. 3.8**). While NE turnover (MHPG:NE) was decreased in the pons ($t_{(9)} = 4.427$, $p = 0.0017$), the increased NE turnover seen in projection regions at 1 week persisted in the PFC ($t_{(9)} = 3.11$, $p = 0.0125$) and hippocampus ($t_{(9)} = 2.697$, $p = 0.0245$) at 6 weeks (**Fig. 3.8**). Furthermore, DA turnover was increased in the hippocampus of hTyr-injected animals ($t_{(9)} = 2.623$, $p = 0.0277$), likely driven by an increase of the metabolite DOPAC ($t_{(9)} = 3.079$, $p = 0.0132$). No changes in 5-HT, metabolite 5-HIAA, or turnover was found in any region at 6 weeks.

Pigment-mediated neurodegeneration has subtle behavioral effects at 6-weeks. Despite the catastrophic loss of LC neurons and decrease in neurotransmitter levels at 6-weeks, the behavioral effects resulting from prolonged pigment expression were subtle. Novelty-induced anxiety, which was increased in hTyr mice at 1-week, did not differ statistically between groups at 6-weeks (**Fig. 3.9a**). Additionally, there were no differences observed in the context fear testing assay (**Fig. 3.9b**).

3.5 DISCUSSION

The present study characterized the impact of hTyr-induced pigment in the LC of mice, allowing causal relationships between NM expression in noradrenergic neurons, LC-NE integrity, and the development of non-motor symptoms reminiscent of prodromal PD in humans. The expression of pigmentation driven by viral delivery of hTyr is consistent with prior work focused on the SN (Carballo-Carbajal et al., 2019). In our model, neuronal dysfunction is evident as early as 1-week post-infusion. Even at this early time point, we found a modest decrease in the number of cell bodies present in the LC, as well as dramatically decreased NET immunoreactivity in the pons, PFC, and hippocampus of hTyr mice compared to controls. These findings are consistent with other reports of early LC axon loss in neurodegenerative diseases (Weinshenker, 2018; Doppler et al., 2021). Concurrent with fiber loss was a depletion of NE and its primary metabolite MHPG in the hippocampus and PFC. We also found elevated MHPG:NE ratio, a well validated measure of NE turnover, in projection regions, which may suggest compensatory hyperactivity of surviving LC fibers. This feature has been described in other rodent models of LC neurodegeneration (Hallman and Jonsson, 1984; Iannitelli et al., 2022) and is also consistent with LC neurodegeneration in humans (Francis et al., 1985; Raskind et al., 1999; Jacobs et al., 2021b).

An overactive NE transmission phenotype would be congruent with the pre-degenerative LC dysfunction seen in humans with AD and PD (Weinshenker, 2018). Indeed, pigment-expressing mice displayed elevated novelty-induced anxiety-like behavior, indicating increased noradrenergic neurotransmission (Lustberg et al., 2020b). These results were perhaps surprising given the significant loss of noradrenergic fibers and NE in projections. However, the increased NE turnover suggests that surviving fibers compensate for the loss of neighboring LC neuron terminals, and we and others have observed adrenergic receptor hypersensitivity following neurotoxic lesions of LC terminals that may also be present here (Wolfman et al., 1994; Szot et al., 2010; Iannitelli et al., 2022). Finally, increased turnover of DA in the pons and PFC at 1-week could be contributing to the anxiety-like and arousal phenotypes seen in pigment-expressing mice at this time point.

On a molecular level, we found that hTyr expression led to the upregulation of several important pathways. Isolation of LC-mRNA with TRAP yielded several hundred genes dysregulated between hTyr and EYFP controls. While many of these genes were significantly – but not robustly on a fold-change level – dysregulated on an individual level, pathway analyses revealed these subtle changes may have a concomitant impact on cellular health and functioning. Unsurprisingly, metabolism of the amino acids tyrosine and tryptophan, in addition to the metabolism of DA itself, were highly enriched in pigmented LC neurons. Similar increases were seen in macroautophagy and lysosome activity, indicating a cellular attempt to clear granules from the cytosol. Importantly, lysosomal dysfunction has been closely linked to PD (Nguyen et al., 2019). The upregulation of several additional pathways were directly linked to the production of pigment granules. These include increases in peroxisome activity (involved in oxidation), the

response to heavy metal ions iron and manganese, and in the pigment metabolic process and pigment granule formation.

Perhaps the most intriguing results from our pathway analyses were the upregulation of specific stress response systems, immune reactions, and subsequent apoptosis in pigmented neurons. Reliable increases in P53 signaling pathways were found throughout each of our analyses, indicating severe cellular stress. Endoplasmic reticulum stress was also a consistent finding in the gene ontology biological processes analysis, revealing that cellular pigment has a severe impact on the crucial function that the endoplasmic reticulum plays in calcium storage, protein synthesis and lipid metabolism. Antigen presentation via MHC-I was the most enriched pathway in all of our analyses, providing a clue about how LC neurons respond to pigment burden. The primary function of MHC-I is to present endogenous particles to signal cytotoxic T-cells, an intervention which leads to cellular destruction. Remarkably, catecholamine neurons are the only neurons known to express MHC-I (Cebrian et al., 2014), providing a tantalizing link between the unique possession of NM and a mechanism for dealing with this burden once it becomes harmful to the cell. In line with this theory, several apoptotic and cell-death-related pathways were also upregulated in our analyses. While these preliminary transcriptomic analyses are informative, further investigation into the specific genes driving these pathway changes is warranted. However, these findings provide preliminary evidence of potential links between our rodent model LC pigmentation and real PD-related symptoms seen in human patients.

Substantial cell death was visible by 6- to 8-weeks post-infusion, and was accompanied by a robust glial response. While microglia are most often associated with clearing extracellular debris, we found that the astrocyte response was dominant in our model. One potential explanation could be the timing of our histological experiments. As others have reported an early microglial

response to pigmented neurons (Carballo-Carbajal et al., 2019), it is possible that the assessment of glia several weeks post-injection represents a late or prolonged immune response, which may be dominated by astrocytes. For this reason, glial responses at the 1-week will be a critical analysis in our future investigations of this rodent model. Neuroinflammation is a well-appreciated aspect of PD (Tansey et al., 2022), and our data suggest that the presence of pigmentation in degenerating LC neurons could be contributing to the neuroimmune response.

This loss of noradrenergic neurons resulted in a decrease of NE and its metabolite in the pons itself, as well as a near-total depletion in both terminal fields assessed. NE turnover was decreased in the pons, but similar to the results obtained at 1-week, turnover was increased in the hippocampus and PFC. DA turnover was also increased in the hippocampus at the 6-week timepoint. This dysregulation may account for the subtle behavioral changes seen despite the significant loss of LC neurons at this end-point. There were no differences between groups in novelty-induced anxiety nor contextual fear memory. The loss of an anxiety-like phenotype at 6-weeks may be explained by a near-total loss of LC-NE, which is required for this behavior (Lustberg et al., 2020c). While contextual fear memory should also require LC innervation of the hippocampus (McGaugh, 2013), recent studies have also implicated DA in hippocampal function and fear memory (Likhtik and Johansen, 2019; Stubbendorff and Stevenson, 2021). Thus, the increase in DA turnover in the hippocampus at 6-weeks may account for the lack of behavioral differences seen in the contextual fear task.

The present study describes the first analysis of pigment induction in the rodent LC, providing critical insight into the consequences of granule accumulation in noradrenergic neurons. We found that pigment expression dysregulates LC neurons on a cellular and molecular level at 1 week, triggering phenotypes reminiscent of non-motor symptoms in prodromal PD. As the

pigment accumulates, immune response and neurodegeneration ensue. By 6-weeks post-infusion, the LC has nearly entirely degenerated, having detrimental effects on neurotransmission but not on mouse behavior. Future work should focus on a mid-point which represents moderate neurodegeneration, as well as a later end-point representing a total loss of LC neurons. Furthermore, pigment-mediated changes in noradrenergic and dopaminergic neurons should be compared to assess the differences in responding and rate of cell death between LC-NM and SN-NM. Indeed, it was reported that hTyr-expressing SN-DA neurons took many months to degenerate (Carballo-Carbajal et al., 2019). It is not clear whether this reflects differences with our model in the virus itself (whatever they used vs Cre-dependent AAV5), species (rat vs mouse), or a true greater vulnerability of LC neurons. Ultimately, this model of pigment induction in rodent catecholamine neurons may be critical for uncovering the role NM plays in PD onset and progression.

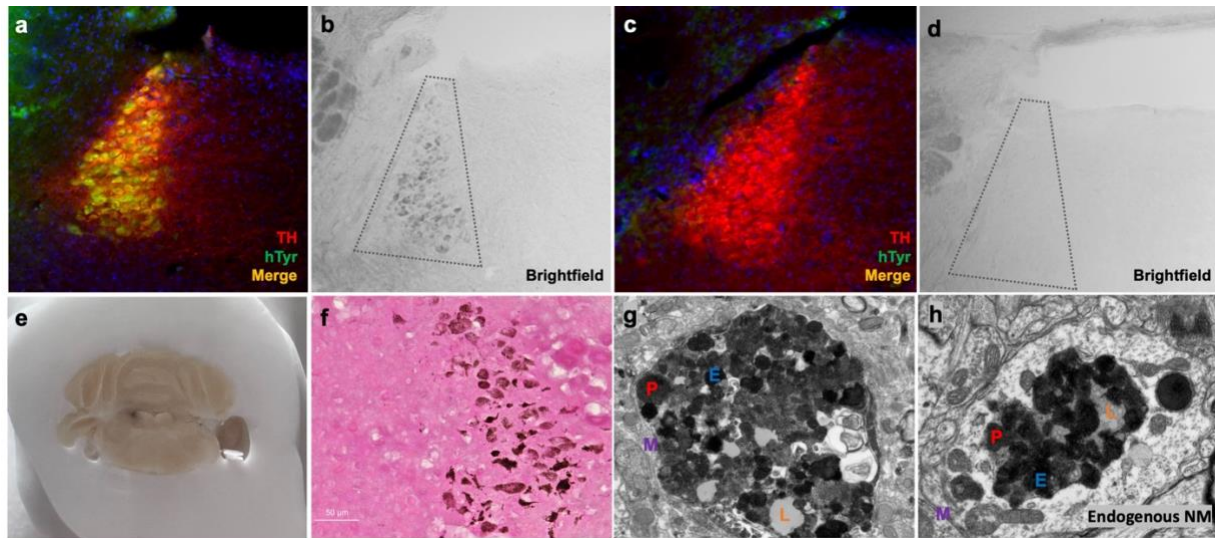


Fig. 3.1. hTyr induces pigmentation in the LC reminiscent of endogenous NM. Mice received stereotaxic injection of AAV5-DIO-hTyr into the LC, driving expression of human Tyrosinase in TH-Cre⁺ experimental animals (a) but not in TH-Cre⁻ controls (c). Although rodents (TH-Cre⁺ image shown here) do not display endogenous NM (d), the presence of hTyr resulted in LC pigmentation visible by brightfield microscopy (b) and gross anatomical inspection (e). This hTyr-derived pigment stained positive for melanin components with Fontana-Masson (f), and electron microscopic analysis of these granules (g) showed they contain several features characteristic of endogenous NM from aged rhesus macaques (h), including pheomelanin (P, red), eumelanin (E, blue), lipid droplets (L, orange), and enclosure in a membrane (M, purple).

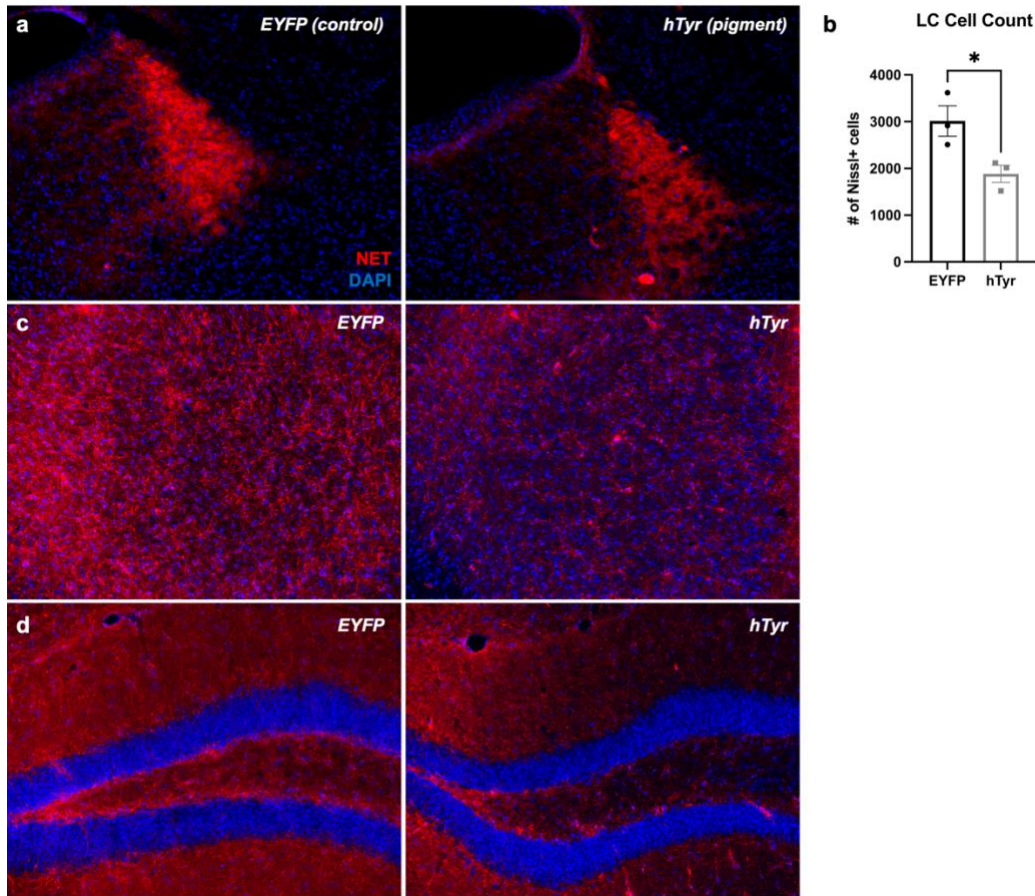


Fig. 3.2. The presence of NM-like pigmentation damages LC cell bodies and fibers at 1-week.

TH-Cre mice received LC infusion of AAV5-DIO-hTyr or EYFP control and were assessed for locus coeruleus (LC) neuron damage 1 week later. hTyr-induced pigment expression resulted in substantial loss of axon terminals as measured by norepinephrine transporter (NET) immunoreactivity in the dentate gyrus (DG) (d) and anterior cingulate cortex (ACC) (c), with a similar decrease in NET also present in the LC itself (a). Concurrent with NE fiber damage was a decrease in LC cell body number as measured by NeuroTrace Nissl immunoreactivity (b). Images acquired at 20X. Data shown as mean \pm SEM. N=3 per group. **p<0.01, ***p<0.001, ****p<0.0001.

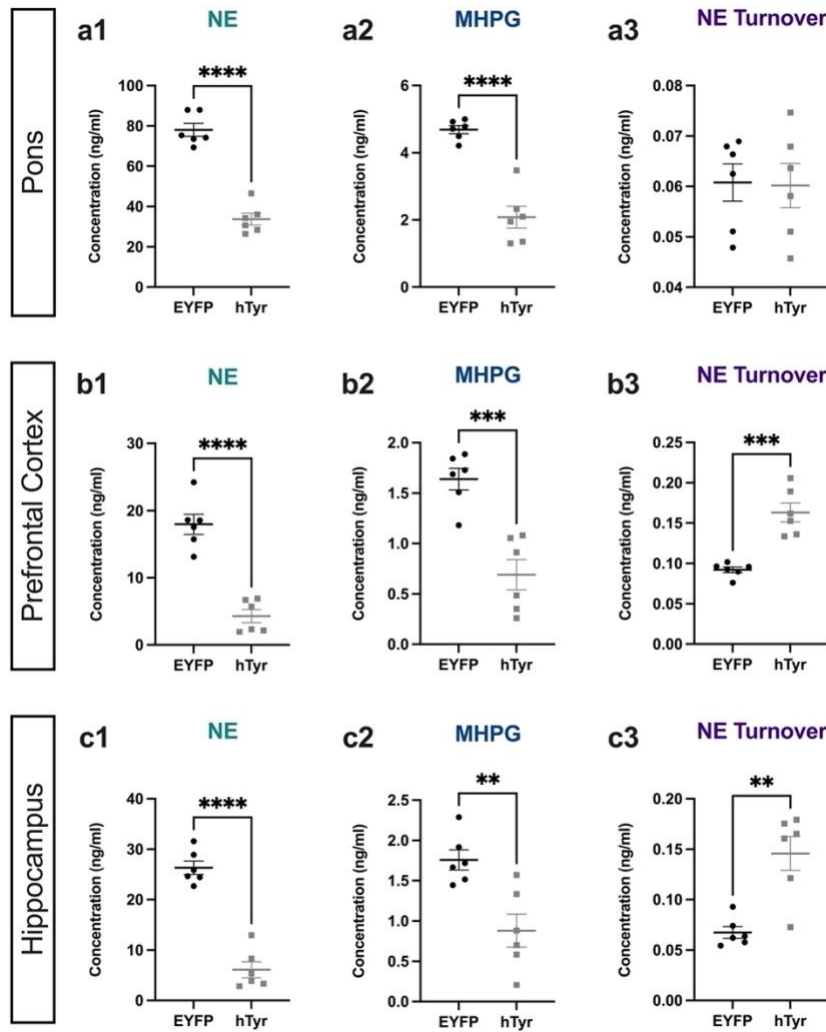


Fig. 3.3. hTyr-induced pigmentation decreases tissue NE and metabolite levels and increases turnover at 1 week. TH-Cre mice received stereotaxic infusion of AAV-DIO-hTyr or EYFP control into the LC, and tissue monoamine and metabolite levels were measured 1 week later by HPLC in the pons, prefrontal cortex (PFC), and hippocampus. hTyr significantly decreased NE and its primary metabolite MHPG in the pons (**a1-2**), PFC (**b1-2**), and hippocampus (**c1-2**). NE turnover, defined as the MHPG:NE ratio, was increased in PFC (**b3**) and hippocampus (**c3**). Data shown as mean \pm SEM. N=6 per group. * p <0.05, ** p <0.01, **** p <0.0001.

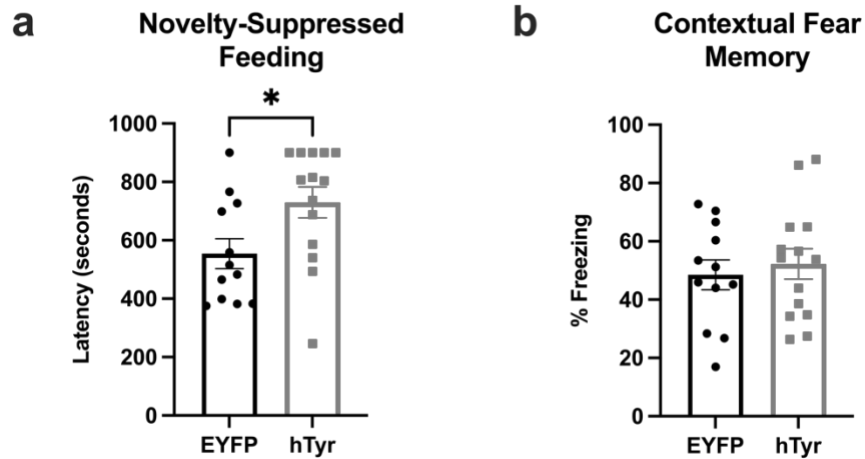


Fig. 3.4. hTyr-induced pigmentation increases novelty-induced anxiety but not contextual fear memory at 1 week. TH-Cre mice received stereotaxic infusion of AAV-DIO-hTyr or EYFP control into the LC, and behavior was assessed 1 week later. hTyr-expressing mice increased latency to bite the food pellet in the novelty-suppressed feeding test (**a**), but no difference in freezing behavior in the contextual conditioning fear assay (**b**) (N=12-14 per group).

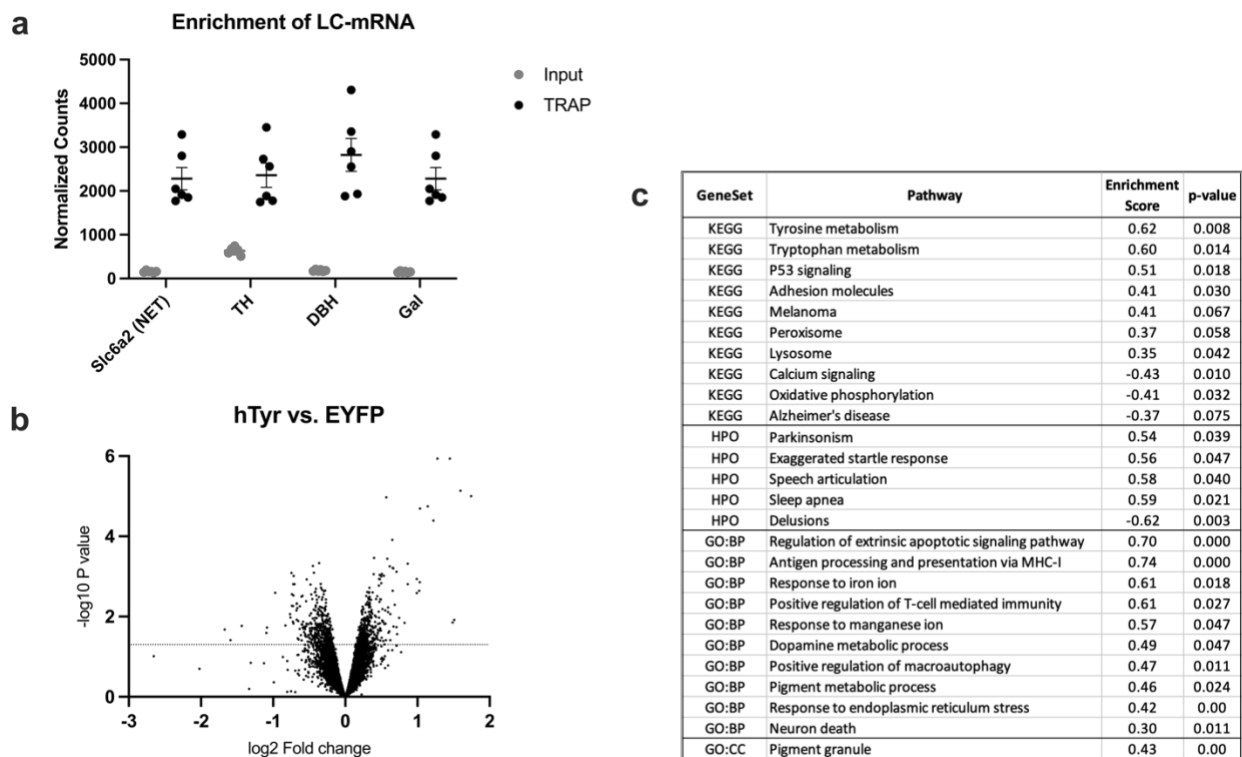


Fig. 3.5. hTyr-driven pigmentation triggers changes in the LC transcriptome. TH-Cre; Slc6a2-eGFP/Rpl10a mice received viral infusion of AAV5-DIO-hTyr or EYFP control in the LC, and gene expression was assessed 1 week later. We confirmed LC-mRNA enrichment in TRAP samples over hindbrain input, and found elevated levels of noradrenergic genes in the immunoprecipitated TRAP samples (a). Volcano plot of all filtered, normalized genes (~11,500) displaying spread of up- and down-regulated genes (b). Table highlighting significantly enriched KEGG, Human Phenotype Ontology (HPO), Gene Ontology Biological Process (GO:BP) and Gene Ontology Cellular Component (GO:CC) pathways of interest in our LC data (c).

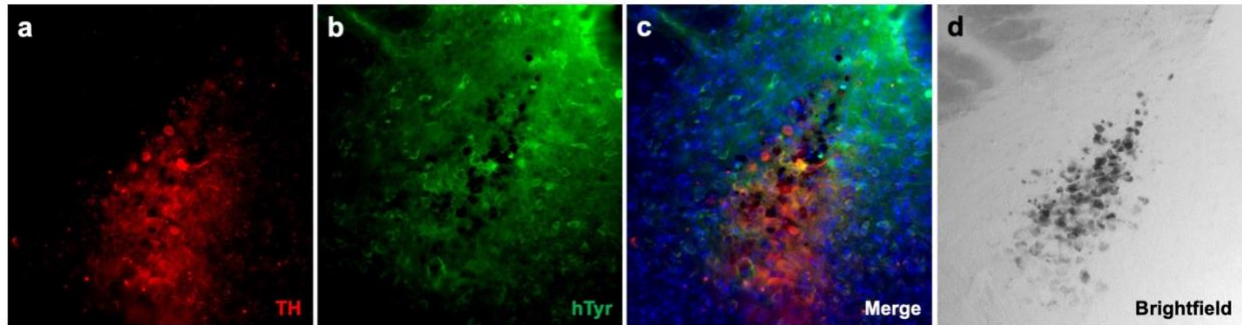


Fig. 3.6: Prolonged pigment expression results in granule accumulation and LC degeneration. TH-Cre mice received stereotaxic infusion of AAV-DIO-hTyr into the LC and aged for 8 weeks prior to tissue extraction and immunohistochemical assessment of LC integrity with noradrenergic marker tyrosine hydroxylase (TH) (**a**). Although expression of hTyr has diminished by 8-weeks post-injection, presumably due to loss of LC cell bodies (**b**), pigmentation remains robust in the region (**d**).

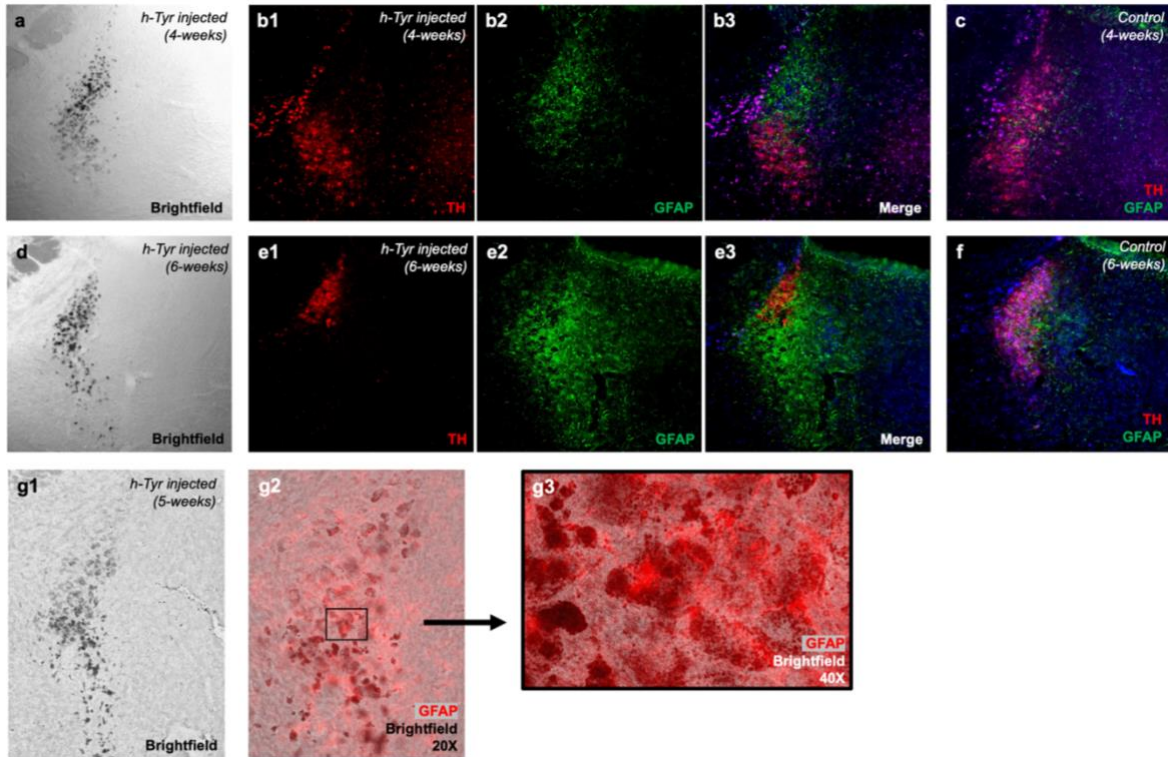


Fig. 3.7: Pigment-induced neurodegeneration triggers astrocyte responses in and around the LC. TH-Cre mice received AAV5-DIO-hTyr, and tissue was assessed for neuroinflammation as a result of pigment accumulation at 4-6 weeks. Over time, hTyr-induced pigmentation accumulated and darkened in the LC (**a**). Representative images show that astrocyte reactivity, as measured by GFAP immunostaining, was appreciably increased in the LC of hTyr-injected (**b**), but not non-expressing control mice (**c**). This process was exacerbated over time, with pigmentation becoming even more robust by 6-weeks (**d**) despite the near-total loss of TH-positive neurons (**e1**). LC neurodegeneration was accompanied by glial scarring of the region (**e**) that is not seen in non-expressing controls (**f**). Overlaying brightfield and fluorescent micrographs of the region revealed a potential interaction between astrocytes and pigment granules (**g**).

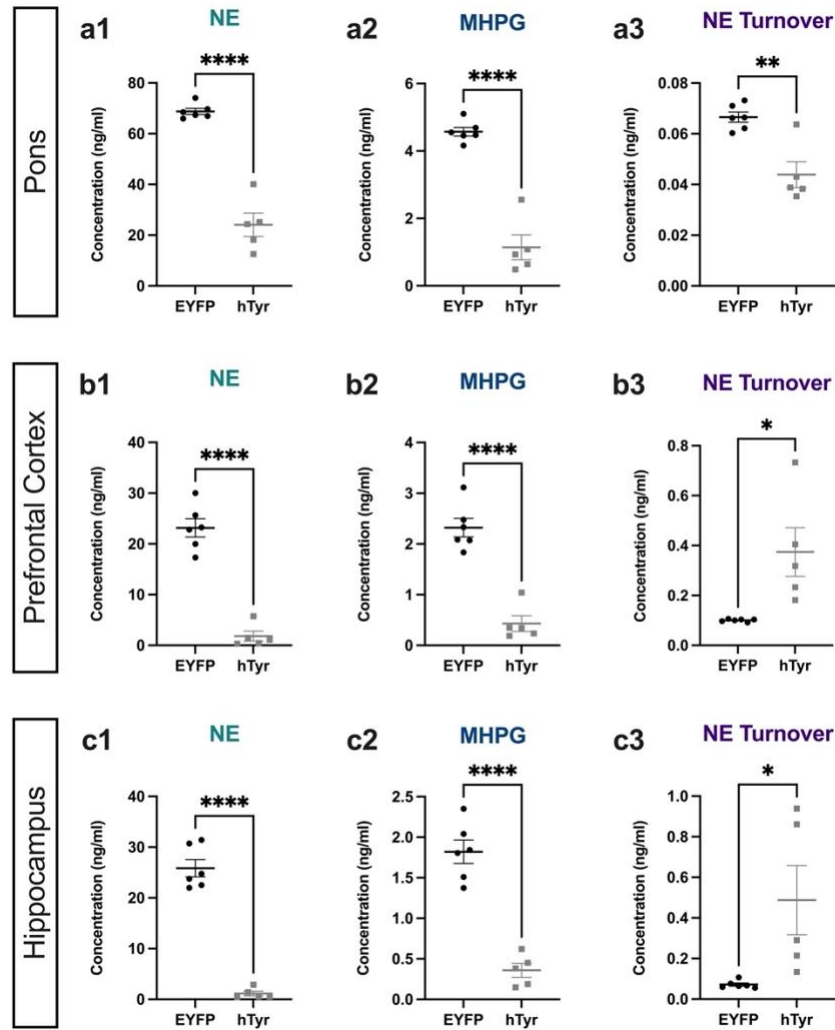


Fig. 3.8. hTyr-induced pigmentation depletes tissue NE and metabolite levels and dysregulates turnover at 6 weeks. TH-Cre mice received stereotaxic infusion of AAV5-DIO-hTyr or EYFP control into the LC, and tissue monoamine and metabolite levels were measured 6 weeks later by HPLC in the pons, prefrontal cortex (PFC), and hippocampus. hTyr significantly and robustly decreased NE and metabolite MHPG in the pons (**a1-2**), PFC (**b1-2**), and hippocampus (**c1-2**). NE turnover (MHPG:NE ratio) was decreased in the pons (**a3**), but decreased in the PFC (**b3**) and hippocampus (**c3**). Data shown as mean \pm SEM. N=8 per group. * p <0.05, ** p <0.01, **** p <0.0001.

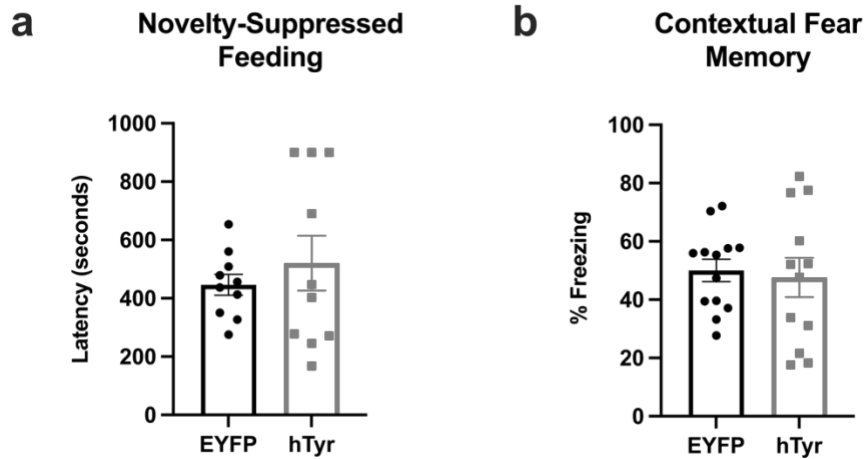


Fig. 3.9. Pigment accumulation and subsequent neurodegeneration does not affect novelty-induced anxiety or contextual fear memory by 6-weeks. TH-Cre mice received stereotaxic infusion of AAV5-DIO-hTyr or EYFP control into the LC, and behavior was assessed 6 weeks later. hTyr-expressing mice displayed no difference in latency to bite the food pellet in the novelty-suppressed feeding test at 6-week post-infusion (**a**), and no difference in freezing behavior in the contextual fear assay (**b**) (N=12-14 per group).

CHAPTER 4: DISCUSSION

4.1 SUMMARY

This dissertation sought to understand noradrenergic dysfunction in the context of neurodegenerative diseases. To accomplish this, we utilized the LC-specific neurotoxin DSP-4 and developed a novel model of LC pigmentation in mice. We assessed both models on a molecular, cellular, and behavioral level to fully characterize the impact these insults have on LC survival and functioning. We demonstrated that noradrenergic fiber damage, which precedes outright cell loss, has a profound effect on the transcriptional profile and cellular functioning of the LC, which leads to behavioral changes reminiscent of the prodromal aspects of neurodegenerative diseases. Once the cell bodies begin to die, these molecular, cellular, and behavioral changes are coupled with a robust neuroinflammatory response. Due to the widespread innervation by the LC-NE system, this dysfunction and subsequent degeneration of noradrenergic neurons has downstream effects impacting the entire brain. Ultimately, we believe that these features contribute to the early, prodromal symptoms patients experience in both Alzheimer's and Parkinson's diseases (AD; PD).

4.2 CONCLUSIONS AND FUTURE DIRECTIONS

4.2.1 DSP-4

Although the LC-specific neurotoxin DSP-4 has been used to study noradrenergic dysfunction for several decades, the precise molecular mechanisms underlying the ultimate effects of this compound are not fully understood. One obstacle to comprehensively understanding the consequences of DSP-4 has been the use of several different model organisms and dosing regimens between experiments. This has made results difficult to integrate and interpret between studies. Additionally, previous work has been mostly confined to studying just one feature of LC dysfunction, such as cell firing or changes in behavior. Furthermore, prior characterizations of this

model have mostly lacked molecular genetic assessments due to the technical limitations of studying effects in such a small nucleus. Thus, our study sought to comprehensively assess the effects of DSP-4 on a molecular, cellular, and behavioral level in the same species in tandem experiments.

In line with previous work (Grzanna et al., 1989; Theron et al., 1993; Wolfman et al., 1994; Harro et al., 1999; Szot et al., 2010), we found that two administrations of DSP-4 (50 mg/kg), spaced one week apart, resulted in LC terminal damage and a concurrent depletion of NE and its metabolite MHPG in the pons itself, as well as in hippocampal and cortical projection regions. Despite a decrease in the concentration of these catechols, rate of NE turnover, as measured by the ratio of MHPG:NE, was increased significantly in the pons and prefrontal cortex (PFC), with similar trends also seen in the hippocampus, potentially signifying compensatory elevation of NE release from surviving fibers (Jacobs, 2019; van Hooren et al., 2021; Gilvesy et al., 2022). These changes, combined with receptor hypersensitivity following DSP-4 administration (Wolfman et al., 1994; Szot et al., 2010), likely contribute to the behavioral phenotypes we saw in DSP-4 treated animals.

DSP-4 administration led to an increase in novelty-induced anxiety and locomotor activity in our studies, results which are consistent with previous reports that surgical or neurotoxin ablation of the LC in rats induces similar anxiety-like phenotypes that reflect responses to novelty stress (Martin-Iverson et al., 1982; Harro et al., 1995). This novelty-induced anxiety was coupled with an increase in Arc immunoreactivity, a marker for neuronal activity which is induced by stimulation of adrenergic receptors (Essali and Sanders, 2016). Despite these changes, baseline firing of LC neurons was unaffected in DSP-4-treated mice, indicating that the anxiogenic effects

of this treatment are more reflective of compensatory changes in NE release and postsynaptic transmission than a change in cell body activity.

This study presented the first population-wide transcriptional analysis of the LC following DSP-4 treatment. In line with immunohistochemical observations (Grzanna et al., 1989; Theron et al., 1993; Wolfman et al., 1994; Harro et al., 1999), we observed a downregulation of several LC-enriched genes that encode noradrenergic specification and/or function, including *Th*, *Slc6a2* (NET), *Dbh*, *Phox2a*, and *Gal*. The suppression of these genes in the LC of DSP-4 treated mice indicates a loss of critical functioning in these cells as they become damaged and are unable to maintain their noradrenergic identity.

Future directions of this work should focus on answering several questions regarding DSP-4 treatment in mice. The first issue that should be addressed is whether the behavioral and metabolic changes we observed as a result of DSP-4 administration are indicative of increased NE transmission from the remaining LC fibers. While our data suggest that increased NE transmission can account for the Arc immunoreactivity, increased NE turnover, and novelty-induced anxiety results, the methods utilized in the present study did not measure NE release directly. Thus, future experiments should utilize emerging techniques for measuring neurotransmission, such as the GPCR activation-based (GRAB) sensors developed for the detection of NE (Feng et al., 2019). The employment of GRAB-NE sensors would allow for temporally-sensitive measurements of NE release in awake, behaving animals, which would be particularly useful for measuring NE release in the stress paradigms that showed increased Arc activity. However, a potential limitation is that the profound decrease in total NE with DSP-4 administration may result in extracellular levels of NE below the limit of detection for GRAB-NE sensors.

In addition to this, electrophysiological recordings from unanesthetized animals may also provide insights into the activity of LC neurons in response to various stimuli. DSP-4-treated mice displayed increased anxiety-like behavior in both the novelty-suppressed feeding and marble burying tasks, indicating an increase in LC firing. As we did not observe any differences in baseline firing in our electrophysiological recordings, these data may indicate that LC hyperactivation in DSP-4-treated mice may be context-specific. Thus, recordings from awake, behaving mice would allow for the assessment of LC activation in a novel context. Based on the behavioral output, we anticipate that treated mice would display increased LC firing specifically during these tasks.

Finally, our TRAP results have provided a wealth of information regarding the molecular changes LC neurons undergo in response to DSP-4. The most robustly and significantly downregulated genes were those involved in catecholamine synthesis and transmission. Several of these pathways, such as those involved in cancer-related cellular stress, were unexpected. However, they do provide a framework for future hypotheses regarding DSP-4-mediated neurodegeneration of the LC. Below, I present several methods for manipulating gene expression *in vivo*, including viral vector delivery and genetic knockout. If specific genes of interest are identified in the TRAP data, these methods could also be employed for mediating the effects of DSP-4.

4.2.2 Neuromelanin

Along with substantia nigra DA neurons, the LC is the only structure in the brain that produces appreciable amounts of neuromelanin (NM), a dark brown cytoplasmic pigment. It has been proposed that these NM granules initially play a protective role by sequestering toxic catecholamine metabolites and heavy metals, but become harmful during aging and particularly in

PD as they overwhelm cellular machinery and get released during neurodegeneration. Because rodents do not naturally produce NM, the study of this pigment has been mostly limited to human postmortem studies, and it has not been possible to establish causal relationships between NM and PD-associated LC pathology. We adapted a viral-mediated approach for expression of human tyrosinase (hTyr), the enzyme responsible for peripheral melanin production, to promote pigmentation in rodent LC neurons.

In chapter 3, I presented the first characterization of a rodent model of LC-NM expression. We found that expression of hTyr in the LC drives visible pigmentation as early as 1-week post-infusion. Importantly, the pigment granules expressed by this rodent model contain several key features of endogenous NM. Electron microscopy revealed ultrastructural similarities between the enzyme-derived pigment and natural pigment obtained from aged Rhesus macaques, including the presence of both pheomelanin and eumelanin, large lipid droplets, and a double-membrane surrounding the granule. Pigment from this mouse model also stained positive for melanin components with the Fontana-Masson stain.

Pigment expression resulted in mild LC degeneration and a depletion of catecholamine levels as early as 1 week post-injection. However, rates of NE turnover were increased in both the PFC and hippocampus, which may contribute to the emergence of anxiety-like behavior observed in pigment-expressing mice. Concurrent with these changes were several dysregulated genes and pathways.

The most notable transcriptional changes were those related to cell death pathways, endoplasmic reticulum stress, and antigen presentation. Because pigmentation induces LC degeneration, it is perhaps unsurprising that we found many apoptotic pathways enriched in samples from hTyr mice. Although the mechanism of this NM-mediated cell death is not well

understood, our data provide compelling evidence for the upregulation of antigen presentation via MHC-I. Unlike MHC-II, which is involved in the innate immune response, MHC-I is critical for adaptive immunity. Once MHC-I identifies an endogenous threat, it presents the antigen on the cell surface. This antigen presentation signals for cytotoxic T-cells to intervene and destroy the cell. Interestingly, catecholamine neurons are the only neurons known to express MHC-I (Cebrian et al., 2014). As they are also the only neurons to possess endogenous pigmented granules, which can become burdensome to the cell over time, the link between these two characteristics is intriguing. Our transcriptomic results provide evidence to support a link between NM and MHC-I-mediated cell death, as this pathway was the most robustly and significantly upregulated in our mouse model of LC pigmentation. Based on these data, we believe that the unique presence of MHC-I on catecholamine neurons may help these cells self-immolate by presenting neuromelanin particles to trigger the immune response. One way of testing this hypothesis is by expressing hTyr in the LC of MHC-I knockout mice. If antigen presentation by MHC-I is mediating the neurodegenerative response to NM-like pigmentation, then these mice should display decreased or delayed noradrenergic neuron loss in response to pigment granules.

Further support for this theory is found in the robust immune response of hTyr mice after several weeks of pigment expression. As the LC neurons die, astrocytes infiltrate the region and form a glial scar. Work has been done characterizing the relationship between T-cells and astrocytes, particularly in neurodegenerative disease (Xie and Yang, 2015). To more thoroughly understand this interaction, future research with this model should employ astrocyte primary cultures to investigate their specific reactions to LC-NM.

By 6 weeks, the accumulation of this pigment results in severe LC neurodegeneration in our rodent model. Concurrent with this cell loss is a near-total depletion of tissue NE and

metabolite levels. Despite this loss of cellular integrity and functioning, LC-sensitive behavioral responses are surprisingly unchanged between pigment-expressing and control animals. Perhaps this is due to the increased NE and DA turnover at this time point, indicating that the surviving neurons are compensating for the loss. Alternatively, the normalization of anxiety-like behavior in 6-week animals may reflect the progressive loss of LC-NE, which prevents any increased turnover from the few surviving terminals from promoting anxiety. Further investigations should assess behavior at later time points, when all LC neurons and projections are lost.

Many of these molecular and early behavioral phenotypes are reminiscent of LC dysfunction in PD, validating the utility of this model for studying the consequences of pigment accumulation in the LC as it relates to neurodegenerative disease. As this is a novel rodent model of NM-like pigment expression in the LC, its characterization will inform many lines of future work. In order to achieve this, though, issues with viral vector consistency must be addressed to ensure that each batch of virus has similar effects *in vivo*. To combat this issue, I propose the development of a transgenic model expressing hTyr under an LC-specific promoter, such as NET or Dbh. This will allow for consistency between experiments, but also will potentially slow the progression of pigment accumulation due to the use of weaker promoters, allowing for more thorough analysis of time points when cells are expressing pigment but have not yet died.

Additionally, the molecular composition of these granules should be investigated further with techniques such as mass spectrometry. Electron microscopy allowed for ultrastructural visualization of these granules, however, there are several known components of true NM that are not visible with brightfield microscopy alone. These features are also difficult to stain for with immunohistochemical techniques because antibodies cannot penetrate the membrane-bound granules. Thus, methods like the laser-capture mass spectrometry technique MALDI (Rompp and

Spengler, 2013) would permit the analysis of their lipid, metal ion, and protein components directly from brain sections. These results could be compared to the mass spectrometry studies of human NM granules (Zecca et al., 1992), providing insight into the similarities and differences between hTyr-induced pigmentation and endogenous NM.

A promising future study should examine the effects overexpressing vesicular monoamine transporter 2 (VMAT2), which sequesters catecholamines in synaptic vesicles, has on NM accumulation and toxicity in both the LC and SN. Cytoplasmic NE, DA, and their metabolites are significant contributors to NM (Sulzer et al., 2000; Zecca et al., 2001), and I hypothesize that facilitating vesicular packaging of NE and DA will reduce their cytoplasmic concentration and subsequent conversion into toxic metabolites, which should slow the rate of NM accumulation. VMAT2-HI transgenic mice have a twofold increase in transporter expression in all catecholamine neurons (Lohr et al., 2014), which protects against MPTP and methamphetamine toxicity (Lohr et al., 2016). I predict that this mechanism will also be sufficient to protect neurons from deleterious hTyr-induced NM granule accumulation. However, if this transgenic overexpression is not robust enough, a viral vector-based strategy may also be adapted to drive even higher expression.

Additionally, the potential of metal chelation for mitigating harmful NM accumulation should also be investigated. NM granules contain appreciable amounts of heavy metals, most notably iron and copper (Zecca et al., 2003b). The SN and LC have some of the highest heavy metal loads within the brain, as iron is produced as a byproduct of DA synthesis, while copper is required by the NE synthesis enzyme dopamine beta-hydroxylase (DBH). Furthermore, it has been suggested that heavy metal exposure from the environment is a contributing factor to the development of PD (Lan and Jiang, 1997; Freire and Koifman, 2012), as these molecules directly contribute to oxidative stress and glial responses (Dichtl et al., 2018). Metal chelation therapy has

been successfully employed to treat rodent models of leukemia (Chan et al., 2021), and thus, future work should adapt these approaches to buffer the harmful effects of NM in the LC and SN. NM-expressing mice can be treated with either an iron chelator (e.g. deferasirox), or a copper chelator (e.g. Penicillamine). I predict that administration of metal chelators will significantly suppress hTyr-induced NM accumulation in catecholamine neurons, slowing the rate of neurodegeneration. The transcriptomic data obtained in my thesis experiments has identified dysregulated genes and pathways resulting from NM burden in neurons, many of which have been studied in the context of PD. Manipulating these novel pathways to intervene in NM-driven neurodegeneration is a promising line of future research.

This model can also be used to investigate the interactions between NM and neurodegenerative disease pathologies. For example, whether endogenous mouse hyperphosphorylated tau or a-syn is contained within the pigment granules should be assessed. If there is no incorporation of these protein aggregates at baseline, we should employ transgenic and viral vector strategies for driving pathological tau and a-syn in the LC, and determine whether the combination of these models can provide insights into the way NM granules interact with AD and PD pathology.

5.3 CONCLUDING REMARKS

This dissertation assessed noradrenergic dysfunction in neurodegenerative disease using two separate but complimentary mouse models of disease. I found that the LC-specific neurotoxin DSP-4 recapitulates behavioral aspects of prodromal AD and PD, including novelty-induced anxiety, while leaving cellular mechanisms largely intact. This model is particularly useful for studying the earliest prodromal aspects of neurodegeneration, when LC fiber damage

predominates. On the other hand, hTyr-induced LC pigmentation recapitulates a true neurodegenerative phenotype in mice with robust cell body loss. This model allowed us to assess the impact of noradrenergic neuron loss as it relates to AD and PD, and compared to DSP-4, we found that hTyr-injected mice showed more severe cellular and molecular changes. Thus, these models are complimentary for assessing the full array of LC dysfunction in disease. While DSP-4 mimics early changes related to axon damage, hTyr-induced pigmentation allows for investigation into the late-stage effects of LC degeneration. The development of these models will enable future research focused on specific aspects of noradrenergic dysfunction in neurodegenerative disease, allowing for the research and development of treatments focused on the prodromal, LC-associated symptoms of AD and PD.

REFERENCES

- (2022) 2022 Alzheimer's disease facts and figures. *Alzheimers Dement* 18:700-789.
- Aghajanian GK, Cedarbaum JM, Wang RY (1977) Evidence for norepinephrine-mediated collateral inhibition of locus coeruleus neurons. *Brain Res* 136:570-577.
- Ahmed H, Abushouk AI, Gabr M, Negida A, Abdel-Daim MM (2017) Parkinson's disease and pesticides: A meta-analysis of disease connection and genetic alterations. *Biomed Pharmacother* 90:638-649.
- Alhayek S, Preuss CV (2022) Beta 1 Receptors. In: *StatPearls*. Treasure Island (FL).
- Allen B, Ingram E, Takao M, Smith MJ, Jakes R, Virdee K, Yoshida H, Holzer M, Craxton M, Emson PC, Atzori C, Migheli A, Crowther RA, Ghetti B, Spillantini MG, Goedert M (2002) Abundant tau filaments and nonapoptotic neurodegeneration in transgenic mice expressing human P301S tau protein. *J Neurosci* 22:9340-9351.
- Allen MT, Levy LS (2013) Parkinson's disease and pesticide exposure--a new assessment. *Crit Rev Toxicol* 43:515-534.
- Alonso AC, Grundke-Iqbal I, Iqbal K (1996) Alzheimer's disease hyperphosphorylated tau sequesters normal tau into tangles of filaments and disassembles microtubules. *Nat Med* 2:783-787.
- Antila H, Kwak I, Choi A, Pisciotti A, Covarrubias I, Baik J, Eisch A, Beier K, Thomas S, Weber F, Chung S (2022) A noradrenergic-hypothalamic neural substrate for stress-induced sleep disturbances. *Proc Natl Acad Sci U S A* 119:e2123528119.
- Arnulf I, Leu-Semenescu S (2009) Sleepiness in Parkinson's disease. *Parkinsonism Relat Disord* 15 Suppl 3:S101-104.

Aston-Jones G, Bloom FE (1981) Activity of norepinephrine-containing locus coeruleus neurons in behaving rats anticipates fluctuations in the sleep-waking cycle. *J Neurosci* 1:876-886.

Aston-Jones G, Rajkowski J, Cohen J (1999) Role of locus coeruleus in attention and behavioral flexibility. *Biol Psychiatry* 46:1309-1320.

Aurora RN, Zak RS, Auerbach SH, Casey KR, Chowdhuri S, Karippot A, Maganti RK, Ramar K, Kristo DA, Bista SR, Lamm CI, Morgenthaler TI, Standards of Practice C, American Academy of Sleep M (2010) Best practice guide for the treatment of nightmare disorder in adults. *J Clin Sleep Med* 6:389-401.

Balestrino R, Schapira AHV (2020) Parkinson disease. *Eur J Neurol* 27:27-42.

Barden H, Levine S (1983) Histochemical observations on rodent brain melanin. *Brain Res Bull* 10:847-851.

Bartfai T, Iverfeldt K, Fisone G, Serfozo P (1988) Regulation of the release of coexisting neurotransmitters. *Annu Rev Pharmacol Toxicol* 28:285-310.

Beitz JM (2014) Parkinson's disease: a review. *Front Biosci (Schol Ed)* 6:65-74.

Bekris LM, Mata IF, Zabetian CP (2010a) The genetics of Parkinson disease. *J Geriatr Psychiatry Neurol* 23:228-242.

Bekris LM, Yu CE, Bird TD, Tsuang DW (2010b) Genetics of Alzheimer disease. *J Geriatr Psychiatry Neurol* 23:213-227.

Belkin MR, Schwartz TL (2015) Alpha-2 receptor agonists for the treatment of posttraumatic stress disorder. *Drugs Context* 4:212286.

Berger Z, Roder H, Hanna A, Carlson A, Rangachari V, Yue M, Wszolek Z, Ashe K, Knight J, Dickson D, Andorfer C, Rosenberry TL, Lewis J, Hutton M, Janus C (2007) Accumulation

- of pathological tau species and memory loss in a conditional model of tauopathy. *J Neurosci* 27:3650-3662.
- Berridge CW, Foote SL (1996) Enhancement of behavioral and electroencephalographic indices of waking following stimulation of noradrenergic beta-receptors within the medial septal region of the basal forebrain. *J Neurosci* 16:6999-7009.
- Bissette G, Klimek V, Pan J, Stockmeier C, Ordway G (2003) Elevated concentrations of CRF in the locus coeruleus of depressed subjects. *Neuropsychopharmacology* 28:1328-1335.
- Blennow K, Zetterberg H (2018) Biomarkers for Alzheimer's disease: current status and prospects for the future. *J Intern Med* 284:643-663.
- Bonifati V, Rizzu P, Squitieri F, Krieger E, Vanacore N, van Swieten JC, Brice A, van Duijn CM, Oostra B, Meco G, Heutink P (2003) DJ-1 (PARK7), a novel gene for autosomal recessive, early onset parkinsonism. *Neurol Sci* 24:159-160.
- Bonifati V et al. (2005) Early-onset parkinsonism associated with PINK1 mutations: frequency, genotypes, and phenotypes. *Neurology* 65:87-95.
- Bouret S, Sara SJ (2005) Network reset: a simplified overarching theory of locus coeruleus noradrenaline function. *Trends Neurosci* 28:574-582.
- Braak H, Braak E (1995) Staging of Alzheimer's disease-related neurofibrillary changes. *Neurobiol Aging* 16:271-278; discussion 278-284.
- Braak H, Braak E (2000) Pathoanatomy of Parkinson's disease. *J Neurol* 247 Suppl 2:II3-10.
- Braak H, Thal DR, Ghebremedhin E, Del Tredici K (2011) Stages of the pathologic process in Alzheimer disease: age categories from 1 to 100 years. *J Neuropathol Exp Neurol* 70:960-969.

- Bremner JD, Krystal JH, Southwick SM, Charney DS (1996a) Noradrenergic mechanisms in stress and anxiety: I. Preclinical studies. *Synapse* 23:28-38.
- Bremner JD, Krystal JH, Southwick SM, Charney DS (1996b) Noradrenergic mechanisms in stress and anxiety: II. Clinical studies. *Synapse* 23:39-51.
- Brunden KR, Trojanowski JQ, Lee VM (2009) Advances in tau-focused drug discovery for Alzheimer's disease and related tauopathies. *Nat Rev Drug Discov* 8:783-793.
- Brundin P, Melki R (2017) Prying into the Prion Hypothesis for Parkinson's Disease. *J Neurosci* 37:9808-9818.
- Budson AE, Price BH (2005) Memory dysfunction. *N Engl J Med* 352:692-699.
- Busch C, Bohl J, Ohm TG (1997) Spatial, temporal and numeric analysis of Alzheimer changes in the nucleus coeruleus. *Neurobiol Aging* 18:401-406.
- Bush WD, Garguilo J, Zucca FA, Albertini A, Zecca L, Edwards GS, Nemanich RJ, Simon JD (2006) The surface oxidation potential of human neuromelanin reveals a spherical architecture with a pheomelanin core and a eumelanin surface. *Proc Natl Acad Sci U S A* 103:14785-14789.
- Butkovich LM, Houser MC, Chalermplanupap T, Porter-Stransky KA, Iannitelli AF, Boles JS, Lloyd GM, Coomes AS, Eidson LN, De Sousa Rodrigues ME, Oliver DL, Kelly SD, Chang J, Bengoa-Vergniory N, Wade-Martins R, Giasson BI, Joers V, Weinshenker D, Tansey MG (2020) Transgenic Mice Expressing Human alpha-Synuclein in Noradrenergic Neurons Develop Locus Coeruleus Pathology and Nonmotor Features of Parkinson's Disease. *J Neurosci* 40:7559-7576.
- Butkovich LM, Houser, M.C., Chalermplanupap, T., Porter-Stransky, K.A., Eidson, L.N., De Sousa Rodrigues, M. E., Oliver, D.L., Kelly, S.D., Chang, J., Bengoa-Vergniory, N.,

- Wade-Martins, R., Weinshenker, D., Tansey, M.G. (2019) Transgenic mice expressing human alpha-synuclein in noradrenergic neurons develop locus coeruleus pathology and non-motor features of Parkinson's disease. *BioRxiv*.
- Carballo-Carbajal I, Laguna A, Romero-Gimenez J, Cuadros T, Bove J, Martinez-Vicente M, Parent A, Gonzalez-Sepulveda M, Penuelas N, Torra A, Rodriguez-Galvan B, Ballabio A, Hasegawa T, Bortolozzi A, Gelpi E, Vila M (2019) Brain tyrosinase overexpression implicates age-dependent neuromelanin production in Parkinson's disease pathogenesis. *Nat Commun* 10:973.
- Carter ME, Yizhar O, Chikahisa S, Nguyen H, Adamantidis A, Nishino S, Deisseroth K, de Lecea L (2010) Tuning arousal with optogenetic modulation of locus coeruleus neurons. *Nat Neurosci* 13:1526-1533.
- Cassidy CM, Therriault J, Pascoal TA, Cheung V, Savard M, Tuominen L, Chamoun M, McCall A, Celebi S, Lussier F, Massarweh G, Soucy JP, Weinshenker D, Tardif C, Ismail Z, Gauthier S, Rosa-Neto P (2022) Association of locus coeruleus integrity with Braak stage and neuropsychiatric symptom severity in Alzheimer's disease. *Neuropsychopharmacology* 47:1128-1136.
- Castellano JM, Kim J, Stewart FR, Jiang H, DeMattos RB, Patterson BW, Fagan AM, Morris JC, Mawuenyega KG, Cruchaga C, Goate AM, Bales KR, Paul SM, Bateman RJ, Holtzman DM (2011) Human apoE isoforms differentially regulate brain amyloid-beta peptide clearance. *Sci Transl Med* 3:89ra57.
- Cebrian C, Zucca FA, Mauri P, Steinbeck JA, Studer L, Scherzer CR, Kanter E, Budhu S, Mandelbaum J, Vonsattel JP, Zecca L, Loike JD, Sulzer D (2014) MHC-I expression

- renders catecholaminergic neurons susceptible to T-cell-mediated degeneration. *Nat Commun* 5:3633.
- Cerf E, Gustot A, Goormaghtigh E, Ruyschaert JM, Raussens V (2011) High ability of apolipoprotein E4 to stabilize amyloid-beta peptide oligomers, the pathological entities responsible for Alzheimer's disease. *FASEB J* 25:1585-1595.
- Chalermphanupap T, Schroeder JP, Rorabaugh JM, Liles LC, Lah JJ, Levey AI, Weinshenker D (2018) Locus Coeruleus Ablation Exacerbates Cognitive Deficits, Neuropathology, and Lethality in P301S Tau Transgenic Mice. *J Neurosci* 38:74-92.
- Chan LSA, Gu LC, Wells RA (2021) The effects of secondary iron overload and iron chelation on a radiation-induced acute myeloid leukemia mouse model. *BMC Cancer* 21:509.
- Chan-Palay V (1991a) Locus coeruleus and norepinephrine in Parkinson's disease. *Jpn J Psychiatry Neurol* 45:519-521.
- Chan-Palay V (1991b) Alterations in the locus coeruleus in dementias of Alzheimer's and Parkinson's disease. *Prog Brain Res* 88:625-630.
- Cicchetti F, Lapointe N, Roberge-Tremblay A, Saint-Pierre M, Jimenez L, Ficke BW, Gross RE (2005) Systemic exposure to paraquat and maneb models early Parkinson's disease in young adult rats. *Neurobiol Dis* 20:360-371.
- Cohen D, Eisdorfer C, Gorelick P, Paveza G, Luchins DJ, Freels S, Ashford JW, Semla T, Levy P, Hirschman R (1993) Psychopathology associated with Alzheimer's disease and related disorders. *J Gerontol* 48:M255-260.
- Cohen RM, Rezai-Zadeh K, Weitz TM, Rentsendorj A, Gate D, Spivak I, Bholat Y, Vasilevko V, Glabe CG, Breunig JJ, Rakic P, Davtyan H, Agadjanyan MG, Kepe V, Barrio JR, Bannykh S, Szekely CA, Pechnick RN, Town T (2013) A transgenic Alzheimer rat with plaques, tau

- pathology, behavioral impairment, oligomeric abeta, and frank neuronal loss. *J Neurosci* 33:6245-6256.
- Conner JM, Lauterborn JC, Yan Q, Gall CM, Varon S (1997) Distribution of brain-derived neurotrophic factor (BDNF) protein and mRNA in the normal adult rat CNS: evidence for anterograde axonal transport. *J Neurosci* 17:2295-2313.
- Costello S, Cockburn M, Bronstein J, Zhang X, Ritz B (2009) Parkinson's disease and residential exposure to maneb and paraquat from agricultural applications in the central valley of California. *Am J Epidemiol* 169:919-926.
- Cuchillo-Ibanez I, Seereeram A, Byers HL, Leung KY, Ward MA, Anderton BH, Hanger DP (2008) Phosphorylation of tau regulates its axonal transport by controlling its binding to kinesin. *FASEB J* 22:3186-3195.
- Curtis AL, Lechner SM, Pavcovich LA, Valentino RJ (1997) Activation of the locus coeruleus noradrenergic system by intracoeular microinfusion of corticotropin-releasing factor: effects on discharge rate, cortical norepinephrine levels and cortical electroencephalographic activity. *J Pharmacol Exp Ther* 281:163-172.
- D'Amato RJ, Lipman ZP, Snyder SH (1986) Selectivity of the parkinsonian neurotoxin MPTP: toxic metabolite MPP⁺ binds to neuromelanin. *Science* 231:987-989.
- Davies RR, Graham KS, Xuereb JH, Williams GB, Hodges JR (2004) The human perirhinal cortex and semantic memory. *Eur J Neurosci* 20:2441-2446.
- de Rijk MC, Launer LJ, Berger K, Breteler MM, Dartigues JF, Baldereschi M, Fratiglioni L, Lobo A, Martinez-Lage J, Trenkwalder C, Hofman A (2000) Prevalence of Parkinson's disease in Europe: A collaborative study of population-based cohorts. Neurologic Diseases in the Elderly Research Group. *Neurology* 54:S21-23.

- Del Tredici K, Braak H (2013) Dysfunction of the locus coeruleus-norepinephrine system and related circuitry in Parkinson's disease-related dementia. *J Neurol Neurosurg Psychiatry* 84:774-783.
- Del Tredici K, Rub U, De Vos RA, Bohl JR, Braak H (2002) Where does parkinson disease pathology begin in the brain? *J Neuropathol Exp Neurol* 61:413-426.
- DeMattei M, Levi AC, Fariello RG (1986) Neuromelanin pigment in substantia nigra neurons of rats and dogs. *Neurosci Lett* 72:37-42.
- Devoto P, Flore G (2006) On the origin of cortical dopamine: is it a co-transmitter in noradrenergic neurons? *Curr Neuropharmacol* 4:115-125.
- Devoto P, Flore G, Saba P, Fa M, Gessa GL (2005) Co-release of noradrenaline and dopamine in the cerebral cortex elicited by single train and repeated train stimulation of the locus coeruleus. *Bmc Neurosci* 6:31.
- Dexter DT, Jenner P, Schapira AH, Marsden CD (1992) Alterations in levels of iron, ferritin, and other trace metals in neurodegenerative diseases affecting the basal ganglia. The Royal Kings and Queens Parkinson's Disease Research Group. *Ann Neurol* 32 Suppl:S94-100.
- Dichtl S, Haschka D, Nairz M, Seifert M, Volani C, Lutz O, Weiss G (2018) Dopamine promotes cellular iron accumulation and oxidative stress responses in macrophages. *Biochem Pharmacol* 148:193-201.
- Dixit R, Ross JL, Goldman YE, Holzbaur EL (2008) Differential regulation of dynein and kinesin motor proteins by tau. *Science* 319:1086-1089.
- Doppler CEJ, Kinnerup MB, Brune C, Farrher E, Betts M, Fedorova TD, Schaldemose JL, Knudsen K, Ismail R, Seger AD, Hansen AK, Staer K, Fink GR, Brooks DJ, Nahimi A,

- Borghammer P, Sommerauer M (2021) Regional locus coeruleus degeneration is uncoupled from noradrenergic terminal loss in Parkinson's disease. *Brain*.
- Du B, Zhang Y, Liang M, Du Z, Li H, Fan C, Zhang H, Jiang Y, Bi X (2021) N6-methyladenosine (m6A) modification and its clinical relevance in cognitive dysfunctions. *Aging (Albany NY)* 13:20716-20737.
- Duff K, Eckman C, Zehr C, Yu X, Prada CM, Perez-tur J, Hutton M, Buee L, Harigaya Y, Yager D, Morgan D, Gordon MN, Holcomb L, Refolo L, Zenk B, Hardy J, Younkin S (1996) Increased amyloid-beta42(43) in brains of mice expressing mutant presenilin 1. *Nature* 383:710-713.
- Espana RA, Schmeichel BE, Berridge CW (2016) Norepinephrine at the nexus of arousal, motivation and relapse. *Brain Res* 1641:207-216.
- Essali N, Sanders J (2016) Interdependent adrenergic receptor regulation of Arc and Zif268 mRNA in cerebral cortex. *Neurosci Lett* 612:38-42.
- Fang X, Han D, Cheng Q, Zhang P, Zhao C, Min J, Wang F (2018) Association of Levels of Physical Activity With Risk of Parkinson Disease: A Systematic Review and Meta-analysis. *JAMA Netw Open* 1:e182421.
- Fawcett JP, Bamji SX, Causing CG, Aloyz R, Ase AR, Reader TA, McLean JH, Miller FD (1998) Functional evidence that BDNF is an anterograde neuronal trophic factor in the CNS. *J Neurosci* 18:2808-2821.
- Fedorow H, Tribl F, Halliday G, Gerlach M, Riederer P, Double KL (2005) Neuromelanin in human dopamine neurons: comparison with peripheral melanins and relevance to Parkinson's disease. *Prog Neurobiol* 75:109-124.

- Feng J, Zhang C, Lischinsky JE, Jing M, Zhou J, Wang H, Zhang Y, Dong A, Wu Z, Wu H, Chen W, Zhang P, Zou J, Hires SA, Zhu JJ, Cui G, Lin D, Du J, Li Y (2019) A Genetically Encoded Fluorescent Sensor for Rapid and Specific In Vivo Detection of Norepinephrine. *Neuron* 102:745-761 e748.
- Ferreira JJ et al. (2013) Summary of the recommendations of the EFNS/MDS-ES review on therapeutic management of Parkinson's disease. *Eur J Neurol* 20:5-15.
- Foote SL, Bloom FE, Aston-Jones G (1983) Nucleus locus ceruleus: new evidence of anatomical and physiological specificity. *Physiol Rev* 63:844-914.
- Francis PT, Palmer AM, Sims NR, Bowen DM, Davison AN, Esiri MM, Neary D, Snowden JS, Wilcock GK (1985) Neurochemical studies of early-onset Alzheimer's disease. Possible influence on treatment. *N Engl J Med* 313:7-11.
- Freire C, Koifman S (2012) Pesticide exposure and Parkinson's disease: epidemiological evidence of association. *Neurotoxicology* 33:947-971.
- Fritsch T, Smyth KA, Wallendal MS, Hyde T, Leo G, Geldmacher DS (2012) Parkinson disease: research update and clinical management. *South Med J* 105:650-656.
- Fritschy JM, Grzanna R (1991) Selective effects of DSP-4 on locus coeruleus axons: are there pharmacologically different types of noradrenergic axons in the central nervous system? *Prog Brain Res* 88:257-268.
- Fritschy JM, Geffard M, Grzanna R (1990) The response of noradrenergic axons to systemically administered DSP-4 in the rat: an immunohistochemical study using antibodies to noradrenaline and dopamine-beta-hydroxylase. *J Chem Neuroanat* 3:309-321.
- Funayama M, Hasegawa K, Kowa H, Saito M, Tsuji S, Obata F (2002) A new locus for Parkinson's disease (PARK8) maps to chromosome 12p11.2-q13.1. *Ann Neurol* 51:296-301.

- Games D, Adams D, Alessandrini R, Barbour R, Berthelette P, Blackwell C, Carr T, Clemens J, Donaldson T, Gillespie F, et al. (1995) Alzheimer-type neuropathology in transgenic mice overexpressing V717F beta-amyloid precursor protein. *Nature* 373:523-527.
- Gami-Patel P, Scarioni M, Bouwman FH, Boon BDC, van Swieten JC, Brain Bank N, Rozemuller AJM, Smit AB, Pijnenburg YAL, Hoozemans JJM, Dijkstra AA (2022) The severity of behavioural symptoms in FTD is linked to the loss of GABRQ-expressing VENs and pyramidal neurons. *Neuropathol Appl Neurobiol* 48:e12798.
- Gant JC, Chen KC, Kadish I, Blalock EM, Thibault O, Porter NM, Landfield PW (2015) Reversal of Aging-Related Neuronal Ca²⁺ Dysregulation and Cognitive Impairment by Delivery of a Transgene Encoding FK506-Binding Protein 12.6/1b to the Hippocampus. *J Neurosci* 35:10878-10887.
- Gant JC, Blalock EM, Chen KC, Kadish I, Porter NM, Norris CM, Thibault O, Landfield PW (2014) FK506-binding protein 1b/12.6: a key to aging-related hippocampal Ca²⁺ dysregulation? *Eur J Pharmacol* 739:74-82.
- Gao J, Liu R, Zhao E, Huang X, Nalls MA, Singleton AB, Chen H (2015) Head injury, potential interaction with genes, and risk for Parkinson's disease. *Parkinsonism Relat Disord* 21:292-296.
- Gash DM, Rutland K, Hudson NL, Sullivan PG, Bing G, Cass WA, Pandya JD, Liu M, Choi DY, Hunter RL, Gerhardt GA, Smith CD, Slevin JT, Prince TS (2008) Trichloroethylene: Parkinsonism and complex 1 mitochondrial neurotoxicity. *Ann Neurol* 63:184-192.
- Gazewood JD, Richards DR, Clebak K (2013) Parkinson disease: an update. *Am Fam Physician* 87:267-273.

- Gilvesy A, Husen E, Magloczky Z, Mihaly O, Hortobagyi T, Kanatani S, Heinsen H, Renier N, Hokfelt T, Mulder J, Uhlen M, Kovacs GG, Adori C (2022) Spatiotemporal characterization of cellular tau pathology in the human locus coeruleus-pericoerulear complex by three-dimensional imaging. *Acta Neuropathol* 144:651-676.
- Glenner GG, Wong CW (1984) Alzheimer's disease: initial report of the purification and characterization of a novel cerebrovascular amyloid protein. *Biochem Biophys Res Commun* 120:885-890.
- Gloeckner CJ, Kinkl N, Schumacher A, Braun RJ, O'Neill E, Meitinger T, Kolch W, Prokisch H, Ueffing M (2006) The Parkinson disease causing LRRK2 mutation I2020T is associated with increased kinase activity. *Hum Mol Genet* 15:223-232.
- Gold CA, Budson AE (2008) Memory loss in Alzheimer's disease: implications for development of therapeutics. *Expert Rev Neurother* 8:1879-1891.
- Goldman SM, Quinlan PJ, Ross GW, Marras C, Meng C, Bhudhikanok GS, Comyns K, Korell M, Chade AR, Kasten M, Priestley B, Chou KL, Fernandez HH, Cambi F, Langston JW, Tanner CM (2012) Solvent exposures and Parkinson disease risk in twins. *Ann Neurol* 71:776-784.
- Goldstein DS (2021) The Catecholaldehyde Hypothesis for the Pathogenesis of Catecholaminergic Neurodegeneration: What We Know and What We Do Not Know. *Int J Mol Sci* 22.
- Goodman AM, Langner BM, Jackson N, Alex C, McMahon LL (2021) Heightened Hippocampal beta-Adrenergic Receptor Function Drives Synaptic Potentiation and Supports Learning and Memory in the TgF344-AD Rat Model during Prodromal Alzheimer's Disease. *J Neurosci* 41:5747-5761.

- Grace AA, Bunney BS (1983) Intracellular and extracellular electrophysiology of nigral dopaminergic neurons--3. Evidence for electrotonic coupling. *Neuroscience* 10:333-348.
- Grant MM, Weiss JM (2001) Effects of chronic antidepressant drug administration and electroconvulsive shock on locus coeruleus electrophysiologic activity. *Biol Psychiatry* 49:117-129.
- Greco G (2014) Neuromelanin and Parkinson's Disease. In: *Handbook of Neurotoxicity*. New York, NY: Springer.
- Grella SL, Neil JM, Edison HT, Strong VD, Odintsova IV, Walling SG, Martin GM, Marrone DF, Harley CW (2019) Locus Coeruleus Phasic, But Not Tonic, Activation Initiates Global Remapping in a Familiar Environment. *J Neurosci* 39:445-455.
- Grzanna R, Berger U, Fritschy JM, Geffard M (1989) Acute action of DSP-4 on central norepinephrine axons: biochemical and immunohistochemical evidence for differential effects. *J Histochem Cytochem* 37:1435-1442.
- Guerin D, Sacquet J, Mandairon N, Jourdan F, Didier A (2009) Early locus coeruleus degeneration and olfactory dysfunctions in Tg2576 mice. *Neurobiol Aging* 30:272-283.
- Haass C, Schlossmacher MG, Hung AY, Vigo-Pelfrey C, Mellon A, Ostaszewski BL, Lieberburg I, Koo EH, Schenk D, Teplow DB, et al. (1992) Amyloid beta-peptide is produced by cultured cells during normal metabolism. *Nature* 359:322-325.
- Halliday GM, Li YW, Blumbergs PC, Joh TH, Cotton RG, Howe PR, Blessing WW, Geffen LB (1990) Neuropathology of immunohistochemically identified brainstem neurons in Parkinson's disease. *Ann Neurol* 27:373-385.
- Hallman H, Jonsson G (1984) Monoamine neurotransmitter metabolism in microencephalic rat brain after prenatal methylazoxymethanol treatment. *Brain Res Bull* 13:383-389.

- Hardy J, Selkoe DJ (2002) The amyloid hypothesis of Alzheimer's disease: progress and problems on the road to therapeutics. *Science* 297:353-356.
- Harro J, Oreland L, Vasar E, Bradwejn J (1995) Impaired exploratory behaviour after DSP-4 treatment in rats: implications for the increased anxiety after noradrenergic denervation. *Eur Neuropsychopharmacol* 5:447-455.
- Harro J, Pahkla R, Modiri AR, Harro M, Kask A, Oreland L (1999) Dose-dependent effects of noradrenergic denervation by DSP-4 treatment on forced swimming and beta-adrenoceptor binding in the rat. *J Neural Transm (Vienna)* 106:619-629.
- Hawkes CH, Del Tredici K, Braak H (2007) Parkinson's disease: a dual-hit hypothesis. *Neuropathol Appl Neurobiol* 33:599-614.
- Heneka MT, Nadrigny F, Regen T, Martinez-Hernandez A, Dumitrescu-Ozimek L, Terwel D, Jardanhazi-Kurutz D, Walter J, Kirchhoff F, Hanisch UK, Kummer MP (2010) Locus ceruleus controls Alzheimer's disease pathology by modulating microglial functions through norepinephrine. *Proc Natl Acad Sci U S A* 107:6058-6063.
- Heneka MT, Ramanathan M, Jacobs AH, Dumitrescu-Ozimek L, Bilkei-Gorzo A, Debeir T, Sastre M, Galldiks N, Zimmer A, Hoehn M, Heiss WD, Klockgether T, Staufenbiel M (2006) Locus ceruleus degeneration promotes Alzheimer pathogenesis in amyloid precursor protein 23 transgenic mice. *J Neurosci* 26:1343-1354.
- Heneka MT et al. (2015) Neuroinflammation in Alzheimer's disease. *Lancet Neurol* 14:388-405.
- Henjum K, Watne LO, Godang K, Halaas NB, Eldholm RS, Blennow K, Zetterberg H, Saltvedt I, Bollerslev J, Knapskog AB (2022) Cerebrospinal fluid catecholamines in Alzheimer's disease patients with and without biological disease. *Transl Psychiatry* 12:151.

- Henrich MT, Geibl FF, Lee B, Chiu WH, Koprach JB, Brotchie JM, Timmermann L, Decher N, Matschke LA, Oertel WH (2018) A53T-alpha-synuclein overexpression in murine locus coeruleus induces Parkinson's disease-like pathology in neurons and glia. *Acta Neuropathol Commun* 6:39.
- Hernan MA, Takkouche B, Caamano-Isorna F, Gestal-Otero JJ (2002) A meta-analysis of coffee drinking, cigarette smoking, and the risk of Parkinson's disease. *Ann Neurol* 52:276-284.
- Herrmann N, Lanctot KL, Khan LR (2004) The role of norepinephrine in the behavioral and psychological symptoms of dementia. *J Neuropsychiatry Clin Neurosci* 16:261-276.
- Hinson VK, Delambo A, Elm J, Turner T (2017) A Randomized Clinical Trial of Atomoxetine for Mild Cognitive Impairment in Parkinson's Disease. *Mov Disord Clin Pract* 4:416-423.
- Hirata H, Aston-Jones G (1994) A novel long-latency response of locus coeruleus neurons to noxious stimuli: mediation by peripheral C-fibers. *J Neurophysiol* 71:1752-1761.
- Hirsch E, Graybiel AM, Agid YA (1988) Melanized dopaminergic neurons are differentially susceptible to degeneration in Parkinson's disease. *Nature* 334:345-348.
- Hoffmeister JD, Kelm-Nelson CA, Ciucci MR (2021) Quantification of brainstem norepinephrine relative to vocal impairment and anxiety in the Pink1^{-/-} rat model of Parkinson disease. *Behav Brain Res* 414:113514.
- Holets VR, Hokfelt T, Rokaeus A, Terenius L, Goldstein M (1988) Locus coeruleus neurons in the rat containing neuropeptide Y, tyrosine hydroxylase or galanin and their efferent projections to the spinal cord, cerebral cortex and hypothalamus. *Neuroscience* 24:893-906.

Hoogendijk WJ, Feenstra MG, Botterblom MH, Gilhuis J, Sommer IE, Kamphorst W, Eikelenboom P, Swaab DF (1999) Increased activity of surviving locus ceruleus neurons in Alzheimer's disease. *Ann Neurol* 45:82-91.

Hoover BR, Reed MN, Su J, Penrod RD, Kotilinek LA, Grant MK, Pitstick R, Carlson GA, Lanier LM, Yuan LL, Ashe KH, Liao D (2010) Tau mislocalization to dendritic spines mediates synaptic dysfunction independently of neurodegeneration. *Neuron* 68:1067-1081.

Howells FM, Stein DJ, Russell VA (2012) Synergistic tonic and phasic activity of the locus coeruleus norepinephrine (LC-NE) arousal system is required for optimal attentional performance. *Metab Brain Dis* 27:267-274.

Hunsley MS, Palmiter RD (2004) Altered sleep latency and arousal regulation in mice lacking norepinephrine. *Pharmacol Biochem Behav* 78:765-773.

Iannitelli AF, Kelberman MA, Lustberg DJ, Korukonda A, McCann KE, Mulvey B, Segal A, Liles LC, Sloan SA, Dougherty JD, Weinshenker D (2022) The Neurotoxin DSP-4 Dysregulates the Locus Coeruleus-Norepinephrine System and Recapitulates Molecular and Behavioral Aspects of Prodromal Neurodegenerative Disease. *bioRxiv:2022.2009.2027.509797*.

Iranzo A, Tolosa E, Gelpi E, Molinuevo JL, Valldeoriola F, Serradell M, Sanchez-Valle R, Vilaseca I, Lomena F, Vilas D, Llado A, Gaig C, Santamaria J (2013) Neurodegenerative disease status and post-mortem pathology in idiopathic rapid-eye-movement sleep behaviour disorder: an observational cohort study. *Lancet Neurol* 12:443-453.

Iravani MM, Sadeghian M, Rose S, Jenner P (2014) Loss of locus coeruleus noradrenergic neurons alters the inflammatory response to LPS in substantia nigra but does not affect nigral cell loss. *J Neural Transm (Vienna)* 121:1493-1505.

- Iro CM, Hamati R, El Mansari M, Blier P (2021) Repeated but Not Single Administration of Ketamine Prolongs Increases of the Firing Activity of Norepinephrine and Dopamine Neurons. *Int J Neuropsychopharmacol* 24:570-579.
- Ito G, Okai T, Fujino G, Takeda K, Ichijo H, Katada T, Iwatsubo T (2007) GTP binding is essential to the protein kinase activity of LRRK2, a causative gene product for familial Parkinson's disease. *Biochemistry* 46:1380-1388.
- Jacobs HIL (2019) Focus on the blue locus for learning. *Nat Hum Behav* 3:1143-1144.
- Jacobs HIL, Riphagen JM, Ramakers I, Verhey FRJ (2021a) Alzheimer's disease pathology: pathways between central norepinephrine activity, memory, and neuropsychiatric symptoms. *Mol Psychiatry* 26:897-906.
- Jacobs HIL, Becker JA, Kwong K, Engels-Dominguez N, Prokopiou PC, Papp KV, Properzi M, Hampton OL, d'Oleire Uquillas F, Sanchez JS, Rentz DM, El Fakhri G, Normandin MD, Price JC, Bennett DA, Sperling RA, Johnson KA (2021b) In vivo and neuropathology data support locus coeruleus integrity as indicator of Alzheimer's disease pathology and cognitive decline. *Sci Transl Med* 13:eabj2511.
- Jankowsky JL, Slunt HH, Ratovitski T, Jenkins NA, Copeland NG, Borchelt DR (2001) Co-expression of multiple transgenes in mouse CNS: a comparison of strategies. *Biomol Eng* 17:157-165.
- Johnson RD, Iuvone PM, Minneman KP (1987) Regulation of alpha-1 adrenergic receptor density and functional responsiveness in rat brain. *J Pharmacol Exp Ther* 242:842-849.
- Jonsson G, Hallman H, Ponzio F, Ross S (1981) DSP4 (N-(2-chloroethyl)-N-ethyl-2-bromobenzylamine)--a useful denervation tool for central and peripheral noradrenaline neurons. *Eur J Pharmacol* 72:173-188.

Ju YE, Lucey BP, Holtzman DM (2014) Sleep and Alzheimer disease pathology--a bidirectional relationship. *Nat Rev Neurol* 10:115-119.

Kalia LV, Lang AE (2015) Parkinson's disease. *The Lancet* 386:896-912.

Kalinin S, Gavriilyuk V, Polak PE, Vasser R, Zhao J, Heneka MT, Feinstein DL (2007) Noradrenaline deficiency in brain increases beta-amyloid plaque burden in an animal model of Alzheimer's disease. *Neurobiol Aging* 28:1206-1214.

Kang SS, Ahn EH, Zhang Z, Liu X, Manfredsson FP, Sandoval IM, Dhakal S, Iuvone PM, Cao X, Ye K (2018) alpha-Synuclein stimulation of monoamine oxidase-B and legumain protease mediates the pathology of Parkinson's disease. *EMBO J* 37.

Kang SS, Liu X, Ahn EH, Xiang J, Manfredsson FP, Yang X, Luo HR, Liles LC, Weinshenker D, Ye K (2020) Norepinephrine metabolite DOPEGAL activates AEP and pathological Tau aggregation in locus coeruleus. *J Clin Invest* 130:422-437.

Kang SS, Meng L, Zhang X, Wu Z, Mancieri A, Xie B, Liu X, Weinshenker D, Peng J, Zhang Z, Ye K (2022) Tau modification by the norepinephrine metabolite DOPEGAL stimulates its pathology and propagation. *Nat Struct Mol Biol* 29:292-305.

Karran E, De Strooper B (2022) The amyloid hypothesis in Alzheimer disease: new insights from new therapeutics. *Nat Rev Drug Discov* 21:306-318.

Kehagia AA, Housden CR, Regenthal R, Barker RA, Muller U, Rowe J, Sahakian BJ, Robbins TW (2014) Targeting impulsivity in Parkinson's disease using atomoxetine. *Brain* 137:1986-1997.

Kelberman M, Keilholz S, Weinshenker D (2020) What's That (Blue) Spot on my MRI? Multimodal Neuroimaging of the Locus Coeruleus in Neurodegenerative Disease. *Front Neurosci* 14:583421.

- Kelberman MA, Anderson CR, Chlan E, Rorabaugh JM, McCann KE, Weinshenker D (2022) Consequences of Hyperphosphorylated Tau in the Locus Coeruleus on Behavior and Cognition in a Rat Model of Alzheimer's Disease. *J Alzheimers Dis* 86:1037-1059.
- Kelly L, Seifi M, Ma R, Mitchell SJ, Rudolph U, Viola KL, Klein WL, Lambert JJ, Swinny JD (2021) Identification of intraneuronal amyloid beta oligomers in locus coeruleus neurons of Alzheimer's patients and their potential impact on inhibitory neurotransmitter receptors and neuronal excitability. *Neuropathol Appl Neurobiol* 47:488-505.
- Kelly SC, He B, Perez SE, Ginsberg SD, Mufson EJ, Counts SE (2017) Locus coeruleus cellular and molecular pathology during the progression of Alzheimer's disease. *Acta Neuropathol Commun* 5:8.
- Kim CK, Lee YR, Ong L, Gold M, Kalali A, Sarkar J (2022) Alzheimer's Disease: Key Insights from Two Decades of Clinical Trial Failures. *J Alzheimers Dis* 87:83-100.
- Kinney JW, Bemiller SM, Murtishaw AS, Leisgang AM, Salazar AM, Lamb BT (2018) Inflammation as a central mechanism in Alzheimer's disease. *Alzheimers Dement (N Y)* 4:575-590.
- Kolisnyk B, Al-Onaizi M, Soreq L, Barbash S, Bekenstein U, Haberman N, Hanin G, Kish MT, Souza da Silva J, Fahnestock M, Ule J, Soreq H, Prado VF, Prado MAM (2017) Cholinergic Surveillance over Hippocampal RNA Metabolism and Alzheimer's-Like Pathology. *Cereb Cortex* 27:3553-3567.
- Koylu EO, Smith Y, Couceyro PR, Kuhar MJ (1999) CART peptides colocalize with tyrosine hydroxylase neurons in rat locus coeruleus. *Synapse* 31:309-311.
- Krainc T, Monje MHG, Kinsinger M, Bustos BI, Lubbe SJ (2022) Melanin and Neuromelanin: Linking Skin Pigmentation and Parkinson's Disease. *Mov Disord*.

- Kumbhare D, Holloway KL, Baron MS (2017) Parkinsonism and dystonia are differentially induced by modulation of different territories in the basal ganglia. *Neuroscience* 353:42-57.
- Lan J, Jiang DH (1997) Excessive iron accumulation in the brain: a possible potential risk of neurodegeneration in Parkinson's disease. *J Neural Transm (Vienna)* 104:649-660.
- Lanari A, Amenta F, Silvestrelli G, Tomassoni D, Parnetti L (2006) Neurotransmitter deficits in behavioural and psychological symptoms of Alzheimer's disease. *Mech Ageing Dev* 127:158-165.
- Lang R, Gundlach AL, Holmes FE, Hobson SA, Wynick D, Hokfelt T, Kofler B (2015) Physiology, signaling, and pharmacology of galanin peptides and receptors: three decades of emerging diversity. *Pharmacol Rev* 67:118-175.
- Langfelder P, Zhang B, Horvath S (2008) Defining clusters from a hierarchical cluster tree: the Dynamic Tree Cut package for R. *Bioinformatics* 24:719-720.
- Le Maitre E, Barde SS, Palkovits M, Diaz-Heijtz R, Hokfelt TG (2013) Distinct features of neurotransmitter systems in the human brain with focus on the galanin system in locus coeruleus and dorsal raphe. *Proc Natl Acad Sci U S A* 110:E536-545.
- Levey AI et al. (2022) A phase II study repurposing atomoxetine for neuroprotection in mild cognitive impairment. *Brain* 145:1924-1938.
- Li Y, Tomiyama H, Sato K, Hatano Y, Yoshino H, Atsumi M, Kitaguchi M, Sasaki S, Kawaguchi S, Miyajima H, Toda T, Mizuno Y, Hattori N (2005) Clinicogenetic study of PINK1 mutations in autosomal recessive early-onset parkinsonism. *Neurology* 64:1955-1957.

- Li Y, Wang C, Wang J, Zhou Y, Ye F, Zhang Y, Cheng X, Huang Z, Liu K, Fei G, Zhong C, Zeng M, Jin L (2019) Mild cognitive impairment in de novo Parkinson's disease: A neuromelanin MRI study in locus coeruleus. *Mov Disord* 34:884-892.
- Likhtik E, Johansen JP (2019) Neuromodulation in circuits of aversive emotional learning. *Nat Neurosci* 22:1586-1597.
- Lim SY, Lang AE (2010) The nonmotor symptoms of Parkinson's disease--an overview. *Mov Disord* 25 Suppl 1:S123-130.
- Liu L, Luo S, Zeng L, Wang W, Yuan L, Jian X (2013) Degenerative alterations in noradrenergic neurons of the locus coeruleus in Alzheimer's disease. *Neural Regen Res* 8:2249-2255.
- Liu M, Choi DY, Hunter RL, Pandya JD, Cass WA, Sullivan PG, Kim HC, Gash DM, Bing G (2010) Trichloroethylene induces dopaminergic neurodegeneration in Fisher 344 rats. *J Neurochem* 112:773-783.
- Liu Y, Yoo MJ, Savonenko A, Stirling W, Price DL, Borchelt DR, Mamounas L, Lyons WE, Blue ME, Lee MK (2008) Amyloid pathology is associated with progressive monoaminergic neurodegeneration in a transgenic mouse model of Alzheimer's disease. *J Neurosci* 28:13805-13814.
- Logue MP, Growdon JH, Coviella IL, Wurtman RJ (1985) Differential effects of DSP-4 administration on regional brain norepinephrine turnover in rats. *Life Sci* 37:403-409.
- Lohle M, Storch A, Reichmann H (2009) Beyond tremor and rigidity: non-motor features of Parkinson's disease. *J Neural Transm (Vienna)* 116:1483-1492.
- Lohr KM, Chen M, Hoffman CA, McDaniel MJ, Stout KA, Dunn AR, Wang M, Bernstein AI, Miller GW (2016) Vesicular Monoamine Transporter 2 (VMAT2) Level Regulates MPTP

- Vulnerability and Clearance of Excess Dopamine in Mouse Striatal Terminals. *Toxicol Sci* 153:79-88.
- Lohr KM, Bernstein AI, Stout KA, Dunn AR, Lazo CR, Alter SP, Wang M, Li Y, Fan X, Hess EJ, Yi H, Vecchio LM, Goldstein DS, Guillot TS, Salahpour A, Miller GW (2014) Increased vesicular monoamine transporter enhances dopamine release and opposes Parkinson disease-related neurodegeneration in vivo. *Proc Natl Acad Sci U S A* 111:9977-9982.
- Lucking CB, Durr A, Bonifati V, Vaughan J, De Michele G, Gasser T, Harhangi BS, Meco G, Deneffe P, Wood NW, Agid Y, Brice A, French Parkinson's Disease Genetics Study G, European Consortium on Genetic Susceptibility in Parkinson's D (2000) Association between early-onset Parkinson's disease and mutations in the parkin gene. *N Engl J Med* 342:1560-1567.
- Lustberg D, Iannitelli AF, Tillage RP, Pruitt M, Liles LC, Weinshenker D (2020a) Central norepinephrine transmission is required for stress-induced repetitive behavior in two rodent models of obsessive-compulsive disorder. *Psychopharmacology (Berl)*.
- Lustberg D, Tillage RP, Bai Y, Pruitt M, Liles LC, Weinshenker D (2020b) Noradrenergic circuits in the forebrain control affective responses to novelty. *Psychopharmacology (Berl)* 237:3337-3355.
- Lustberg D, Iannitelli AF, Tillage RP, Pruitt M, Liles LC, Weinshenker D (2020c) Central norepinephrine transmission is required for stress-induced repetitive behavior in two rodent models of obsessive-compulsive disorder. *Psychopharmacology (Berl)* 237:1973-1987.
- Lustberg DJ, Liu JQ, Iannitelli AF, Vanderhoof SO, Liles LC, McCann KE, Weinshenker D (2022) Norepinephrine and dopamine contribute to distinct repetitive behaviors induced by novel odorant stress in male and female mice. *Horm Behav* 144:105205.

Lyons WE, Fritschy JM, Grzanna R (1989) The noradrenergic neurotoxin DSP-4 eliminates the coeruleospinal projection but spares projections of the A5 and A7 groups to the ventral horn of the rat spinal cord. *J Neurosci* 9:1481-1489.

Madar IH, Sultan G, Tayubi IA, Hasan AN, Pahi B, Rai A, Sivanandan PK, Loganathan T, Begum M, Rai S (2021) Identification of marker genes in Alzheimer's disease using a machine-learning model. *Bioinformatics* 17:348-355.

Mandelkow EM, Stamer K, Vogel R, Thies E, Mandelkow E (2003) Clogging of axons by tau, inhibition of axonal traffic and starvation of synapses. *Neurobiol Aging* 24:1079-1085.

Mann DM, Yates PO (1974) Lipoprotein pigments--their relationship to ageing in the human nervous system. II. The melanin content of pigmented nerve cells. *Brain* 97:489-498.

Mann DM, Yates PO (1983) Possible role of neuromelanin in the pathogenesis of Parkinson's disease. *Mech Ageing Dev* 21:193-203.

Marras C, Beck JC, Bower JH, Roberts E, Ritz B, Ross GW, Abbott RD, Savica R, Van Den Eeden SK, Willis AW, Tanner CM, Parkinson's Foundation PG (2018) Prevalence of Parkinson's disease across North America. *NPJ Parkinsons Dis* 4:21.

Martin-Iverson MT, Pisa M, Chan E, Fibiger HC (1982) Enhanced neophobia but normal plasma corticosterone levels in rats with dorsal noradrenergic bundle lesions. *Pharmacol Biochem Behav* 17:639-643.

Mata IF, Ross OA, Kachergus J, Huerta C, Ribacoba R, Moris G, Blazquez M, Guisasola LM, Salvador C, Martinez C, Farrer M, Alvarez V (2006) LRRK2 mutations are a common cause of Parkinson's disease in Spain. *Eur J Neurol* 13:391-394.

Mata IF et al. (2010) SNCA variant associated with Parkinson disease and plasma alpha-synuclein level. *Arch Neurol* 67:1350-1356.

- Mather M, Harley CW (2016) The Locus Coeruleus: Essential for Maintaining Cognitive Function and the Aging Brain. *Trends Cogn Sci* 20:214-226.
- Matschke LA, Komadowski MA, Stohr A, Lee B, Henrich MT, Griesbach M, Rinne S, Geibl FF, Chiu WH, Koprach JB, Brotchie JM, Kiper AK, Dolga AM, Oertel WH, Decher N (2022) Enhanced firing of locus coeruleus neurons and SK channel dysfunction are conserved in distinct models of prodromal Parkinson's disease. *Sci Rep* 12:3180.
- Matsukawa M, Nakadate K, Ishihara I, Okado N (2003) Synaptic loss following depletion of noradrenaline and/or serotonin in the rat visual cortex: a quantitative electron microscopic study. *Neuroscience* 122:627-635.
- Matsumine H et al. (1997) Localization of a gene for an autosomal recessive form of juvenile Parkinsonism to chromosome 6q25.2-27. *Am J Hum Genet* 60:588-596.
- Mavridis M, Degryse AD, Lategan AJ, Marien MR, Colpaert FC (1991) Effects of locus coeruleus lesions on parkinsonian signs, striatal dopamine and substantia nigra cell loss after 1-methyl-4-phenyl-1,2,3,6-tetrahydropyridine in monkeys: a possible role for the locus coeruleus in the progression of Parkinson's disease. *Neuroscience* 41:507-523.
- McCall JG, Al-Hasani R, Siuda ER, Hong DY, Norris AJ, Ford CP, Bruchas MR (2015) CRH Engagement of the Locus Coeruleus Noradrenergic System Mediates Stress-Induced Anxiety. *Neuron* 87:605-620.
- McCarter SJ, Boswell CL, St Louis EK, Dueffert LG, Slocumb N, Boeve BF, Silber MH, Olson EJ, Tippmann-Peikert M (2013) Treatment outcomes in REM sleep behavior disorder. *Sleep Med* 14:237-242.
- McGaugh JL (2013) Making lasting memories: remembering the significant. *Proc Natl Acad Sci U S A* 110 Suppl 2:10402-10407.

- McIntyre CK, Miyashita T, Setlow B, Marjon KD, Steward O, Guzowski JF, McGaugh JL (2005) Memory-influencing intra-basolateral amygdala drug infusions modulate expression of Arc protein in the hippocampus. *Proc Natl Acad Sci U S A* 102:10718-10723.
- McKhann G, Drachman D, Folstein M, Katzman R, Price D, Stadlan EM (1984) Clinical diagnosis of Alzheimer's disease: report of the NINCDS-ADRDA Work Group under the auspices of Department of Health and Human Services Task Force on Alzheimer's Disease. *Neurology* 34:939-944.
- McReynolds JR, Anderson KM, Donowho KM, McIntyre CK (2014) Noradrenergic actions in the basolateral complex of the amygdala modulate Arc expression in hippocampal synapses and consolidation of aversive and non-aversive memory. *Neurobiol Learn Mem* 115:49-57.
- Metz GA (2007) Stress as a modulator of motor system function and pathology. *Rev Neurosci* 18:209-222.
- Miller EC, Teravskis PJ, Dummer BW, Zhao X, Haganir RL, Liao D (2014) Tau phosphorylation and tau mislocalization mediate soluble Abeta oligomer-induced AMPA glutamate receptor signaling deficits. *Eur J Neurosci* 39:1214-1224.
- Mitchell HA, Weinshenker D (2010) Good night and good luck: norepinephrine in sleep pharmacology. *Biochem Pharmacol* 79:801-809.
- Monzani E, Nicolis S, Dell'Acqua S, Capucciati A, Bacchella C, Zucca FA, Mosharov EV, Sulzer D, Zecca L, Casella L (2019) Dopamine, Oxidative Stress and Protein-Quinone Modifications in Parkinson's and Other Neurodegenerative Diseases. *Angew Chem Int Ed Engl* 58:6512-6527.

- Mootha VK et al. (2003) PGC-1alpha-responsive genes involved in oxidative phosphorylation are coordinately downregulated in human diabetes. *Nat Genet* 34:267-273.
- Mouton PR, Pakkenberg B, Gundersen HJ, Price DL (1994) Absolute number and size of pigmented locus coeruleus neurons in young and aged individuals. *J Chem Neuroanat* 7:185-190.
- Mulvey B, Bhatti DL, Gyawali S, Lake AM, Kriaucionis S, Ford CP, Bruchas MR, Heintz N, Dougherty JD (2018) Molecular and Functional Sex Differences of Noradrenergic Neurons in the Mouse Locus Coeruleus. *Cell Rep* 23:2225-2235.
- Murchison CF, Zhang XY, Zhang WP, Ouyang M, Lee A, Thomas SA (2004) A distinct role for norepinephrine in memory retrieval. *Cell* 117:131-143.
- Myhre R, Steinkjer S, Stormyr A, Nilsen GL, Abu Zayyad H, Horany K, Nusier MK, Klungland H (2008) Significance of the parkin and PINK1 gene in Jordanian families with incidences of young-onset and juvenile parkinsonism. *BMC Neurol* 8:47.
- Naegeli C, Zeffiro T, Piccirelli M, Jaillard A, Weilenmann A, Hassanpour K, Schick M, Rufer M, Orr SP, Mueller-Pfeiffer C (2018) Locus Coeruleus Activity Mediates Hyperresponsiveness in Posttraumatic Stress Disorder. *Biol Psychiatry* 83:254-262.
- Najim al-Din AS, Wriekat A, Mubaidin A, Dasouki M, Hiari M (1994) Pallido-pyramidal degeneration, supranuclear upgaze paresis and dementia: Kufor-Rakeb syndrome. *Acta Neurol Scand* 89:347-352.
- Nguyen M, Wong YC, Ysselstein D, Severino A, Krainc D (2019) Synaptic, Mitochondrial, and Lysosomal Dysfunction in Parkinson's Disease. *Trends Neurosci* 42:140-149.
- Nicholl DJ, Vaughan JR, Khan NL, Ho SL, Aldous DE, Lincoln S, Farrer M, Gayton JD, Davis MB, Piccini P, Daniel SE, Lennox GG, Brooks DJ, Williams AC, Wood NW (2002) Two

- large British kindreds with familial Parkinson's disease: a clinico-pathological and genetic study. *Brain* 125:44-57.
- Nicholls DG (2008) Oxidative stress and energy crises in neuronal dysfunction. *Ann N Y Acad Sci* 1147:53-60.
- Noble W, Pooler AM, Hanger DP (2011) Advances in tau-based drug discovery. *Expert Opin Drug Discov* 6:797-810.
- Oertel WH, Henrich MT, Janzen A, Geibl FF (2019) The locus coeruleus: Another vulnerability target in Parkinson's disease. *Mov Disord* 34:1423-1429.
- Oliveira LM, Tuppy M, Moreira TS, Takakura AC (2017) Role of the locus coeruleus catecholaminergic neurons in the chemosensory control of breathing in a Parkinson's disease model. *Exp Neurol* 293:172-180.
- Ostergren A, Svensson AL, Lindquist NG, Brittebo EB (2005) Dopamine melanin-loaded PC12 cells: a model for studies on pigmented neurons. *Pigment Cell Res* 18:306-314.
- Paisan-Ruiz C et al. (2004) Cloning of the gene containing mutations that cause PARK8-linked Parkinson's disease. *Neuron* 44:595-600.
- Pall HS, Williams AC, Blake DR, Lunec J, Gutteridge JM, Hall M, Taylor A (1987) Raised cerebrospinal-fluid copper concentration in Parkinson's disease. *Lancet* 2:238-241.
- Palmer AM, Francis PT, Bowen DM, Benton JS, Neary D, Mann DM, Snowden JS (1987) Catecholaminergic neurones assessed ante-mortem in Alzheimer's disease. *Brain Res* 414:365-375.
- Peskind ER, Tsuang DW, Bonner LT, Pascualy M, Riekse RG, Snowden MB, Thomas R, Raskind MA (2005) Propranolol for disruptive behaviors in nursing home residents with probable

- or possible Alzheimer disease: a placebo-controlled study. *Alzheimer Dis Assoc Disord* 19:23-28.
- Pezzoli G, Cereda E (2013) Exposure to pesticides or solvents and risk of Parkinson disease. *Neurology* 80:2035-2041.
- Pickett EK et al. (2019) Amyloid Beta and Tau Cooperate to Cause Reversible Behavioral and Transcriptional Deficits in a Model of Alzheimer's Disease. *Cell Rep* 29:3592-3604 e3595.
- Poe GR, Foote S, Eschenko O, Johansen JP, Bouret S, Aston-Jones G, Harley CW, Manahan-Vaughan D, Weinshenker D, Valentino R, Berridge C, Chandler DJ, Waterhouse B, Sara SJ (2020) Locus coeruleus: a new look at the blue spot. *Nat Rev Neurosci* 21:644-659.
- Polymeropoulos MH, Higgins JJ, Golbe LI, Johnson WG, Ide SE, Di Iorio G, Sanges G, Stenroos ES, Pho LT, Schaffer AA, Lazzarini AM, Nussbaum RL, Duvoisin RC (1996) Mapping of a gene for Parkinson's disease to chromosome 4q21-q23. *Science* 274:1197-1199.
- Polymeropoulos MH, Lavedan C, Leroy E, Ide SE, Dehejia A, Dutra A, Pike B, Root H, Rubenstein J, Boyer R, Stenroos ES, Chandrasekharappa S, Athanassiadou A, Papapetropoulos T, Johnson WG, Lazzarini AM, Duvoisin RC, Di Iorio G, Golbe LI, Nussbaum RL (1997) Mutation in the alpha-synuclein gene identified in families with Parkinson's disease. *Science* 276:2045-2047.
- Popova SN, Alafuzoff I (2013) Distribution of SLC10A4, a synaptic vesicle protein in the human brain, and the association of this protein with Alzheimer's disease-related neuronal degeneration. *J Alzheimers Dis* 37:603-610.
- Porter-Stransky KA, Centanni SW, Karne SL, Odil LM, Fekir S, Wong JC, Jerome C, Mitchell HA, Escayg A, Pedersen NP, Winder DG, Mitrano DA, Weinshenker D (2019)

- Noradrenergic Transmission at Alpha1-Adrenergic Receptors in the Ventral Periaqueductal Gray Modulates Arousal. *Biol Psychiatry* 85:237-247.
- Prediger RD, Matheus FC, Schwarzbald ML, Lima MM, Vital MA (2012) Anxiety in Parkinson's disease: a critical review of experimental and clinical studies. *Neuropharmacology* 62:115-124.
- Prokopiou PC, Engels-Dominguez N, Papp KV, Scott MR, Schultz AP, Schneider C, Farrell ME, Buckley RF, Quiroz YT, El Fakhri G, Rentz DM, Sperling RA, Johnson KA, Jacobs HIL (2022) Lower novelty-related locus coeruleus function is associated with Aβ-related cognitive decline in clinically healthy individuals. *Nat Commun* 13:1571.
- Pursiainen V, Korpelainen JT, Haapaniemi TH, Sotaniemi KA, Myllylä VV (2007) Blood pressure and heart rate in parkinsonian patients with and without wearing-off. *Eur J Neurol* 14:373-378.
- Raskind MA, Peskind ER, Holmes C, Goldstein DS (1999) Patterns of cerebrospinal fluid catechols support increased central noradrenergic responsiveness in aging and Alzheimer's disease. *Biol Psychiatry* 46:756-765.
- Remy P, Doder M, Lees A, Turjanski N, Brooks D (2005) Depression in Parkinson's disease: loss of dopamine and noradrenaline innervation in the limbic system. *Brain* 128:1314-1322.
- Rey NL, Jardanhazi-Kurutz D, Terwel D, Kummer MP, Jourdan F, Didier A, Heneka MT (2012) Locus coeruleus degeneration exacerbates olfactory deficits in APP/PS1 transgenic mice. *Neurobiol Aging* 33:426 e421-411.
- Rommelfanger KS, Weinshenker D, Miller GW (2004) Reduced MPTP toxicity in noradrenaline transporter knockout mice. *J Neurochem* 91:1116-1124.

- Rommelfanger KS, Edwards GL, Freeman KG, Liles LC, Miller GW, Weinshenker D (2007) Norepinephrine loss produces more profound motor deficits than MPTP treatment in mice. *Proc Natl Acad Sci U S A* 104:13804-13809.
- Rompp A, Spengler B (2013) Mass spectrometry imaging with high resolution in mass and space. *Histochem Cell Biol* 139:759-783.
- Rorabaugh JM, Chalermplanupap T, Botz-Zapp CA, Fu VM, Lembeck NA, Cohen RM, Weinshenker D (2017) Chemogenetic locus coeruleus activation restores reversal learning in a rat model of Alzheimer's disease. *Brain* 140:3023-3038.
- Rothman SM, Mattson MP (2012) Sleep disturbances in Alzheimer's and Parkinson's diseases. *Neuromolecular Med* 14:194-204.
- Roy A (1988) Cortisol nonsuppression in depression: relationship to clinical variables. *J Affect Disord* 14:265-270.
- Salazar M, Sokoloski TD, Patil PN (1978) Binding of dopaminergic drugs by the neuromelanin of the substantia nigra, synthetic melanins and melanin granules. *Fed Proc* 37:2403-2407.
- Samii A, Nutt JG, Ransom BR (2004) Parkinson's disease. *Lancet* 363:1783-1793.
- Sanchez-Padilla J, Guzman JN, Ilijic E, Kondapalli J, Galtieri DJ, Yang B, Schieber S, Oertel W, Wokosin D, Schumacker PT, Surmeier DJ (2014) Mitochondrial oxidant stress in locus coeruleus is regulated by activity and nitric oxide synthase. *Nat Neurosci* 17:832-840.
- Sara SJ (2009) The locus coeruleus and noradrenergic modulation of cognition. *Nat Rev Neurosci* 10:211-223.
- Sasaki M, Shibata E, Tohyama K, Takahashi J, Otsuka K, Tsuchiya K, Takahashi S, Ehara S, Terayama Y, Sakai A (2006) Neuromelanin magnetic resonance imaging of locus ceruleus and substantia nigra in Parkinson's disease. *Neuroreport* 17:1215-1218.

- Schenck CH, Boeve BF, Mahowald MW (2013) Delayed emergence of a parkinsonian disorder or dementia in 81% of older men initially diagnosed with idiopathic rapid eye movement sleep behavior disorder: a 16-year update on a previously reported series. *Sleep Med* 14:744-748.
- Scheuner D et al. (1996) Secreted amyloid beta-protein similar to that in the senile plaques of Alzheimer's disease is increased in vivo by the presenilin 1 and 2 and APP mutations linked to familial Alzheimer's disease. *Nat Med* 2:864-870.
- Schneider RB, Iourinets J, Richard IH (2017) Parkinson's disease psychosis: presentation, diagnosis and management. *Neurodegener Dis Manag* 7:365-376.
- Selkoe DJ, Hardy J (2016) The amyloid hypothesis of Alzheimer's disease at 25 years. *EMBO Mol Med* 8:595-608.
- Senard JM, Rai S, Lapeyre-Mestre M, Brefel C, Rascol O, Rascol A, Montastruc JL (1997) Prevalence of orthostatic hypotension in Parkinson's disease. *J Neurol Neurosurg Psychiatry* 63:584-589.
- Shamoto-Nagai M, Maruyama W, Akao Y, Osawa T, Tribl F, Gerlach M, Zucca FA, Zecca L, Riederer P, Naoi M (2004) Neuromelanin inhibits enzymatic activity of 26S proteasome in human dopaminergic SH-SY5Y cells. *J Neural Transm (Vienna)* 111:1253-1265.
- Sian-Hulsmann J, Monoranu C, Strobel S, Riederer P (2015) Lewy Bodies: A Spectator or Salient Killer? *CNS Neurol Disord Drug Targets* 14:947-955.
- Simola N, Morelli M, Carta AR (2007) The 6-hydroxydopamine model of Parkinson's disease. *Neurotox Res* 11:151-167.
- Small GW (2006) Diagnostic issues in dementia: neuroimaging as a surrogate marker of disease. *J Geriatr Psychiatry Neurol* 19:180-185.

- Song S, Jiang L, Oyarzabal EA, Wilson B, Li Z, Shih YI, Wang Q, Hong JS (2019a) Loss of Brain Norepinephrine Elicits Neuroinflammation-Mediated Oxidative Injury and Selective Caudo-Rostral Neurodegeneration. *Mol Neurobiol* 56:2653-2669.
- Song S, Wang Q, Jiang L, Oyarzabal E, Riddick NV, Wilson B, Moy SS, Shih YI, Hong JS (2019b) Noradrenergic dysfunction accelerates LPS-elicited inflammation-related ascending sequential neurodegeneration and deficits in non-motor/motor functions. *Brain Behav Immun* 81:374-387.
- Spires-Jones TL, Hyman BT (2014) The intersection of amyloid beta and tau at synapses in Alzheimer's disease. *Neuron* 82:756-771.
- Srinivasan J, Schmidt WJ (2003) Potentiation of parkinsonian symptoms by depletion of locus coeruleus noradrenaline in 6-hydroxydopamine-induced partial degeneration of substantia nigra in rats. *Eur J Neurosci* 17:2586-2592.
- Stamer K, Vogel R, Thies E, Mandelkow E, Mandelkow EM (2002) Tau blocks traffic of organelles, neurofilaments, and APP vesicles in neurons and enhances oxidative stress. *J Cell Biol* 156:1051-1063.
- Stampfer MJ (2006) Cardiovascular disease and Alzheimer's disease: common links. *J Intern Med* 260:211-223.
- Starr JM, Loeffler B, Abousleiman Y, Simonotto E, Marshall I, Goddard N, Wardlaw JM (2005) Episodic and semantic memory tasks activate different brain regions in Alzheimer disease. *Neurology* 65:266-269.
- Steenen SA, van Wijk AJ, van der Heijden GJ, van Westrhenen R, de Lange J, de Jongh A (2016) Propranolol for the treatment of anxiety disorders: Systematic review and meta-analysis. *J Psychopharmacol* 30:128-139.

- Stiasny-Kolster K, Doerr Y, Moller JC, Hoffken H, Behr TM, Oertel WH, Mayer G (2005) Combination of 'idiopathic' REM sleep behaviour disorder and olfactory dysfunction as possible indicator for alpha-synucleinopathy demonstrated by dopamine transporter FP-CIT-SPECT. *Brain* 128:126-137.
- Stubbendorff C, Stevenson CW (2021) Dopamine regulation of contextual fear and associated neural circuit function. *Eur J Neurosci* 54:6933-6947.
- Subramanian A, Tamayo P, Mootha VK, Mukherjee S, Ebert BL, Gillette MA, Paulovich A, Pomeroy SL, Golub TR, Lander ES, Mesirov JP (2005) Gene set enrichment analysis: a knowledge-based approach for interpreting genome-wide expression profiles. *Proc Natl Acad Sci U S A* 102:15545-15550.
- Sulzer D, Surmeier DJ (2013) Neuronal vulnerability, pathogenesis, and Parkinson's disease. *Mov Disord* 28:715-724.
- Sulzer D, Mosharov E, Tallozy Z, Zucca FA, Simon JD, Zecca L (2008) Neuronal pigmented autophagic vacuoles: lipofuscin, neuromelanin, and ceroid as macroautophagic responses during aging and disease. *J Neurochem* 106:24-36.
- Sulzer D, Bogulavsky J, Larsen KE, Behr G, Karatekin E, Kleinman MH, Turro N, Krantz D, Edwards RH, Greene LA, Zecca L (2000) Neuromelanin biosynthesis is driven by excess cytosolic catecholamines not accumulated by synaptic vesicles. *Proc Natl Acad Sci U S A* 97:11869-11874.
- Surmeier DJ, Guzman JN, Sanchez-Padilla J (2010) Calcium, cellular aging, and selective neuronal vulnerability in Parkinson's disease. *Cell Calcium* 47:175-182.
- Szot P, White SS, Greenup JL, Leverenz JB, Peskind ER, Raskind MA (2006) Compensatory changes in the noradrenergic nervous system in the locus ceruleus and hippocampus of

- postmortem subjects with Alzheimer's disease and dementia with Lewy bodies. *J Neurosci* 26:467-478.
- Szot P, Miguelez C, White SS, Franklin A, Sikkema C, Wilkinson CW, Ugedo L, Raskind MA (2010) A comprehensive analysis of the effect of DSP4 on the locus coeruleus noradrenergic system in the rat. *Neuroscience* 166:279-291.
- Szot P, Knight L, Franklin A, Sikkema C, Foster S, Wilkinson CW, White SS, Raskind MA (2012) Lesioning noradrenergic neurons of the locus coeruleus in C57Bl/6 mice with unilateral 6-hydroxydopamine injection, to assess molecular, electrophysiological and biochemical changes in noradrenergic signaling. *Neuroscience* 216:143-157.
- Szot P, Franklin A, Miguelez C, Wang Y, Vidaurrazaga I, Ugedo L, Sikkema C, Wilkinson CW, Raskind MA (2016) Depressive-like behavior observed with a minimal loss of locus coeruleus (LC) neurons following administration of 6-hydroxydopamine is associated with electrophysiological changes and reversed with precursors of norepinephrine. *Neuropharmacology* 101:76-86.
- Takeuchi T, Duzkiewicz AJ, Sonneborn A, Spooner PA, Yamasaki M, Watanabe M, Smith CC, Fernandez G, Deisseroth K, Greene RW, Morris RG (2016) Locus coeruleus and dopaminergic consolidation of everyday memory. *Nature* 537:357-362.
- Tansey MG, Lee JK (2015) Inflammation in nervous system disorders. Introduction. *Neuroscience* 302:1.
- Tansey MG, Wallings RL, Houser MC, Herrick MK, Keating CE, Joers V (2022) Inflammation and immune dysfunction in Parkinson disease. *Nat Rev Immunol*.

- Tao Y, Han Y, Yu L, Wang Q, Leng SX, Zhang H (2020) The Predicted Key Molecules, Functions, and Pathways That Bridge Mild Cognitive Impairment (MCI) and Alzheimer's Disease (AD). *Front Neurol* 11:233.
- Taylor BN, Cassagnol M (2022) Alpha Adrenergic Receptors. In: *StatPearls*. Treasure Island (FL).
- Taylor KM, Saint-Hilaire MH, Sudarsky L, Simon DK, Hersh B, Sparrow D, Hu H, Weisskopf MG (2016) Head injury at early ages is associated with risk of Parkinson's disease. *Parkinsonism Relat Disord* 23:57-61.
- Thakur S, Dhapola R, Sarma P, Medhi B, Reddy DH (2022) Neuroinflammation in Alzheimer's Disease: Current Progress in Molecular Signaling and Therapeutics. *Inflammation*.
- Thal DR, Rub U, Orantes M, Braak H (2002) Phases of A beta-deposition in the human brain and its relevance for the development of AD. *Neurology* 58:1791-1800.
- Theofilas P, Ehrenberg AJ, Dunlop S, Di Lorenzo Alho AT, Nguy A, Leite REP, Rodriguez RD, Mejia MB, Suemoto CK, Ferretti-Rebustini REL, Polichiso L, Nascimento CF, Seeley WW, Nitrini R, Pasqualucci CA, Jacob Filho W, Rueb U, Neuhaus J, Heinsen H, Grinberg LT (2017) Locus coeruleus volume and cell population changes during Alzheimer's disease progression: A stereological study in human postmortem brains with potential implication for early-stage biomarker discovery. *Alzheimers Dement* 13:236-246.
- Theron CN, de Villiers AS, Taljaard JJ (1993) Effects of DSP-4 on monoamine and monoamine metabolite levels and on beta adrenoceptor binding kinetics in rat brain at different times after administration. *Neurochem Res* 18:1321-1327.
- Tillage RP, Wilson GE, Liles LC, Holmes PV, Weinshenker D (2020a) Chronic Environmental or Genetic Elevation of Galanin in Noradrenergic Neurons Confers Stress Resilience in Mice. *J Neurosci* 40:7464-7474.

- Tillage RP, Foster SL, Lustberg D, Liles LC, McCann KE, Weinshenker D (2021) Co-released norepinephrine and galanin act on different timescales to promote stress-induced anxiety-like behavior. *Neuropsychopharmacology* 46:1535-1543.
- Tillage RP, Sciolino NR, Plummer NW, Lustberg D, Liles LC, Hsiang M, Powell JM, Smith KG, Jensen P, Weinshenker D (2020b) Elimination of galanin synthesis in noradrenergic neurons reduces galanin in select brain areas and promotes active coping behaviors. *Brain Struct Funct* 225:785-803.
- Tippett LJ, Meier SL, Blackwood K, Diaz-Asper C (2007) Category specific deficits in Alzheimer's disease: fact or artefact? *Cortex* 43:907-920.
- Tomlinson BE, Blessed G, Roth M (1970) Observations on the brains of demented old people. *J Neurol Sci* 11:205-242.
- Tomlinson BE, Irving D, Blessed G (1981) Cell loss in the locus coeruleus in senile dementia of Alzheimer type. *J Neurol Sci* 49:419-428.
- Troade J, Marien M, Darios F, Hartmann A, Ruberg M, Colpaert F, Michel PP (2001) Noradrenaline provides long-term protection to dopaminergic neurons by reducing oxidative stress. *J Neurochem* 79:200-210.
- Trojano L, Papagno C (2018) Cognitive and behavioral disorders in Parkinson's disease: an update. II: behavioral disorders. *Neurol Sci* 39:53-61.
- Valente EM, Bentivoglio AR, Dixon PH, Ferraris A, Ialongo T, Frontali M, Albanese A, Wood NW (2001) Localization of a novel locus for autosomal recessive early-onset parkinsonism, PARK6, on human chromosome 1p35-p36. *Am J Hum Genet* 68:895-900.
- Valentino RJ (1988) CRH effects on central noradrenergic neurons: relationship to stress. *Adv Exp Med Biol* 245:47-64.

- Valentino RJ, Van Bockstaele E (2008) Convergent regulation of locus coeruleus activity as an adaptive response to stress. *Eur J Pharmacol* 583:194-203.
- Van Egroo M, Koshmanova E, Vandewalle G, Jacobs HIL (2022) Importance of the locus coeruleus-norepinephrine system in sleep-wake regulation: Implications for aging and Alzheimer's disease. *Sleep Med Rev* 62:101592.
- van Hooren L, Vaccaro A, Ramachandran M, Vazaios K, Libard S, van de Walle T, Georganaki M, Huang H, Pietila I, Lau J, Ulvmar MH, Karlsson MCI, Zetterling M, Mangsbo SM, Jakola AS, Olsson Bontell T, Smits A, Essand M, Dimberg A (2021) Agonistic CD40 therapy induces tertiary lymphoid structures but impairs responses to checkpoint blockade in glioma. *Nat Commun* 12:4127.
- Vankov A, Herve-Minvielle A, Sara SJ (1995) Response to novelty and its rapid habituation in locus coeruleus neurons of the freely exploring rat. *Eur J Neurosci* 7:1180-1187.
- Vazey EM, Aston-Jones G (2012) The emerging role of norepinephrine in cognitive dysfunctions of Parkinson's disease. *Front Behav Neurosci* 6:48.
- Villemagne VL, Pike KE, Chetelat G, Ellis KA, Mulligan RS, Bourgeat P, Ackermann U, Jones G, Szoek C, Salvado O, Martins R, O'Keefe G, Mathis CA, Klunk WE, Ames D, Masters CL, Rowe CC (2011) Longitudinal assessment of Abeta and cognition in aging and Alzheimer disease. *Ann Neurol* 69:181-192.
- Von Coelln R, Thomas B, Savitt JM, Lim KL, Sasaki M, Hess EJ, Dawson VL, Dawson TM (2004) Loss of locus coeruleus neurons and reduced startle in parkin null mice. *Proc Natl Acad Sci U S A* 101:10744-10749.

- Wagner-Altendorf TA, Fischer B, Roeper J (2019) Axonal projection-specific differences in somatodendritic alpha2 autoreceptor function in locus coeruleus neurons. *Eur J Neurosci* 50:3772-3785.
- Wakamatsu K, Tabuchi K, Ojika M, Zucca FA, Zecca L, Ito S (2015) Norepinephrine and its metabolites are involved in the synthesis of neuromelanin derived from the locus coeruleus. *J Neurochem* 135:768-776.
- Wang J, Li Y, Huang Z, Wan W, Zhang Y, Wang C, Cheng X, Ye F, Liu K, Fei G, Zeng M, Jin L (2018) Neuromelanin-sensitive magnetic resonance imaging features of the substantia nigra and locus coeruleus in de novo Parkinson's disease and its phenotypes. *Eur J Neurol* 25:949-e973.
- Wang X, Michaelis EK (2010) Selective neuronal vulnerability to oxidative stress in the brain. *Front Aging Neurosci* 2:12.
- Wang Y, Musich PR, Serrano MA, Zou Y, Zhang J, Zhu MY (2014) Effects of DSP4 on the noradrenergic phenotypes and its potential molecular mechanisms in SH-SY5Y cells. *Neurotox Res* 25:193-207.
- Weinshenker D (2018) Long Road to Ruin: Noradrenergic Dysfunction in Neurodegenerative Disease. *Trends Neurosci* 41:211-223.
- West AB, Moore DJ, Biskup S, Bugayenko A, Smith WW, Ross CA, Dawson VL, Dawson TM (2005) Parkinson's disease-associated mutations in leucine-rich repeat kinase 2 augment kinase activity. *Proc Natl Acad Sci U S A* 102:16842-16847.
- Wilson RS, Nag S, Boyle PA, Hizel LP, Yu L, Buchman AS, Schneider JA, Bennett DA (2013) Neural reserve, neuronal density in the locus ceruleus, and cognitive decline. *Neurology* 80:1202-1208.

- Woitecki AM, Muller JA, van Loo KM, Sowade RF, Becker AJ, Schoch S (2016) Identification of Synaptotagmin 10 as Effector of NPAS4-Mediated Protection from Excitotoxic Neurodegeneration. *J Neurosci* 36:2561-2570.
- Wolfman C, Abo V, Calvo D, Medina J, Dajas F, Silveira R (1994) Recovery of central noradrenergic neurons one year after the administration of the neurotoxin DSP4. *Neurochem Int* 25:395-400.
- Wszolek ZK, Pfeiffer RF, Tsuboi Y, Uitti RJ, McComb RD, Stoessl AJ, Strongosky AJ, Zimprich A, Muller-Myhsok B, Farrer MJ, Gasser T, Calne DB, Dickson DW (2004) Autosomal dominant parkinsonism associated with variable synuclein and tau pathology. *Neurology* 62:1619-1622.
- Xie L, Yang SH (2015) Interaction of astrocytes and T cells in physiological and pathological conditions. *Brain Res* 1623:63-73.
- Xu Q, Park Y, Huang X, Hollenbeck A, Blair A, Schatzkin A, Chen H (2010) Physical activities and future risk of Parkinson disease. *Neurology* 75:341-348.
- Yamasaki M, Takeuchi T (2017) Locus Coeruleus and Dopamine-Dependent Memory Consolidation. *Neural Plast* 2017:8602690.
- Yan D, Zhang Y, Liu L, Shi N, Yan H (2018) Pesticide exposure and risk of Parkinson's disease: Dose-response meta-analysis of observational studies. *Regul Toxicol Pharmacol* 96:57-63.
- Yoshiyama Y, Higuchi M, Zhang B, Huang SM, Iwata N, Saido TC, Maeda J, Suhara T, Trojanowski JQ, Lee VM (2007) Synapse loss and microglial activation precede tangles in a P301S tauopathy mouse model. *Neuron* 53:337-351.

- Zarow C, Lyness SA, Mortimer JA, Chui HC (2003) Neuronal loss is greater in the locus coeruleus than nucleus basalis and substantia nigra in Alzheimer and Parkinson diseases. *Arch Neurol* 60:337-341.
- Zecca L, Mecacci C, Seraglia R, Parati E (1992) The chemical characterization of melanin contained in substantia nigra of human brain. *Biochim Biophys Acta* 1138:6-10.
- Zecca L, Zucca FA, Wilms H, Sulzer D (2003a) Neuromelanin of the substantia nigra: a neuronal black hole with protective and toxic characteristics. *Trends Neurosci* 26:578-580.
- Zecca L, Youdim MB, Riederer P, Connor JR, Crichton RR (2004a) Iron, brain ageing and neurodegenerative disorders. *Nat Rev Neurosci* 5:863-873.
- Zecca L, Tampellini D, Gerlach M, Riederer P, Fariello RG, Sulzer D (2001) Substantia nigra neuromelanin: structure, synthesis, and molecular behaviour. *Mol Pathol* 54:414-418.
- Zecca L, Fariello R, Riederer P, Sulzer D, Gatti A, Tampellini D (2002) The absolute concentration of nigral neuromelanin, assayed by a new sensitive method, increases throughout the life and is dramatically decreased in Parkinson's disease. *FEBS Lett* 510:216-220.
- Zecca L, Zucca FA, Costi P, Tampellini D, Gatti A, Gerlach M, Riederer P, Fariello RG, Ito S, Gallorini M, Sulzer D (2003b) The neuromelanin of human substantia nigra: structure, synthesis and molecular behaviour. *J Neural Transm Suppl*:145-155.
- Zecca L, Wilms H, Geick S, Claasen JH, Brandenburg LO, Holzknecht C, Panizza ML, Zucca FA, Deuschl G, Sievers J, Lucius R (2008a) Human neuromelanin induces neuroinflammation and neurodegeneration in the rat substantia nigra: implications for Parkinson's disease. *Acta Neuropathol* 116:47-55.
- Zecca L, Stroppolo A, Gatti A, Tampellini D, Toscani M, Gallorini M, Giaveri G, Arosio P, Santambrogio P, Fariello RG, Karatekin E, Kleinman MH, Turro N, Hornykiewicz O,

- Zucca FA (2004b) The role of iron and copper molecules in the neuronal vulnerability of locus coeruleus and substantia nigra during aging. *Proc Natl Acad Sci U S A* 101:9843-9848.
- Zecca L, Bellei C, Costi P, Albertini A, Monzani E, Casella L, Gallorini M, Bergamaschi L, Moscatelli A, Turro NJ, Eisner M, Crippa PR, Ito S, Wakamatsu K, Bush WD, Ward WC, Simon JD, Zucca FA (2008b) New melanic pigments in the human brain that accumulate in aging and block environmental toxic metals. *Proc Natl Acad Sci U S A* 105:17567-17572.
- Zhang B, Horvath S (2005) A general framework for weighted gene co-expression network analysis. *Stat Appl Genet Mol Biol* 4:Article17.
- Zhang W, Phillips K, Wielgus AR, Liu J, Albertini A, Zucca FA, Faust R, Qian SY, Miller DS, Chignell CF, Wilson B, Jackson-Lewis V, Przedborski S, Joset D, Loike J, Hong JS, Sulzer D, Zecca L (2011) Neuromelanin activates microglia and induces degeneration of dopaminergic neurons: implications for progression of Parkinson's disease. *Neurotox Res* 19:63-72.
- Zhang X, Zuo DM, Yu PH (1995) Neuroprotection by R(-)-deprenyl and N-2-hexyl-N-methylpropargylamine on DSP-4, a neurotoxin, induced degeneration of noradrenergic neurons in the rat locus coeruleus. *Neurosci Lett* 186:45-48.
- Zhao Y, Hu D, Wang R, Sun X, Ropelewski P, Hubler Z, Lundberg K, Wang Q, Adams DJ, Xu R, Qi X (2022) ATAD3A oligomerization promotes neuropathology and cognitive deficits in Alzheimer's disease models. *Nat Commun* 13:1121.
- Zhou Y, Zhao WJ, Quan W, Qiao CM, Cui C, Hong H, Shi Y, Niu GY, Zhao LP, Shen YQ (2021) Dynamic changes of activated AHR in microglia and astrocytes in the substantia nigra-

- striatum system in an MPTP-induced Parkinson's disease mouse model. *Brain Res Bull* 176:174-183.
- Zhu M, Li M, Ye D, Jiang W, Lei T, Shu K (2016) Sensory symptoms in Parkinson's disease: Clinical features, pathophysiology, and treatment. *J Neurosci Res* 94:685-692.
- Zimprich A et al. (2004) The PARK8 locus in autosomal dominant parkinsonism: confirmation of linkage and further delineation of the disease-containing interval. *Am J Hum Genet* 74:11-19.
- Zucca FA, Vanna R, Cupaioli FA, Bellei C, De Palma A, Di Silvestre D, Mauri P, Grassi S, Prinetti A, Casella L, Sulzer D, Zecca L (2018) Neuromelanin organelles are specialized autolysosomes that accumulate undegraded proteins and lipids in aging human brain and are likely involved in Parkinson's disease. *NPJ Parkinsons Dis* 4:17.
- Zweig RM, Cardillo JE, Cohen M, Giere S, Hedreen JC (1993) The locus ceruleus and dementia in Parkinson's disease. *Neurology* 43:986-991.